

AD _____

Award Number: DAMD17-02-1-0438

TITLE: Breast Cancer in Context: New Tools and Paradigms for the Millennium

PRINCIPAL INVESTIGATOR: Mina J. Bissell, Ph.D.

CONTRACTING ORGANIZATION: Ernest O. Lawrence Berkeley National Laboratory
Berkeley, Ca 94720

REPORT DATE: July 2007

TYPE OF REPORT: Final

PREPARED FOR: U.S. Army Medical Research and Materiel Command
Fort Detrick, Maryland 21702-5012

DISTRIBUTION STATEMENT: Approved for Public Release;
Distribution Unlimited

The views, opinions and/or findings contained in this report are those of the author(s) and should not be construed as an official Department of the Army position, policy or decision unless so designated by other documentation.

REPORT DOCUMENTATION PAGE

Form Approved
OMB No. 0704-0188

Public reporting burden for this collection of information is estimated to average 1 hour per response, including the time for reviewing instructions, searching existing data sources, gathering and maintaining the data needed, and completing and reviewing this collection of information. Send comments regarding this burden estimate or any other aspect of this collection of information, including suggestions for reducing this burden to Department of Defense, Washington Headquarters Services, Directorate for Information Operations and Reports (0704-0188), 1215 Jefferson Davis Highway, Suite 1204, Arlington, VA 22202-4302. Respondents should be aware that notwithstanding any other provision of law, no person shall be subject to any penalty for failing to comply with a collection of information if it does not display a currently valid OMB control number. **PLEASE DO NOT RETURN YOUR FORM TO THE ABOVE ADDRESS.**

1. REPORT DATE 01-07-2007			2. REPORT TYPE Final		3. DATES COVERED 1 Jul 2002 – 30 Jun 2007	
4. TITLE AND SUBTITLE Breast Cancer in Context: New Tools and Paradigms for the Millennium					5a. CONTRACT NUMBER	
					5b. GRANT NUMBER DAMD17-02-1-0438	
					5c. PROGRAM ELEMENT NUMBER	
6. AUTHOR(S) Mina J. Bissell, Ph.D. Email: MJBissell@lbl.gov					5d. PROJECT NUMBER	
					5e. TASK NUMBER	
					5f. WORK UNIT NUMBER	
7. PERFORMING ORGANIZATION NAME(S) AND ADDRESS(ES) Ernest O. Lawrence Berkeley National Laboratory Berkeley, Ca 94720					8. PERFORMING ORGANIZATION REPORT NUMBER	
9. SPONSORING / MONITORING AGENCY NAME(S) AND ADDRESS(ES) U.S. Army Medical Research and Materiel Command Fort Detrick, Maryland 21702-5012					10. SPONSOR/MONITOR'S ACRONYM(S)	
					11. SPONSOR/MONITOR'S REPORT NUMBER(S)	
12. DISTRIBUTION / AVAILABILITY STATEMENT Approved for Public Release; Distribution Unlimited						
13. SUPPLEMENTARY NOTES						
14. ABSTRACT We hypothesized that breast tumors are capable of multiple differentiation pathways. A finite number of interconnected pathways establish homeostasis in normal tissues which, if still functional in tumors, may be manipulated for therapy. Our goal was to characterize a large number of breast cancer cell lines with known genomic profiles as surrogates for human breast cancers utilizing a robust 3-dimensional assay with laminin-rich extracellular matrix (3D IrECM) with the aim of discovering new pathways to be targeted by combinations of drugs. In this assay non-malignant mammary epithelial cells form breast-like acinar structures whereby cells growth arrest and polarize while tumorigenic cells proliferate as a disorganized mass. Tumor cells treated with a number of signaling inhibitors alone or in combination are phenotypically "reverted" or killed. We have found that tumor cell lines adopt one of 4 distinct 3D morphologies which provide a finer delineation than hierarchical clustering of expression profiles of cell lines in 2D alone and that these morphologies may be reflective of their biological origin and phenotypic properties, such as degree of invasiveness. We have also found that the 3D microenvironment exerts common changes in expression profiles across all cell lines that are associated with signal transduction activity. Most importantly, we have shown that response to chemotherapeutic agents and radiation are fundamentally different in 2D and 3D assays with the latter more closely predicting in vivo response.						
15. SUBJECT TERMS Breast Cancer						
16. SECURITY CLASSIFICATION OF:				17. LIMITATION OF ABSTRACT	18. NUMBER OF PAGES	19a. NAME OF RESPONSIBLE PERSON USAMRMC
a. REPORT U	b. ABSTRACT U	c. THIS PAGE U	19b. TELEPHONE NUMBER (include area code)			
				UU	57	

Table of Contents

	<u>Page</u>
Introduction.....	4
Body.....	4
Key Research Accomplishments.....	13
Reportable Outcomes.....	14
Conclusion.....	19
References.....	19
Appendices.....	27

Innovator Award 2007 Final Report
Breast Cancer in Context: New Tools and Paradigms for the Millennium

Introduction

Hypothesis

Breast tumors are capable of multiple differentiation pathways. As a finite number of interconnected pathways establish homeostasis in normal tissues, these pathways, if still functional, could be manipulated in tumors. Further, that these pathways can be used to discern therapeutic candidates and manipulated in 3D organotypic cultures as accurate surrogates for human cancer.

Background

Microenvironmental regulators, including the extracellular matrix (ECM), its receptors – most notably integrins and dystroglycan – cell-cell and stromal-epithelial interactions, are critical determinants of both homeostasis and malignancy. How abnormal environments can contribute to genomic instability, and conversely, how an overtly malignant genome could be controlled by seemingly simple manipulations of the extracellular milieu or surface receptors, have only begun to be explored; our challenge is to reconcile the mutation paradigm with the role of the microenvironment (“context”) to create a unified theory of cancer.

This project was designed to gain a broad picture of how the microenvironment influences the development of cancer and how manipulation of microenvironment-cell interactions could be used to identify the interconnected pathways that would be potential therapeutic targets. We hypothesized that the 3D assay which was developed in this laboratory and was additionally modified during the course of the award would lend itself for discovering accurate therapeutic candidates singly or in combination.

To this end we proposed to characterize ~60 breast cancer cell lines with known genomic profiles (by CGH analysis), utilizing a robust three dimensional laminin-rich extracellular matrix assay (3D IrECM). In this assay non-malignant mammary epithelial cells form acinar, *in vivo*-like structures in which the cells withdraw from the cell cycle, polarize, and form a central lumen whereas tumorigenic cells continue to proliferate and form a disorganized mass. Treatment of the tumorigenic cells with a variety of signaling inhibitors, either singly or in combination, is capable of either phenotypically reverting “normal” structures or killing a variety of breast cancer cell lines in the 3D IrECM assay.

Body

A summary of major accomplishments across the entire period of the award is described below; however results from previous years are presented in an abbreviated format and from the current perspective of the completed term of the award. For additional details and figures please refer to previous annual reports.

Year 1

In the first year of this project we focused on standardization of culture conditions and streamlining the assays so that all data generated in forthcoming years could be directly comparable. It was critical to establish these conditions before embarking on the full

characterization of the entire set of cell lines. We obtained 31 of the proposed 60 breast cell lines from Dr. Joe Gray's laboratory at the UCSF SPORE. These cell lines had already been characterized by comparative genomic hybridization (CGH) and Affymetrix technology in 2D. As we received the cell lines, we expanded them and generated stocks to ensure our laboratory had its own independent and reliable supply. Several pilot experiments were performed to define culture conditions, and the minimal culture volume to obtain the requisite amount of material for downstream analysis. We also performed time course experiments to determine the earliest time point at which the phenotypic differences between non-malignant and malignant cells could be clearly discerned. We developed a new 3D "on top" assay and concluded that the panel of cells should be cultured in H14 medium containing 1% FCS for 4 days in the on top assay instead of 10 days in the 3D "embedded" assay. This new procedure also saved a considerable amount of money due to the reduction of IrECM to a third of the amount required by the embedded assay originally developed. The 3D morphology of all cell lines received at that point were then characterized preliminarily under these conditions.

An initial set of four breast cancer cell lines, CAMA-1, HCC1500, BT-20 and MCF-12A were then selected for full characterization. These cell lines were analyzed in parallel to the HMT-3522 S1 (non-malignant) and T4-2 (malignant) human breast cells which have been extensively characterized in our laboratory in the 3D IrECM assay. Culture of the HMT-3522 cell lines served as controls for 3D culture as well as normalization of western blotting, allowing us to compare experiments across the project in a semi-quantitative manner. (It is noteworthy that we discovered in Year 5 that the cell line BT-20 had been misidentified by previous providers, and was in actuality MDA-MB-231; please see further discussion of this issue below.)

Colony size, 3D morphology, basal polarity, and proliferation were measured in these cell lines. Expression profiles were analyzed utilizing RNA labeled by Genisphere Submicro protocol and hybridized to LBNL-generated cDNA microarrays containing 8,000 sequence verified clones from Research Genetics. A pool of RNA from S1 cells grown in 2D was used as a reference for each of these hybridizations. Western blotting was performed to look at levels of signaling proteins we know to be significant in tumorigenesis. We also tested the potential of single inhibitor treatments to revert these cell lines.

The experiments performed in Year 1 established the types of analysis we would perform in following years. We also began to learn that the characterization of so many cell lines in 3D would not be as straightforward as manipulating one or two and would be a much more time-consuming effort requiring much additional attention to detail. However, we used our "proof of principle" human breast tumor cell line, the HMT-3522 to continuously learn about the integration of pathways in a model of tumor reversion during the entire duration of the award with much exciting data leading to a number of important publications listed at the end of this report. The lessons learned and the pathways discovered were continuously applied to the design of the experiments throughout the award period.

Year 2

In Year 2 we expanded our in depth characterization to a second set of cell lines: T-47D, MPE-600, MDA-MB-436 and MDA-MB-468. We began to suspect that the panel of cell lines previously studied fell into roughly four morphological categories in 3D. Thus we selected these particular cell lines as the representatives of each group. We had also planned on receiving additional cell lines from the Gray laboratory for preliminary morphological characterizations and cell stock establishment, but as they were in the process of moving from UCSF to LBNL, we

were not able to proceed with this goal as intended. But we did perform the same panel of experiments outlined in Year 1 with the above cell lines.

In Year 2, we had to change our expression analysis approach. In Year 1 we had utilized in-house cDNA microarrays to determine expression profiles. However, there were major flaws in the design and quality of these microarrays and additionally the pre-existing 2D expression profiles were generated by the Gray lab using an Affymetrix platform. We performed a series of experiments to confirm that we would achieve similar, but higher quality results utilizing the Affymetrix U133A human gene chip. Although this switch was time-consuming and expensive at the surface, in retrospect it was highly worthwhile to change platforms both for the sake of data quality and the ability to compare profiles across samples. We subsequently performed Affymetrix hybridizations utilizing RNA from the eight cell lines fully characterized.

We also identified 7 genes of interest that showed differential expression by microarray amongst morphologically distinct cell lines. Whereas we had begun work to validate the expression of these genes and planned to continue focusing on them in later years, we eventually determined that we would have a better chance of identifying functionally significant genes if we used a much larger data set. This is because the panel of cell lines was very heterogeneous and we did not want to allocate undue time and funds to genes that could seem significant only due to the small size of the initial data set

Year 3

In Year 3, we continued our in-depth characterization of additional cell lines, but at a higher rate than previous years. We refined our morphological characterizations by adding the immunolocalization of actin structure to phase contrast morphology analysis. This allowed us to refine our definitions to six distinct morphologies: round, round mass, irregular mass, grape-like, grape-like stellate and invasive stellate. We would eventually switch over completely to utilizing F-actin localization as our major immunofluorescent marker of colony structure. Previously we had primarily probed localization of $\alpha 6$ integrin as a marker of basal polarity and β -catenin as a basolateral marker and additionally because we were interested in whether we might observe nuclear relocation of the latter. However, expression of both these markers was often not as high, and a much better signal was achieved with phalloidin staining, allowing the organization of cell colonies to be observed much more accurately. We thus added this new parameter.

As mentioned above, we had switched our expression profile analysis to the Affymetrix platform in Year 2, in particular the cartridge format U133A chip. However at the same time, LBNL was in the process of establishing an expression core utilizing the newer high throughput Affymetrix (HTA) format, in which 96 U133A chips could be arrayed simultaneously in a plate format. We were advised by bioinformaticians that subtle differences in the layout and controls between the cartridge and HTA formats made direct comparisons of these data sets very difficult if not impossible. Therefore the eight cell lines arrayed in Year 2 were rerun yet again using the newer HTA format so that we would be able to make comparisons with future data. The Gray lab began the process of rerunning their 2D RNA on the HTA format as well. Necessary setup and validation studies on the new HTA system caused a delay in the generation of new expression data. However, we were still able to run 16 additional cultures containing representatives from each of the 6 morphological groups.

GeneSpring analysis software was used to perform hierarchical cluster analysis of these expression profiles and we were able to make some interesting observations. The first was that the distinct cell morphologies were mostly clustered together within tree branches, suggesting

that the 3D analysis may provide a finer delineation or sub-categorization of cell lines than might be obtained from 2D expression profiles confirming our initial hypothesis. The second observation was that the 3 major branches appeared to group the cell lines by their perceived aggressiveness: one branch contained stellate cell lines, which would be expected to be more aggressive than the round, grape and mass cell lines found in a second branch, and a third branch contained the HCC1500 tumor cell line and the HMT-3522 progression series that was derived by continuous culturing of reduction mammaplasty and which we use as our workhorse for modeling, which may be less aggressive cell lines.

This year we also began the shift in our focus away from strictly determining reversion requirements of the tumor cell lines of differing morphologies towards looking more broadly at the main goal of this project, i.e. to identify predictors of therapeutic response. We focused our attention first on the role of the β 1-integrin and ErbB2 signalling pathways. We found that only cells with high levels of ErbB2 responded to Herceptin. (As an aside, we found that the AU-565 cell line, which is supposed to be amplified at the ErbB2 locus and express very high levels of the protein did not respond. At the time we were puzzled by this finding, but in Year 5, we found that the stock of AU-565 cells utilized for this experiment were misidentified and in fact MDA-MB-415 which express low levels of ErbB2!) We now conclude that it is indeed the case that protein levels of total ErbB2 in 3D are a good predictor of therapeutic response to Herceptin.

On the other hand, AIB2 inhibited proliferation in all cell lines tested but to differing degrees. Herceptin on the other hand had little or no effect on the cell lines tested. Live cell imaging as well as characterization of end point cellular structures by F-actin localization revealed that cell lines also had a different morphological response to AIB2 treatment. For example, AIB2 treatment caused a stark decrease of invasive phenotype in MDA-MB-231 cells but had no discernable effect on cell growth, whereas BT-474 cells treated with AIB2 remained as single cells over the duration of culture.

Analysis of the protein levels of the target proteins showed surprisingly that total levels of β 1 integrin did not necessarily correlate with response. Almost all tumor cells tested responded to treatment with inhibitor antibody to β 1 integrin in 3D cultures (total of 14 cell lines) as well as in vivo (two tumor cell lines tested) (Park et al., 2006). Our current results about to be sent for publication reveal that combinatorial treatment of β 1 integrin inhibitory antibody with other drugs enhances response, and that 3D culture experiments predict the *in vivo* response. In particular, we have found that blockade of β 1 integrin signalling sensitizes tumor cell lines in 3D and tumor xenografts *in vivo* to radiation therapy, such that supplementation of a low dose of radiation with AIB2 treatment results in the same decrease in tumor volume as a high dose of radiation alone. Furthermore, this AIB2 treatment is non-toxic to the animal, again corresponding with results obtained with 3D assays, that treatment of non-malignant acini with AIB2 in 3D culture does not affect the cells. Inhibitory antibody to β 1 integrin is a very promising treatment for breast tumor cells which can be studied in 3D assays as a robust surrogate for expensive and time-consuming *in vivo* studies. Furthermore, these results show that the 3D on top model we have developed to simulate the behavior of normal and malignant cells in culture indeed predicts the outcome of drug behavior in mouse models using human tumor cells.

Year 4

We this year began a collaboration with Bahram Parvin, a bioinformaticist at LBNL with extensive experience in quantitative image analysis towards the aim of automating and standardizing our morphological categorization rules. We provided him sample phase images

and confocal sections of F-actin and nuclear staining of various cancer cell lines in 3D IrECM in order for him to begin developing methods to compute morphological descriptors in 3-dimensional space as opposed to 2-dimensional space, which he had previous experience with. The ultimate goal was to be able to feed images into a computational system that would objectively designate a morphological grouping based on predetermined rules.

Expression analysis was performed on the 26 cell lines profiled by Affymetrix to date. We performed hierarchical cluster analysis and confirmed that the cell lines continued to fall into three major clusters, similarly as in Year 3. Additionally we observed that when the clusters were colored by 3D morphologies, they mostly clustered together within the groups, again as before. We were heartened that as our sample size increased from 16 to 26 cell lines that the same major clusters were maintained. However, as we increased the number of cell lines characterized, we found fair variety in the morphologies presented and, depending on the cell line, a certain degree of heterogeneity within the lines themselves. Although we were able to distinguish 6 morphological categories, we considered these categories flexible as we continued to learn about the behavior of this panel of cell lines in 3D IrECM.

We also began to interrogate the differences in the gene expression profiles between matched cell lines in 2D and 3D, and added a small sample size of xenograft profiles. The latter were generated from RNA isolated from cell line xenografts at UCSF. We hypothesized that the gene expression profiles of tumor xenografts would be more like the profiles of the same cells cultured in 3D as opposed to 2D. Although the cell line sources for the 2D and 3D data were not matched with the xenograft data, and the sample size was small ($n = 3$), we excitingly observed in this analysis a cluster of genes strikingly downregulated in 2D in comparison to 3D and xenograft samples. We performed gene ontology analyses on this gene list using GOstat and found that in this group of genes, membrane proteins were significantly overrepresented while the RNA binding, biopolymer metabolism and ubiquitin cycle classes were underrepresented.

We also followed up on the intriguing results that $\beta 1$ integrin blockade resulted in an inhibition of invasive phenotype in the stellate cell line MDA-MB-231. We tested the hypothesis that other stellate cell lines would respond in a similar manner to AIB2 by treating an additional four cell lines with the same 3D morphology. AIB2 blocked the invasive phenotype of all but one cell line (Figure 1). As discussed below, we have found that all cell lines with stellate 3D morphology have been shown to be invasive by *in vitro* assays. Therefore, we may have identified through utilization of the 3D assay that inhibition of $\beta 1$ integrin may also be used as a therapy against the invasive capacity of tumor cells.

Year 5

As we have described in previous years, we had the realization that in order to make this work more applicable to translational research we needed to perform experiments that mimic the actual situation of the tumor in patients. The idea of reverting tumor cells is a useful cell culture concept to elucidate signaling pathways and their underlying mechanisms and we have continued to perform these experiments with our HMT-3522 proof of principle model. On the other hand, we have now developed a system where we can model an actually formed tumor surrogate as well as the normal acinus in 3D IrECM culture, imitating the status of these structures *in vivo*, and then subject them to chemotherapeutic drugs. We have shown that indeed some of the inhibitory compounds we have identified such as AIB2, indeed killed the tumor without affecting the mouse. Therefore we have continued to perform therapeutic response assays under these conditions.

In this final year of the project we have focused on two main goals. The first was to publish our results from Years 1-4 in the form of a complete description of the 26 cell lines fully characterized in 3D, including morphology, selected proteome profiling and expression analysis. The second was to continue our work investigating the response of breast cancer cell lines to inhibitors, but from the broader point of view of therapy as opposed to reversion per se, as discussed above.

Cell line characterization in 3D

In December 2006, the Gray laboratory published their CGH and expression profiling results of the panel of breast cancer cell lines in 2D, as well as similar characterization of breast cancer tissue (Chin et al., 2006; Neve et al., 2006). One of their major conclusions was that the panel of cell lines roughly represents the variety of chromosomal and genetic aberrations found in primary cancer tissue and therefore as a whole is a good model for the study of breast cancer and therapeutic response. These findings provided an additional validation of our initial hypothesis that these cell lines were reasonable models and made our work of characterizing the behavior of these cells and their response to therapeutics in 3D all the more significant. In this past year, we published these results to date in the inaugural issue of *Molecular Oncology* (Kenny et al, 2007, Appendix C).

We now have classified the panel of cell lines into four morphological classes as opposed to six: Round, Mass, Grape-like and Stellate (Figure 2). We opted to utilize four classes for the reasons discussed above; we initially identified four classes into which the cell lines obviously fell, and although we were able to find cause for further delineations, the biological significance of doing this is at best unknown. We concluded that it was best to minimize the amount of subjectivity in the categorization while we lacked wholly objective (i.e. computational) descriptors of morphology, and therefore utilized the lower number of groups.

We reported the 3D morphologies, as described by phase contrast and immunofluorescence microscopy, proliferation indices, and protein profiling of the panel of cell lines. We performed a statistical analysis showing that the proliferation indices of the cell lines was not significantly correlated to morphology, Sorlie/Perou tumor class, ER status, or whether the cell line was derived from a primary tumor or a metastasis. In particular, the data that morphology and proliferation are not correlated refutes the common misconception that 3D morphology is merely reflective of a lower amount of proliferation in more differentiated cells and vice versa.

A major finding from the protein profiling analysis was that each of the Stellate cell lines lacked E-cadherin, while the Grape-like cell lines generally had lower levels than the other two groups. Eight of the nine Grape-Like cells were isolated from tumor metastases. In general, these cells formed less closely associated colonies with reduced cell-cell adhesion compared to cell lines of the other morphologies. This may reflect, in part, the acquisition by these cells of the ability to break away from their neighbors in the primary tumor over the course of their evolution as they acquired the ability to metastasize. These facts provide additional support for the biological relevance of the 3D assay.

Furthermore, our collaborators in the Gray laboratory reported that breast cancer cell lines belonging to the Basal B category were much more invasive by Boyden chamber assay than those belonging to the Basal A and Luminal categories (Neve et al., 2006). The two outliers in this correlation were MCF-10A and MCF-12A, both Basal B but highly uninvase. Interestingly, both of these cell lines are Round by our 3D morphology (Muthuswamy et al., 2001 and Figure 2, Kenny et al, 2007). Of the other eight Basal B cell lines which are highly invasive, six cell

lines are of the Stellate 3D morphology: three are described in full here (BT-549, Hs578T, MDA-MB-231) and we have also characterized the other three as such (HBL-100, MDA-MB-157, SUM 159PT; data not shown). MDA-MB-436 has been shown to be invasive by similar *in vitro* assays. **Thus far, all of the cell lines we have characterized as Stellate have been shown to be invasive in commonly used *in vitro* assays, suggesting the utility of 3D colony morphology as a functional assay for invasive potential and again indicating that the morphologies tumor cell lines form in 3D have biological relevance.**

In previous years, our expression analysis has focused on comparing the profiles of cell lines of different morphologies in 3D. This year we expanded our analysis to a comparison of the profiles of the same cell lines in 2D versus 3D and whether we could identify global changes in gene expression across cell lines due to exposure to a 3D microenvironment. To do so, we tackled one of the major issues during this project, the question of normalization across platforms and our ability to use preexisting data generated using older technology. We therefore collaborated with bioinformaticians to determine whether a robust normalization method could be applied that would enable us to combine data from the large format U133A Affymetrix chips, on which 3D expression profiling from Year 2 resided, as well as the largest set of 2D data, with data from the HTA U133A chips, the format of all later 3D data. Even though we had been told that this would be extremely difficult to do, as discussed in Year 3, the bioinformaticians were successful in generating a method to do this, the details of which we have published (Kenny et al, 2007).

In total, 89 samples from 24 different cell lines were analyzed using this new technique, 47 in 2D and 42 in 3D. These data have been deposited in the Array Express database (<http://www.ebi.ac.uk/arrayexpress/>; accession number E-TABM-244). When hierarchical clustering was performed on these samples, the cell lines grouped into three clusters, Luminal, Basal A and Basal B, as when the 2D samples are clustered alone (Figure 3). S1 and T4-2 cluster with the non-malignant MCF-12A cell line in the Basal B subclass. The HCC1500 cell line is an outlier of this group, distinct from the other cells with a basal phenotype. These findings are very similar to what we had previously reported with fewer cell lines in the set, although the fact that another non-malignant cell line, MCF-12A, is now a member of this cluster gives even more credence to our original hypothesis that these cell lines reflect a more differentiated phenotype than some of the other cell lines in the panel. This is also a distinction which would not have been revealed by simple hierarchical clustering of the 2D data, since nothing in particular distinguishes the morphologies of these cell lines when they are cultured on tissue culture plastic.

While the Basal/Luminal delineation seems to be the strongest driver of the clustering pattern, cell lines of similar morphologies within these sub-types frequently clustered together suggesting that the gene expression pattern of the cells is a strong determinant of colony morphology. All four of the Stellate cell lines are more similar to each other than to cell lines of any other morphology, while all of the Round cell lines of the Basal subtype clustered together. Among the Luminal subtype, five of the seven Grape-Like cell lines cluster together and there is a sub-cluster of two Round cell lines in a larger cluster of mostly Mass cell lines.

From the hierarchical clustering, it is clear that the 2D and 3D expression profiles of the individual cell lines cluster together, independently of the substratum on which they were cultured. However, we observed that the 3D microenvironment clearly did effect significant changes in the gene expression profiles of the cell lines by identifying a set of genes which distinguished cell lines grown in 2D v 3D (ANOVA, cutoff $P < 0.00025$). 96 Affymetrix probes were strongly up/downregulated consistently across the majority of the cell lines (Figure 4). Of

these probes, 41 corresponded to genes with annotated Gene Ontology functions (Figure 5). Of the eight classifications found, one – “signal transducer activity”– was statistically significantly overrepresented in the set of genes which differ between 2D and 3D culture (P-value = 0.0201). The “enzyme regulator activity” class almost reached statistical significance (P-value = 0.0509). These data provide additional support for our hypothesis that regulation of signal transduction is substantially different in cells cultured on 3D basement membrane gels and also show that, although cell line identity and the Luminal/Basal phenotype make a strong contribution to the gene expression profiles, the 3D culture phenotype also exerts important effects, across the entire diverse panel of cell lines.

In Year 5 we also published a protocol that described in particular methods for culturing breast epithelial cells, both malignant and non-malignant, in 3D (Lee et al., 2007). Previously published 3D methods papers focused on the culture of non-malignant epithelial cells and lacked the generalized point of view of this protocol. This protocol is complementary to the Molecular Oncology manuscript and we already know that it has become an excellent resource for the scientific community.

We are continuing with the characterization of the rest of the breast cancer cell lines. In previous years our approach was to analyze a set of cell lines of each morphology at once in the hopes that patterns would immediately emerge from the data. However, as discussed at several points here, it became clear that the best approach would be to glean the largest data set possible and then to perform a large scale analysis. Therefore, our current approach is to culture as many cell lines in 3D as possible and to bank the protein and RNA for analysis all at once. We now have 39 cell lines where we either have a full set of data or materials for later analysis. Of the total set of 51 cell lines we are also still waiting to receive 6 from the Gray lab. Although we are no longer supported by the Innovator award, we will continue this effort under the auspices of an alternate funding source as we believe it is important work to complete and provide to the scientific community, which is now extremely interested in 3D.

We are also continuing to work with Bahram Parvin to perform image analysis for not only automated identification of 3D morphology, but we are also now developing methods for unbiased correlation of baseline expression profiles with morphological parameters either calculated from phase contrast images or nuclear and F-actin fluorescence. At first we believed the analysis of the immunofluorescence data would be more straightforward but the Parvin group is still developing methods for reconstructing and analyzing 3-dimensional (x,y,z) data. We are currently focusing on utilizing the phase contrast data to calculate morphological parameters while these methods are being developed. We hope to be able to report these analyses in a future manuscript including the full panel of cell lines.

Corollary benefits of the research

It is of note that when we were validating the inter-platform expression normalization technique by generating test clusters of all 2D and 3D samples, we recognized that a secondary benefit of this analysis was as a quality control measure. When individual samples were analyzed (i.e. biological replicates not collapsed) we observed that a few individual samples clustered tightly with samples from different cell lines. We were able to use this information to go back through the data and determine whether we believed samples had been misidentified and, if so, also attempted to discern when the error had occurred. For example, BT-20, a cell line studied in Year 1, was determined to have been MDA-MB-231 and misidentified very early on (this error originated in the vial given to us by the Gray laboratory). Although these errors were disheartening to recognize, we were able to go back through the data and confirm that not only

were the expression patterns of the samples similar but the protein profiles, morphology and response to inhibitors virtually identical, speaking well for the robust nature of the 3D assay that work performed by multiple researchers spanning a period of 5 years matched very well.

Finally, we wish to note that we were unable to pursue the proposed Task 5, although we wished to build upon the preliminary analysis in Year 4 that the expression profiles of cell lines in cultured as xenografts seem to be closer to the profiles of the same cell lines cultured in 3D than cultured in 2D. We had established a relationship with Byron Hann at UCSF to do so, but a major technical issue was that their bank of cell lines is independent from either that of our laboratory or the Gray laboratory and we felt it was imperative that the same stocks be used in order to draw a robust comparison amongst the samples. Unfortunately, we were unable to coordinate a solution with the Hann laboratory and were unable to perform these time-consuming experiments ourselves in the final funding year. However, we wish to pursue similar experiments in the future, and expect to validate our hypothesis that the 3D assay is an excellent surrogate for tumor xenograft studies.

Cell line response to therapeutic intervention

In 2006 we had published a new version of our 3D assay in which cells cultured for four days in order to form a tumor prior to addition of inhibitors (Park et al, 2006). This study in particular focused on the effects of utilizing AIIB2 to block $\beta 1$ integrin. We found that addition of AIIB2 to selected established tumors results in an increase in apoptosis and/or a decrease in proliferation. These results were confirmed by experiments in which animals with cell line xenografts were treated with AIIB2, resulting in a decrease in tumor growth. In this year, we began to utilize this assay as opposed to our typical reversion assay in which the inhibitor is added at day zero. We chose to use the endpoints of proliferation as measured by BrdU incorporation and apoptosis as measured by cleaved caspase 3. These are also the same endpoints as are being used by the Gray laboratory for similar experiments, facilitating later comparison of results. We are also collaborating with the Parvin group in developing methods for automated analysis of immunofluorescence images to quantify BrdU and cleaved caspase labeling. Regardless of the method of quantification, either manual or automated, these endpoints may then be easily numerically represented and correlated with baseline expression profiling or profiles of treated cells.

Although we intend to compare response of cell lines to therapy in 3D with response in 2D as shown by the Gray laboratory, we will also be performing 2D experiments ourselves as an additional control. To date we have performed some preliminary experiments and hope to continue with this work with alternate funding in the future.

First, we determined whether the drug concentrations used for the treatment of breast cancer cell lines in 2D, which are based on the average GI50 values of 50 breast cancer cell lines, are also effective in cells grown in 3D culture models. The breast cancer cell lines AU-565 and BT-474 were propagated on top of 3D IrECM for four days until colonies were formed as described above and subsequently treated for 48 hours with different concentrations of the targeted therapeutics Herceptin and Iressa (Figure 1). Both cell lines express HER2, the target of Herceptin, and EGFR, the target of Iressa.

The drug concentrations used for treatment of the breast cancer cell lines in 2D are 21 $\mu\text{g/ml}$ for Herceptin and 5 μM for Iressa. BT-474, a cell line which has been reported to have a robust response to 21 $\mu\text{g/ml}$ Herceptin when grown in 2D (Neve et al., 2006), has a high sensitivity to the same Herceptin concentration when cultured and treated on 3D IrECM. BT-474 cells also

show a clear response to 5 μ M Iressa, the concentration used in the 2D studies. The breast cancer cell line AU-565 has been shown to have a low sensitivity for 21 μ g/ml Herceptin when grown in 2D (Neve et al., 2006), which was also observed when the cells were treated on top of 3D IrECM. Similarly, the response of AU-565 to 5 μ M Iressa in 3D was also less pronounced as for BT-474 cells. We therefore conclude that the concentrations used for studying drug response of breast cancer cells grown in 2D can be adapted for cells grown in 3D culture models.

We also tested the response of the BT-20 cell line to multiple inhibitors in the same assay. These cells were treated for 48 hours with 5 μ M Iressa, 1.5 μ M Lapatinib, 700 nM AKT-inhibitor (Glaxo Smith Kline), 11 nM PLK-inhibitor (Glaxo Smith Kline), and DMSO as control. Cells were assessed by morphological criteria and cell proliferation measured by BrdU incorporation (Figure 6). We observed that BT-20 cultured in 3D show a high resistance to these varied treatments, and that only Iressa induces a 30% reduction of cell proliferation.

We intend to build upon these data by treating selected cell lines with the clinical inhibitors described above and comparing their responses in 2D and 3D. In continued collaboration with the Gray laboratory, we will attempt to then find predictors of response in the baseline expression data of the cell lines using Bayesian or linear spline approaches. We expect to find that for inhibitors for which response is not strongly driven by genetic factors (i.e. PIK3CA or PTEN mutations for Akt pathway inhibitors) that response of tumors in 3D culture as opposed to 2D will provide a more robust assessment of response in human patients. Furthermore this will allow us to identify of subpopulations of patients that should be included in clinical trials for particular targeted inhibitors so that drugs are not classified as “failures” only because they were administered to a broad segment of the population when they may only be expected to affect tumors that express certain markers as identified by the 3D drug screening. We are currently pursuing these types of studies in collaboration with the Gray laboratory and GlaxoSmithKline, based on results funded by this award, and we believe that such ongoing research is a very significant product of the work performed over the past 5 years and that will benefit not only the scientific community directly but patients as well.

Key Research Accomplishments

- Culture conditions and downstream assays for characterization of breast cancer cell lines were defined and standardized.
- A manuscript describing the full characterization of 25 breast cell lines in 3D was published.
- Baseline expression profiles of 25 breast cell lines in 3D are now publicly available.
- A method for inter-platform Affymetrix normalization was developed and published.
- A detailed and generalized protocol for the 3D culture of breast epithelial cells was published.
- To date, 39 cell lines have either been fully characterized or are pending characterization in 3D.
- The distinct morphologies of breast cell lines in 3D may correlate with their stage of tumor progression.

- 3D expression profiles may allow for identification of subtle differences amongst cell lines which are not discerned by 2D expression analysis alone.
- The 3D microenvironment induces a set of consistent gene expression changes over a large panel of tumor cell lines.
- Knowledge gained during the course of this award, including the methodology of 3D cultures and the utility of the assay as a surrogate for *in vivo* studies, has been widely disseminated amongst academia and industry.
 - The recent academic literature utilizing 3D assays has become too large to cite, but of particular note are publications from the laboratories of Joan Brugge and Senthil Muthuswamy, who were trained by us in this assay (see Muthuswamy et al., 2001; Debnath et al, 2002; Reginato et al., 2005; Aranda et al., 2006). In sum total we have trained in excess of 50 laboratories both formally and informally over the period of this award who are now actively utilizing the 3D assay and way of thinking.
 - Dr. Bissell has given many invited lectures at a number of companies who are interested in utilizing the 3D assay and/or collaborating, including Merck Pharmaceuticals, GlaxoSmithKline, FivePrime Therapeutics, and Halozyme Therapeutics. 3D assays are now being utilized to screen therapeutic response at GSK and other companies.

Reportable Outcomes

Manuscripts:

- Weaver VM, Lelievre S, Lakins JN, Chrenek MA, Jones JC, Giancotti F, Werb Z, Bissell MJ (2002). Beta4 integrin-dependent formation of polarized three-dimensional architecture confers resistance to apoptosis in normal and malignant mammary epithelium. *Cancer Cell*. 2002 Sep;2(3):205-16..
- Anders M, Hansen R, Ding RX, Rauen K, Bissell MJ, and Korn WM. (2003) Disruption of 3D tissue integrity facilitates adenovirus infection by deregulating the coxsackievirus and adenovirus receptor. *Proc Natl Acad Sci* 100:4:1943-1948.
- Schmeichel, KL and Bissell MJ. (2003) Modeling tissue-specific signaling and organ function in three dimensions. *J Cell Sci*. 116:2377-2388.
- Park, CC, Henshall-Powell, RL, Erickson, AC, Talhouk, R, Parvin, B, Bissell MJ and Barcellos-Hoff MH. (2003) Ionizing radiation induces heritable disruption of epithelial cell interactions. *Proc Natl Acad Sci* 100:19:10728-10733.
- Itoh M and Bissell MJ (2003). The Organization of Tight Junctions in Epithelia: Implications for Mammary Gland Biology and Breast Tumorigenesis. *J Mammary Gland Biol Neoplasia* (4):449-462.

- Kenny PA and Bissell MJ. (2003) Tumor reversion: Correction of malignant behavior by microenvironmental cues. *Int J Cancer Review* 107(5):588-695.
- Bissell MJ, Rizki A and Mian IS (2003) Tissue architecture: the ultimate regulator of breast epithelial function. *Curr Opin Cell Biol* (6):753-62.
- Liu H, Radisky DC, Wang F and Bissell MJ. (2004) Polarity and proliferation are controlled by distinct signaling pathways downstream of PI3-kinase in breast epithelial tumor cells. *J Cell Biol* 164(4):603-12.
- Alcaraz J, Nelson CM, Bissell MJ (2004). Biomechanical approaches for studying integration of tissue structure and function in mammary epithelia. *J Mammary Gland Biol Neoplasia*. 2004 Oct;9(4):361-74.
- Rizki A and Bissell MJ. (2004) Homeostasis in the breast: it takes a village. *Cancer Cell* 6(1):1-2.
- Bissell MJ and LaBarge MA (2005). Context, tissue plasticity, and cancer: Are tumor stem cells also regulated by the microenvironment? *Cancer Cell (Focus)* 7:17-23.
- Kaminker P, Plachot C, Kim SH, Chung P, Crippen D, Petersen OW, Bissell MJ, Campisi J and Lelievre SA (2005). Higher-order nuclear organization in growth arrest of human mammary epithelial cells: A novel role for telomere-associated protein TIN2. *Journal of Cell Science* 118(6): 1321-1330.
- Liu H, Radisky DC, Bissell MJ (2005). Proliferation and Polarity in Breast Cancer: Untying the Gordian Knot. *Cell Cycle*. 4:5, 646-649.
- Adriance MC, Inman JL, Petersen OW, Bissell MJ (2005). Myoepithelial Cells: Good fences make good neighbors. *Breast Cancer Research* 2005 7(5):190-7.
- Wu W, Xing EP, Myers C, Mian IS and Bissell MJ (2005). Evaluation of normalization Methods for cDNA Microarray Data by k-NN Classification. *BMC Bioinformatics* 6:191.
- Nelson CM and Bissell MJ (2005). Modeling dynamic reciprocity: Engineering three-dimensional culture models of breast architecture, function, and neoplastic transformation. *Semin Cancer Biol*. 15(5):342-52.
- Park CC, Zhang H, Pallavicini M, Gray JW, Baehner F, Park CJ, Bissell MJ (2006). β 1 Integrin Inhibitory Antibody Induces Apoptosis of Breast Cancer Cells, Inhibits Growth, and Distinguishes Malignant from Normal Phenotype in Three Dimensional Cultures and In vivo. *Cancer Research* Feb 1;66(3):1526-35.
- Liu H, Radisky DC, Nelson CM, Zhang H, Fata J and Bissell MJ (2006). Mechanism of Akt1 inhibition of breast cancer cell invasion reveals a protumorigenic role for TSC2. *Proc Natl Acad Sci U S A*. 2006 Mar 14;103(11):4134-9.

- Knowles DW, Sudar D, Bator-Kelly C, Bissell MJ, and Lelievre SA (2006). Automated local bright feature image analysis of nuclear protein distribution identifies changes in tissue phenotype. *Proc Natl Acad Sci U S A*. 2006 Mar 21;103(12):4445-50.
- Kenny PA, Nelson CM and Bissell, MJ (2006). The Ecology of Tumors. *The Scientist* 20, 30-35.
- Fournier MV, Martin KJ, Kenny PA, Xhaja K, Bosch I, Yaswen P and Bissell, MJ (2006). Gene expression signature in organized and growth-arrested mammary acini predicts good outcome in breast cancer. *Cancer Research*. 2006 Jul 15;66(14):7095-102.
- Nelson CM and Bissell MJ (2006). Of extracellular matrix, scaffolds, and signaling: Tissue architecture regulates development, homeostasis, and cancer. *Annual Review of Cell and Developmental Biology* – Review Article for Volume 22. Sep 27 [Epub ahead of print]
- Kenny PA and Bissell MJ (2007) Targeting TACE-dependent EGFR ligand shedding in breast cancer. *Journal Clinical Investigation* 117 (2) 337-345
- Hamilton SR, Fard SF, Paiwand FF, Tolg C, Veisheh M, Wang C, McCarthy JB, Bissell MJ, Koropatnick J, Turley EA (2007). The hyaluronan receptors CD44 and RHAMM (CD168) form complexes with ERK1,2, which sustain high basal motility in breast cancer cells. *Journal Biological Chemistry* 2007 Mar 28.
- Lee GY, Kenny PA, Lee EH, Bissell MJ (2007.) Three-dimensional culture models of normal and malignant breast epithelial cells. *Nat Methods*. 2007 4(4):359-65.
- Villadsen R, Fridriksdottir AJ, Rønnov-Jessen L, Gudjonsson T, Rank F, Labarge MA, Bissell MJ, Petersen OW (2007). Evidence for a Stem Cell Hierarchy in the Adult Human Breast. *The Journal of Cell Biology*. 2007 177(1):87-101
- Kenny PA, Lee GY, Myers CA, Neve RM, Semeiks JR, Spellman PT, Lorenz K, Lee EH, Barcellos-Hoff MH, Petersen OW, Gray JW, Bissell MJ (2007) The morphologies of breast cancer cell lines in three-dimensional assays correlate with their profiles of gene expression. *Molecular Oncology* 1(1): 84-96
- Kenny PA, Lee GY, Bissell MJ (2007). Targeting the tumor microenvironment. *Front Biosci*. 2007 May 1;12:3468-74.
- Itoh M, Nelson CM, Myers CA, Bissell MJ (2007). Rap1 integrates tissue polarity, lumen formation, and tumorigenic potential in human breast epithelial cells. *Cancer Research*. *Cancer Res*. 2007 May 15;67(10):4759-66.
- Myers C, Liu H, Lee E, and Bissell MJ. Three-Dimensional Cultures of Normal and Malignant Human Breast Epithelial Cells to Achieve *in vivo*-like Architecture and Function. In Cell Biology: A Laboratory Handbook, Third Edition, Julio Celis, Editor (In press).

Posters/presentations:

- Scientific lectures: Dr. Bissell has delivered 85 presentations, including dozens of named and distinguished lectures on aspects of this work nationally and internationally including presentations at the following meetings:
 - Molecular Therapeutics Gordon Conference, July 2004.
 - The 3rd International Conference on Tumor Microenvironment, October 2004.
 - Era of Hope, June 2005.

- Drs. Paraic Kenny and Catherine Park and Ms. Genee Lee have delivered more than 10 lectures or posters of aspects of this work including presentations at the following meetings:
 - American Society for Cell Biology, December 2005.
 - Matrix Turnover - Mechanisms and Common Denominators, April 2007.

Patents applied for/received:

- Method of Increasing Radiation Sensitivity by Inhibition of Beta One Integrin, filed 6/2/2005, serial number PCT/US2005/019396.
- Premalignant Breast Epithelial Cell Lines for Use In Identification of Target Premalignant Genes, filed 3/17/2006, serial number 60/783,790.
- Targeting TNF- α Converting Enzyme (TACE)- Dependent Growth Factor Shedding in Cancer Therapy, filed 7/31/06, serial number PCT/US06/30008.

Awards (to Dr. Bissell):

- Elected to the American Academy of Arts and Sciences (2002)
- Komen Foundation Brinker Award (2003)
- Discovery Health Channel Medical Honor and Medal (2004)
- Honorary Doctorate, University of Copenhagen (2004)
- First Distinguished Scientist Fellowship Award in Life Sciences, OBER, US Dept. of Energy (2005)
- Ted Couch Lectureship and Award in Cancer Research, H. Lee Moffitt Cancer Center and Research Institute (2007)

- Pezcoller Foundation–AACR International Award for Cancer Research (2007)
- Elected to the American Philosophical Society (2007)
- FASEB - Excellence In Science Award (2007)

Informatics:

- Raw expression data published in Kenny et al., 2007, have been deposited in an Array Express database (<http://www.ebi.ac.uk/arrayexpress/>), accession number E-TABM-244.

Funding applied for/received:

- Data from this project was an integral part of an application from Dr. Joe Gray's laboratory to the National Institutes of Health Integrative Cancer Biology Program P50 (now U54), of which Dr. Bissell is a co-PI, which was funded in September 2004. Dr. Gray also received funding for a related project from GlaxoSmithKline on the strength of our data as well.
- Data from this project was used in an application from Dr. Bissell's laboratory to the National Institutes of Health Tumor Microenvironment Network U54 which was funded in September 2006.
- Data from this project was used in an application from Vivo Biosciences, Inc. to the National Institutes of Health Small Business Innovation Research Program which was funded in October 2006.
- Data from this project was used in applications from Dr. Catherine Park's laboratory to the National Institutes of Health and the American Cancer Society and both were funded in 2007.

Employment applied for/received:

- Katrin Lorenz, former graduate student, successfully defended her thesis at the University Louis Pasteur, Strasbourg, September 2003.
- Connie Myers, former Project Manager, obtained a position as a Research Lab Manager, Washington University, St. Louis, MO, September 2005.
- Sun-Young Moonlee, graduate student and research associate, will be completing her thesis in December 2007.
- Paraic Kenny, postdoctoral fellow, has multiple offers for an independent research position in the upcoming year.

The following researchers were supported on this award:

- Mina Bissell
- Stephen Capaldi
- Paraic Kenny
- Eva Lee
- Genee Lee
- Dinah Levy
- Katrin Lorenz
- Sun-Young Moonlee
- Connie Myers
- Hui Zhang

Conclusions

The originally proposed work was to completely characterize a panel of breast cancer cell lines and their reversion requirements in 3D. We have been successful in fulfilling a large portion of this ambitious goal. We hypothesized that we would be able to use the 3D assay to show that even tumor cell lines have plasticity and that their behavior might be modulated in a way that cannot be shown in 2D and that these characteristics can be then used for finding new and effective combinations of therapeutic agents. In particular, we succeeded in studying a statistically significant number of breast tumors, using physiological assays to identify classes of tumors that cannot be identified using 2D analysis alone and have identified broad microenvironmental effects on gene expression. Although we have not identified the particular combinatorial inhibitors required to revert the phenotype of each cell line or class, we have confirmed a major umbrella hypothesis of our original proposal, that even across a broad panel of tumor cell lines, their behavior is modulated by the microenvironment, perhaps in a manner that might be utilized for therapy in the future. We will continue to pursue this work in the hopes that particular targets for intervention in each morphological class could be identified. Finally, a major accomplishment achieved was our role in the widespread adoption of the 3D assay in both academia and industry. A vast number of laboratories are now utilizing 3D to properly study epithelial differentiation and as an assay for therapeutic response, including GlaxoSmithKline, with whom we are collaborating to test both established drugs and new drugs in development in 3D assays to assist them to determine which subpopulations of patients should be selected for clinical trials.

References

Aranda V, Haire T, Nolan ME, Calarco JP, Rosenberg AZ, Fawcett JP, Pawson T, Muthuswamy SK (2006). Par6-aPKC uncouples ErbB2 induced disruption of polarized epithelial organization from proliferation control. *Nat Cell Biol.* 2006 Nov;8(11):1235-45.

Chin K, DeVries S, Fridlyand J, Spellman PT, Roydasgupta R, Kuo WL, Lapuk A, Neve RM, Qian Z, Ryder T, Chen F, Feiler H, Tokuyasu T, Kingsley C, Dairkee S, Meng Z, Chew K, Pinkel D, Jain A, Ljung BM, Esserman L, Albertson DG, Waldman FM, Gray JW (2006). Genomic and transcriptional aberrations linked to breast cancer pathophysiologies. *Cancer Cell* 10(6):529-41.

Debnath J, Mills KR, Collins NL, Reginato MJ, Muthuswamy SK, Brugge JS (2002). The role of apoptosis in creating and maintaining luminal space within normal and oncogene-expressing mammary acini. *Cell*. 2002 Oct 4;111(1):29-40. Erratum in: *Cell*. 2002 Nov 27;111(5):757.

Kenny PA, Lee GY, Myers CA, Neve RM, Semeiks JR, Spellman PT, Lorenz K, Lee EH, Barcellos-Hoff MH, Petersen OW, Gray JW, Bissell MJ (2007). The morphologies of breast cancer cell lines in three-dimensional assays correlate with their profiles of gene expression. *Molecular Oncology* 1(1):84-96.

Lee GY, Kenny PA, Lee EH, Bissell MJ (2007). Three-dimensional culture models of normal and malignant breast epithelial cells. *Nat Methods*. 4(4):359-65.

Muthuswamy SK, Li D, Lelievre S, Bissell MJ, Brugge JS (2001). ErbB2, but not ErbB1, reinitiates proliferation and induces luminal repopulation in epithelial acini. *Nat Cell Biol* 3(9):785-92.

Neve RM, Chin K, Fridlyand J, Yeh J, Baehner FL, Fevr T, Clark L, Bayani N, Coppe JP, Tong F, Speed T, Spellman PT, DeVries S, Lapuk A, Wang NJ, Kuo WL, Stilwell JL, Pinkel D, Albertson DG, Waldman FM, McCormick F, Dickson RB, Johnson MD, Lippman M, Ethier S, Gazdar A, Gray JW (2006). A collection of breast cancer cell lines for the study of functionally distinct cancer subtypes. *Cancer Cell* 10(6):515-27.

Park CC, Zhang H, Pallavicini M, Gray JW, Baehner F, Park CJ, Bissell MJ (2006). β 1 Integrin Inhibitory Antibody Induces Apoptosis of Breast Cancer Cells, Inhibits Growth, and Distinguishes Malignant from Normal Phenotype in Three Dimensional Cultures and In vivo. *Cancer Res* 66(3):1526-35

Reginato MJ, Mills KR, Becker EB, Lynch DK, Bonni A, Muthuswamy SK, Brugge JS (2005). Bim regulation of lumen formation in cultured mammary epithelial acini is targeted by oncogenes. *Mol Cell Biol*. 2005 Jun;25(11):4591-601.

Wang F, Hansen RK, Radisky D, Yoneda T, Barcellos-Hoff MH, Petersen OW, Turley EA and Bissell MJ (2002). Phenotypic Reversion or Death of Cancer Cells by Altering Signaling Pathways in Three-Dimensional Contexts. *J. Nat'l Cancer Inst*. 94(19):1494-1503.

Weaver VM, Petersen OW, Wang F, Larabell CA, Briand P, Damsky C, Bissell MJ (1997). Reversion of the malignant phenotype of human breast cells in three-dimensional culture and in vivo by integrin blocking antibodies. *J Cell Biol* 137(1):231-45.

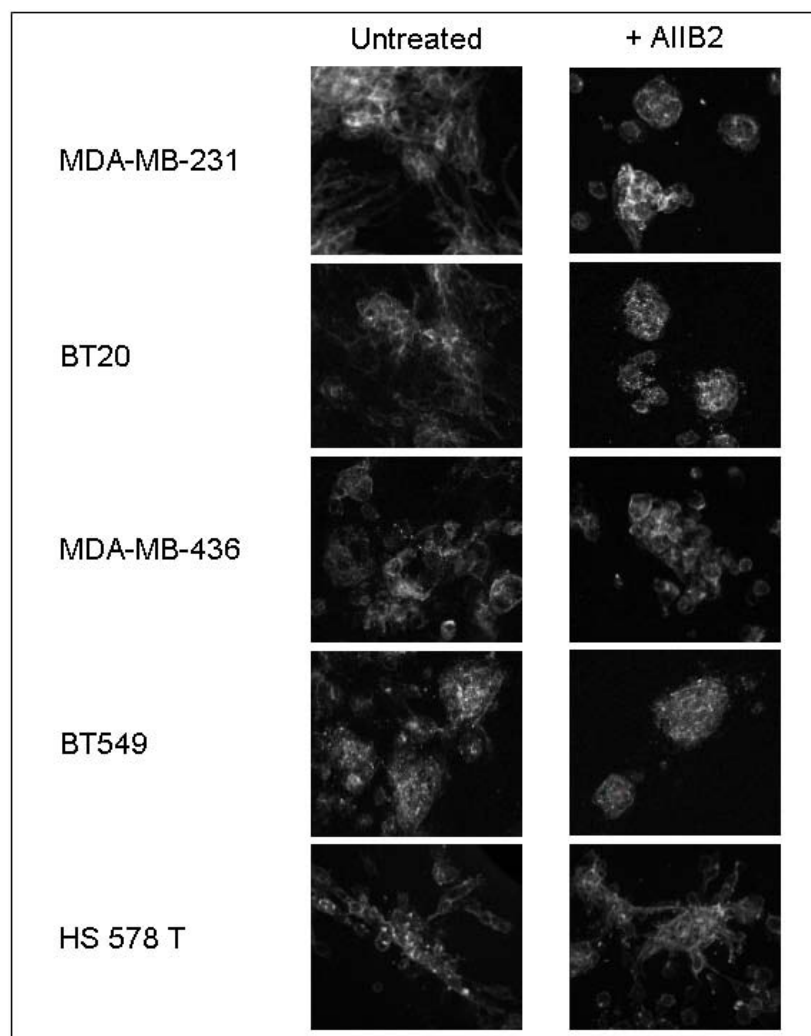
Supporting Data

Figure 1. Three invasive stellate (MDA-MB-231, BT-20, Hs578T) and two grape-like stellate (MDA-MB-436, BT-459) cell lines were treated with AIB2. Z-projections of confocal stacks of F-actin staining are shown. The morphological invasiveness of all cell lines is almost completely inhibited by AIB2, with the exception of Hs578T.

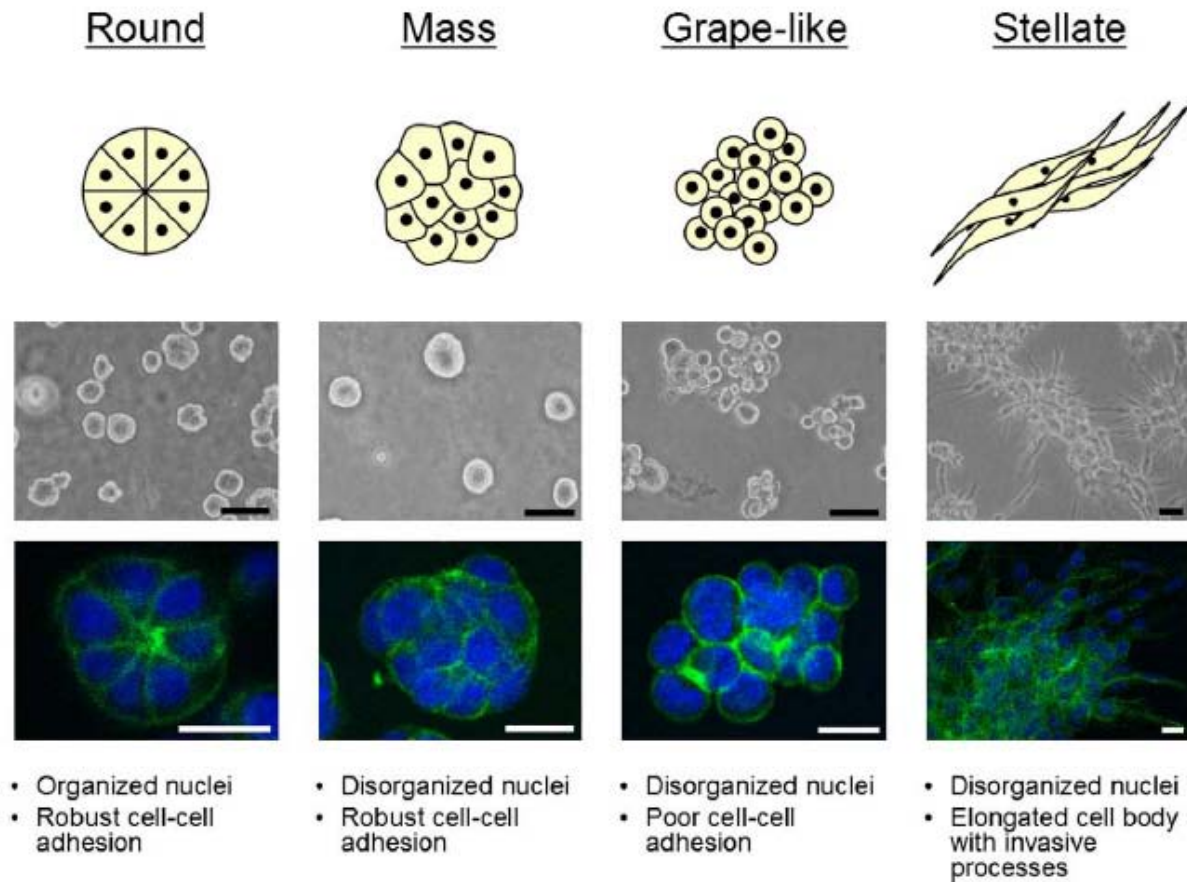


Figure 2. Breast cell line colony morphologies in 3D culture fall into four distinctive groups. A schematic and key descriptors of each morphology is shown in addition to phase contrast and F-actin and nuclear fluorescence images of representative cell lines of each morphology: for Round, S1 is shown; Mass, BT-474; Grape-like, SK-BR-3; and Stellate, MDA-MB-231. Scale bars: phase contrast, 50 μm ; fluorescence, 20 μm .

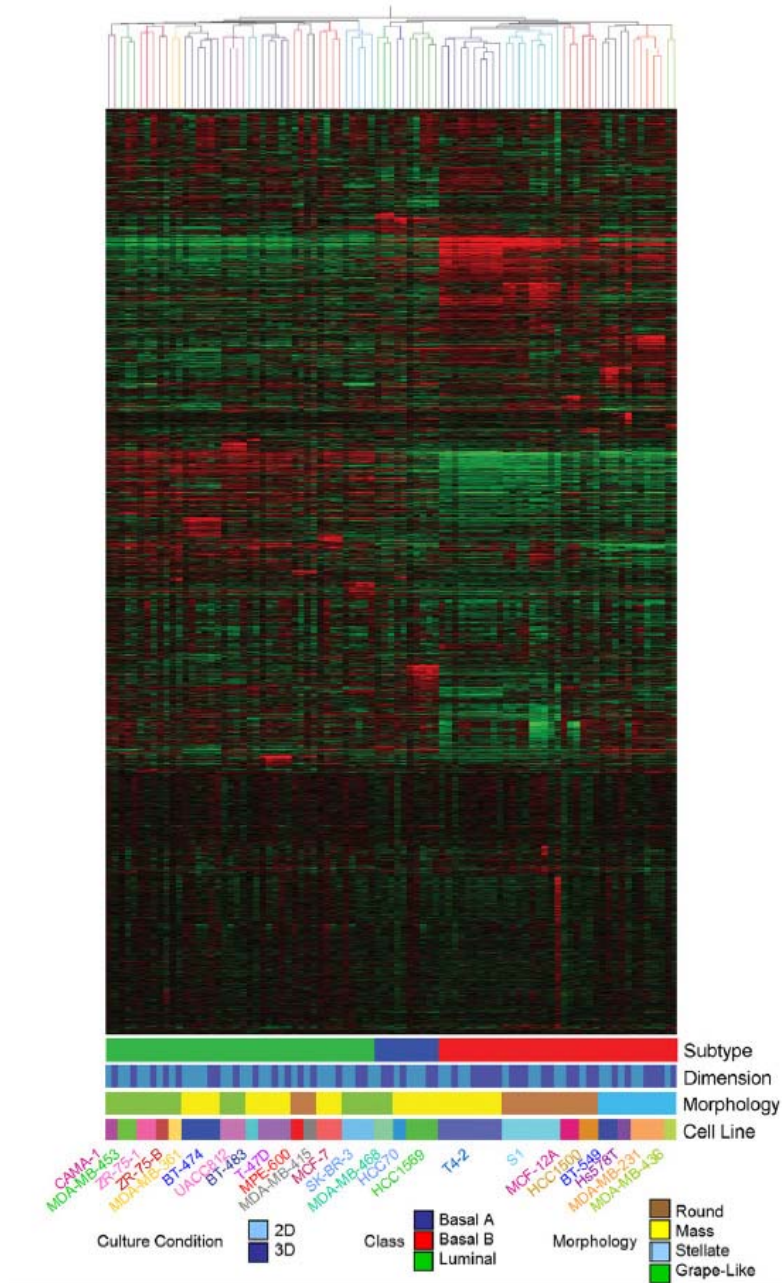


Figure 3. Gene expression profiling of breast cell lines in grown in two and three dimensions. Unsupervised hierarchical clustering of 89 samples representing 24 non-malignant and malignant breast cell lines cultured on either tissue culture plastic (2D) or 3D IrECM (3D). Tree branches are colored to indicate cell line identity (see key on bottom of figure). Also colored in the key are the morphological group and tumor classification to which each cell line belongs.

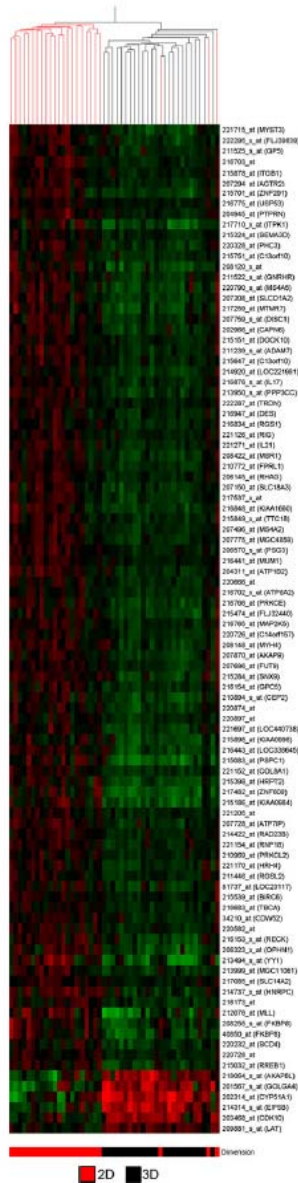


Figure 4. Genes which distinguish 2D and 3D culture conditions. All replicates were averaged so that each condition represents one cell in either 2D or 3D culture. The 22215 Affymetrix probes were tested for association with the parameter, Dimension, using a cutoff of $P < 0.00025$, corrected for multiple comparisons using the Benjamini and Hochberg test. 96 probes significantly distinguished the expression profiles of cells grown on plastic from those grown on IrECM at this level of significance.

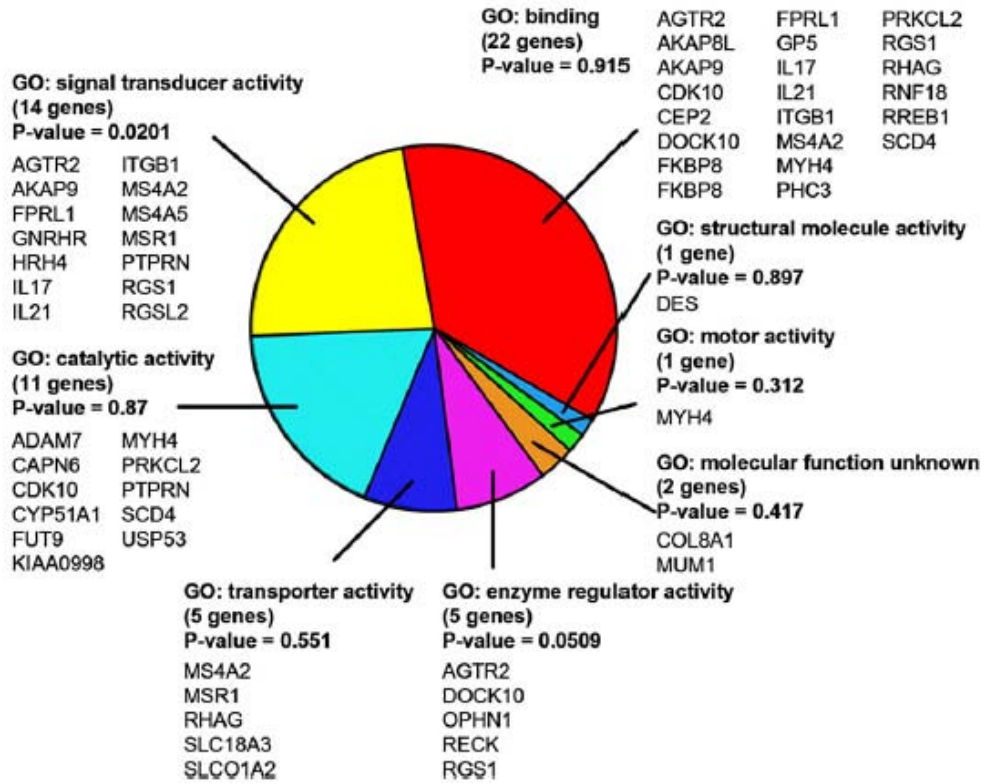


Figure 5. Gene Ontology analysis of the 41 of the 96 genes shown in Figure 4 for which Gene Ontology annotations were available. Genes encoding proteins involved in signal transduction are significantly overrepresented in this set ($P = 0.0201$), while genes encoding proteins involved in the regulation of enzyme activity almost achieved statistical significance ($P = 0.0509$)

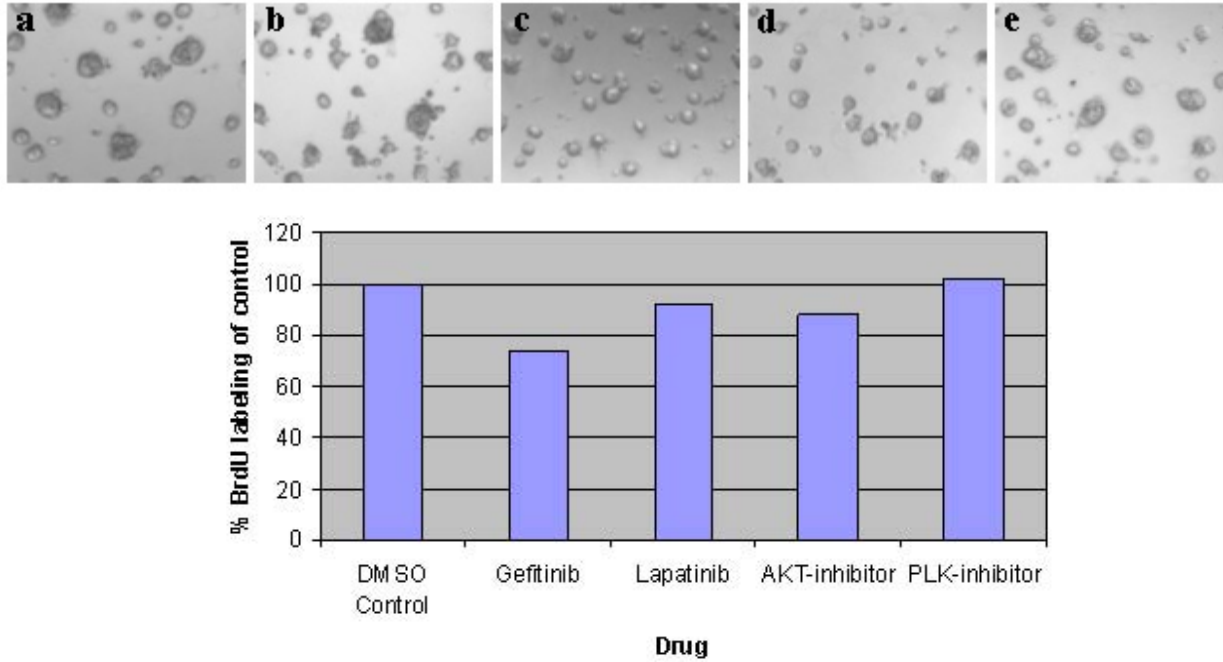


Figure 6. Phase contrast images of BT-20 cells after 48 hours of treatment with: (a) DMSO control, (b) 5 μ M Iressa, (c) 1.5 μ M Lapatinib, (d) 700 nM AKT-inhibitor and (e) 11 nM PLK-inhibitor. (f) Response of BT-20 breast cancer cells to 48 hours of treatment of different inhibitors as measured by BrdU incorporation.

Appendices**Appendix A**

Park CC, Zhang H, Pallavicini M, Gray JW, Baehner F, Park CJ, Bissell MJ (2006). β 1 Integrin Inhibitory Antibody Induces Apoptosis of Breast Cancer Cells, Inhibits Growth, and Distinguishes Malignant from Normal Phenotype in Three Dimensional Cultures and In vivo. *Cancer Research* Feb 1;66(3):1526-35

Appendix B

Lee GY, Kenny PA, Lee EH, Bissell MJ (2007). Three-dimensional culture models of normal and malignant breast epithelial cells. *Nat Methods*. 4(4):359-65.

Appendix C

Kenny PA, Lee GY, Myers CA, Neve RM, Semeiks JR, Spellman PT, Lorenz K, Lee EH, Barcellos-Hoff MH, Petersen OW, Gray JW, Bissell MJ (2007). The morphologies of breast cancer cell lines in three-dimensional assays correlate with their profiles of gene expression. *Molecular Oncology* 1(1):84-96.

β_1 Integrin Inhibitory Antibody Induces Apoptosis of Breast Cancer Cells, Inhibits Growth, and Distinguishes Malignant from Normal Phenotype in Three Dimensional Cultures and *In vivo*

Catherine C. Park,¹ Hui Zhang,³ Maria Pallavicini,⁴ Joe W. Gray,³ Frederick Baehner,² Chong J. Park,⁵ and Mina J. Bissell³

Departments of ¹Radiation Oncology and ²Pathology, University of California, San Francisco, California; ³Life Sciences Division, Ernest Orlando Lawrence Berkeley National Laboratory, Berkeley, California; ⁴School of Natural Sciences, University of California, Merced, California; and ⁵Department of Mathematics and Statistics, San Diego State University, San Diego, California

Abstract

Current therapeutic approaches to cancer are designed to target molecules that contribute to malignant behavior but leave normal tissues intact. β_1 integrin is a candidate target well known for mediating cell-extracellular matrix (ECM) interactions that influence diverse cellular functions; its aberrant expression has been implicated in breast cancer progression and resistance to cytotoxic therapy. The addition of β_1 integrin inhibitory agents to breast cancer cells at a single-cell stage in a laminin-rich ECM (three-dimensional lrECM) culture was shown to down-modulate β_1 integrin signaling, resulting in malignant reversion. To investigate β_1 integrin as a therapeutic target, we modified the three-dimensional lrECM protocol to approximate the clinical situation: before treatment, we allowed nonmalignant cells to form organized acinar structures and malignant cells to form tumor-like colonies. We then tested the ability of β_1 integrin inhibitory antibody, AIB2, to inhibit tumor cell growth in several breast cancer cell lines (T4-2, MDA-MB-231, BT474, SKBR3, and MCF-7) and one nonmalignant cell line (S-1). We show that β_1 integrin inhibition resulted in a significant loss of cancer cells, associated with a decrease in proliferation and increase in apoptosis, and a global change in the composition of residual colonies. In contrast, nonmalignant cells that formed tissue-like structures remained resistant. Moreover, these cancer cell-specific antiproliferative and proapoptotic effects were confirmed *in vivo* with no discernible toxicity to animals. Our findings indicate that β_1 integrin is a promising therapeutic target, and that the three-dimensional lrECM culture assay can be used to effectively distinguish malignant and normal tissue response to therapy. (Cancer Res 2006; 66(3): 1526-35)

Introduction

Development of monoclonal antibody therapies designed to target aberrant cell surface signaling receptors, such as HER-2 and epidermal growth factor receptor (EGFR), have shown great promise in cancer therapy (1, 2). One other class of cell surface receptors that is critical in mediating cell-extracellular matrix

(ECM) interactions is β_1 integrin, a major contributor for growth factor receptor signaling. β_1 integrins belong to a family of heterodimeric transmembrane receptors that transmit biomechanical cues that critically mediate cell-ECM interactions (reviewed in ref. 3). β_1 integrin is aberrantly expressed in human breast carcinomas and has been shown to play a central role in growth, apoptosis, invasion, and metastasis (4–8). In addition to its role in cancer progression, an emerging body of evidence indicates that β_1 integrin signaling plays a significant role in mediating resistance to cytotoxic chemotherapies by enhancing cell survival in hematologic malignancies, lung, and breast cancers (9–12). Inhibition of β_1 integrin has also been shown to abrogate the formation of metastasis in gastric and breast cancer models (13–15). Thus, several aspects of β_1 integrin signaling point to it as a multifaceted target for breast cancer therapy.

Using a three-dimensional lrECM cell culture model, which emulates a more physiologically relevant microenvironment (16), we showed previously that down-modulation of β_1 integrin and growth factor signaling pathways resulted in reversion of the malignant phenotype (17), leading to growth arrest and reformation of tissue polarity (18). In addition, β_1 integrin and growth factor signaling were found to be integrated in the context of the three-dimensional lrECM but not on tissue culture plastic (18, 19).

We reasoned that a modified version of this culture model could provide an accurate surrogate for testing therapies for human breast cancer cells and tumors. We developed the modified three-dimensional lrECM assay and show that inhibition of β_1 integrin results not only in antiproliferative and proapoptotic effects in malignant cell lines in three-dimensional cultures, but that these results were recapitulated also *in vivo*. β_1 integrin inhibition preferentially affected malignant cells both in culture and *in vivo*; the nonmalignant acini and normal tissues were not affected, and remarkably, there was little or no toxicity to the animals.

Materials and Methods

Cell culture. HMT-3522-S1 (S-1) mammary epithelial cells were originally derived from a woman with nonmalignant fibrocystic breast disease (20) and cultured in H14 medium as previously described (17). S-1 cells were propagated on plastic in medium containing 10 ng/mL EGF, and T4-2 cells were grown on collagen type I-coated flasks in the absence of EGF (17). Human breast cancer cell lines MCF-7 and MDA-MB-231 were obtained from the American Type Culture Collection (Manassas, VA), and SKBR-3 and BT474 were a gift from Dr. Joe Gray (University of California in San Francisco, UCSF). Three-dimensional cultures were plated with cells trypsinized from monolayer cultures and plated on top of commercially available matrix produced from Englebreth-Holm-Swarm tumors (Matrigel, Collaborative Research, Waltham, MA). Cell lines were maintained in media described above, conditioned with 5% Matrigel. This assay is distinct from

Note: Supplementary data for this article are available at Cancer Research Online (<http://cancerres.aacrjournals.org/>).

Requests for reprints: Catherine Park, University of California in San Francisco/Mt. Zion Cancer Center, 1600 Divisadero Street H1031, San Francisco, CA 94143-1708. Phone: 415-353-7186; Fax: 415-353-9883; E-mail: park@radonc17.ucsf.edu.

©2006 American Association for Cancer Research.
doi:10.1158/0008-5472.CAN-05-3071

previously published reversion assays that were done with cells completely embedded within Matrigel (17). Cells were plated on day 0. For S-1 cultures, AIB2 was added on day 6 of culture, after acinar formation had occurred. For malignant cell lines, AIB2 was added on day 4 of culture, after cells had undergone several population doublings. All cultures were analyzed after 3 days of AIB2 treatment.

β_1 integrin and HER-2 inhibitory antibodies. AIB2, a β_1 integrin function-blocking antibody (originally a gift from C. Damsky, UCSF) was isolated and prepared from a hybridoma cell line (Sierra Biosources, Milipitas, CA). AIB2 is a rat monoclonal IgG1 that was originally isolated from a human choriocarcinoma hybridoma that specifically binds β_1 integrin extracellular domain (21–23). Experiments using F(ab')₂ fragments of enzyme-digested AIB2 indicated that the epitope-binding portion of the antibody was active and resulted in down-modulation of β_1 integrin-mediated signaling (17, 19). AIB2 was added to culture medium on alternate days. Herceptin is a humanized monoclonal antibody against the erbB2 or HER-2 receptor (24) that was used (20 μ g/mL) to treat SKBR3 cells on day 6. Control cultures for all experiments were treated with the same concentration of nonspecific IgG.

Immunofluorescence. Cells from three-dimensional cultures were fixed onto a glass slide using 4% paraformaldehyde or methanol/acetone. Nonspecific sites were blocked with 0.5% casein/PBS solution for 1 hour at room temperature. Primary β_1 integrin monoclonal rat anti-mouse antibody (PharMingen, San Diego, CA; 1:100) was diluted in blocking buffer and was applied for 1 hour at room temperature in a humidified chamber. Slides were washed in PBS containing 0.1% bovine serum albumin, before incubating in secondary antibody conjugated to FITC (Molecular Probes, Eugene, OR) for 1 hour in a dark humidified chamber at room temperature. The slides were then washed and counterstained with 4',6-diamidino-2-phenylindole before mounting with Vectashield mounting medium (Vector Laboratories, Burlingame, CA).

Confocal microscopy. Confocal images were acquired by using a Zeiss LSM 410 inverted laser scanning confocal microscope equipped with an external argon/krypton laser. Using a Zeiss Fluor $\times 40$ (1.3 numerical aperture) objective, images were captured at the colony midsection. Relative immunofluorescence intensity of images was standardized by comparing only cultures that were processed identically and stained in the same experiment.

Western immunoblot. Cells propagated in three-dimensional IrECM were first treated with ice-cold PBS/EDTA [0.01 mol/L sodium phosphate (pH 7.2) containing 138 mmol/L sodium chloride and 5 mmol/L EDTA] to isolate the cells and then lysed in radioimmunoprecipitation assay buffer as previously described (17). Equal amounts of protein were loaded onto reducing SDS gels. After transfer onto nitrocellulose membrane (Invitrogen, Carlsbad, CA), blots were blocked with 5% nonfat milk and probed. Primary antibodies used include β_1 integrin, clone 18 (1:1,000), phospho-FAK, clone 14 (1:1,000; BD Transduction Laboratories, Lexington, KY); phospho- β_1 integrin (1:1,000; Biosource, Camarillo, CA); β -actin, clone AC-15 (1:5,000; Sigma, St. Louis, MO). Blots were washed, incubated with secondary antibody, and exposed to X-ray film.

Fluorescence-activated cell sorting analysis. Cells were propagated on tissue culture plastic and harvested using 0.25% trypsin. After resuspending in 1 mL DMEM/F-12 media with trypsin inhibitor, cells were spun down and washed in $1 \times$ PBS, 5% fetal bovine serum, and 0.1% sodium azide on ice. Cells were incubated with primary antibody (AIB2, 1:10) at 4°C for 30 minutes to 1 hour, washed, and incubated with a fluorescein-conjugated IgG secondary antibody (1:100) for 30 minutes. After washing, 1 mL of 1% paraformaldehyde solution was added to the pellet and suspended immediately. Cells were analyzed using a Beckman-Coulter EPICS XL-MCL Analyzer. System II Data Acquisition and Display software, version 2.0 was used for data analysis.

Apoptosis and proliferation assays. Apoptosis was assayed in cell culture using a commercially available kit (In Situ Cell Death Detection kit, fluorescein; Roche, Nutley, NJ) designed to detect terminal deoxynucleotidyl transferase (TdT)-mediated nick end labeling (TUNEL). Cells were fixed in 4% paraformaldehyde and permeabilized in cold 0.1% Triton X-100 in 0.1% sodium citrate. After washing in PBS, cells were incubated in

TUNEL reaction mixture at 37°C for 60 minutes, washed, and mounted. Proliferation was detected by indirect immunofluorescence of Ki-67 nuclear antigen. Cells were fixed in methanol/acetone and blocked using 10% goat serum, then incubated in primary rabbit antibody against Ki-67, clone MIB-1 (1:200; Novocastra Laboratories, Norwell, MA) for 1 hour and washed before FITC-conjugated anti-rabbit secondary antibody (The Jackson Laboratory, Bar Harbor, ME) was applied. Nuclei were counterstained with DAPI.

For assay of apoptosis in paraffin-embedded tissues, Apoptag In Situ Apoptosis Detection kit (Intergen, Burlington, MA) was used to detect TUNEL reaction. Paraffin-embedded xenograft tumors were sectioned at 5- to 10- μ m-thick sections. Sections were deparaffinized and rehydrated using xylene and ethanol washes. Tissues were then treated with proteinase K at room temperature, washed, and quenched using 3% hydrogen peroxide. Buffer solution was applied, and sections were incubated in TdT enzyme at 37°C for 1 hour. Stop/wash buffer was used before anti-digoxigenin peroxidase conjugate was applied. Proliferation was assayed in paraffin-embedded tissues using indirect immunohistochemistry. Sections were deparaffinized as above and blocked using 10% normal horse serum, then incubated with mouse monoclonal antibody against Ki-67 (Oncogene, San Diego, CA) overnight at 4°C, and washed in PBS. They were then serially incubated with biotinylated anti-mouse antibody, and streptavidin-horseradish peroxidase and 3,3'-diaminobenzidine (DAPI) medium. After counterstaining with hematoxylin, sections were dehydrated in serial concentrated ethanol and xylene and mounted. Cells were scored by counting the total number of nuclei in five high-power microscopic fields ($\times 40$) using a $\times 10$ objective, or a minimum of 200 nuclei per tumor section.

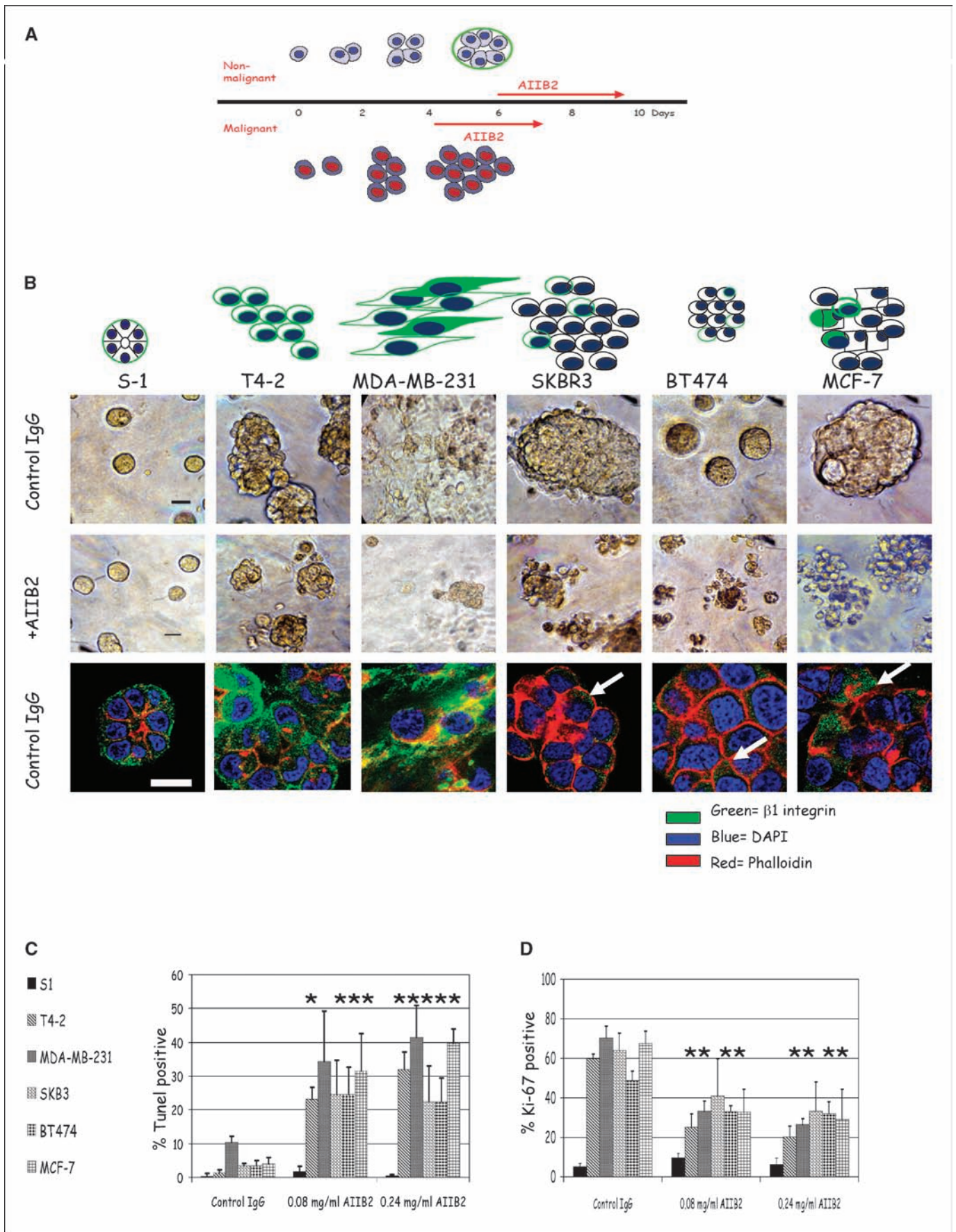
Tumor growth and toxicity assessment *in vivo*. Female nu^{-/-} mice were obtained from Charles River (Wilmington, MA) or Taconic (Germantown, NY) and housed five per cage with chow and water *ad libitum* in a controlled animal barrier. Animals were injected s.c. with 5 to 10 $\times 10^6$ T4-2 cells or 10⁷ MCF-7 cells into the upper back posterior to the right front limb. Estradiol pellets were inserted s.c. above the tail for animals bearing MCF-7 xenografts. AIB2 antibody or nonspecific rat IgG was injected into the i.p. cavity biweekly beginning on day 4 or day 28 after cell implantation. Tumor dimensions (width, height, and depth) were measured biweekly. At the time of sacrifice, animals were euthanized, and tumors were harvested and either immediately frozen in ornithine carbonyl transferase or fixed in formalin. Serum was collected using cardiac puncture techniques.

Animals were monitored for evidence of toxicity by measuring weight, assessing overall activity, and necropsy. Additional toxicity studies were done using β_1 integrin inhibitory antibody, clone Ha 2/5 (PharMingen), which specifically recognizes murine β_1 integrin. Antibody was administered at doses of 1 to 20 mg/kg biweekly over 4 weeks. All experimental procedures were followed according to the UCSF, and LBNL Animal Welfare Committees approved policies and guidelines.

Statistical analysis. For each dose of AIB2 or control IgG in culture, pairwise differences in Ki-67 or TUNEL were tested among the six cell lines using Student's *t* test (25). Multivariate ANOVA was used for analysis of tumor volume at each time point. For each dose of AIB2 or control IgG *in vivo*, pairwise Student's *t* test or χ^2 comparison was used to analyze differences between TUNEL and Ki-67 expression. MINITAB (Minitab, Inc., State College, PA) statistical software was used for all calculations.

Results

β_1 integrin inhibition results in cytostasis and apoptosis in breast cancer cell colonies treated in three-dimensional cultures. We showed previously that down-modulation of β_1 integrin downstream signaling pathways in *single* cancer cells embedded within three-dimensional IrECM was associated with phenotypic reversion, exemplified by growth arrest and acinar differentiation (17, 26), whereas *single* nonmalignant mammary epithelial cells underwent apoptosis (27). We sought to explore whether there is a role for β_1 integrin as a molecular target in



breast cancer, which relies on the differential response between normal and malignant tissues. In patients, tumors are commonly discovered *after* a multicellular three-dimensional tumor has already been formed, and normal cells are found in an organized three-dimensional context. We reasoned that this scenario could be emulated also in the three-dimensional lrECM assay. In addition, we wanted to know whether we could then distinguish between the response of normal and malignant structures. Accordingly, we modified the three-dimensional lrECM assay to test these concerns.

When cultured on top of three-dimensional lrECM gels with 5% Matrigel conditioned media, nonmalignant breast cells undergo morphogenesis and, after 6 days, form acini with polarized cells oriented around a central lumen with a well organized basement membrane, recapitulating normal acinar structures found *in vivo* (Fig. 1A; for review, see ref. 28). In contrast, all malignant breast cell lines tested (T4-2, MDA-MB-231, SKBR3, BT474, and MCF-7) continued to proliferate and formed disorganized tumor colonies (Fig. 1A). Our previous studies have shown that β_1 integrin inhibitory monoclonal antibody, AIIB2, or its F(ab')₂ fragments applied to single cells were capable of down-modulating β_1 integrin signaling pathways (17, 19). In the present studies, breast cancer cell lines were propagated in three-dimensional lrECM until colonies were formed (4 days) and were then treated with AIIB2 at doses ranging from 0.08 to 0.24 mg/mL, or with isotype-matched nonspecific rat IgG1 as control (Fig. 1B). Using confocal microscopy, we show that β_1 integrin was appropriately localized to the basolateral surfaces of the S-1 cells within the acini, as is the case *in vivo*. In contrast, it was diffusely distributed around the surfaces of each cell within T4-2 and MDA-MB-231 colonies in three-dimensional lrECM, and little expression was seen on three of the other cell lines (Fig. 1B).

In assays starting from single cells, AIIB2 concentrations of 0.10 to 0.16 mg/mL were sufficient to induce reversion (17, 19). In the current procedure, colonies were analyzed for percentage of proliferating cells using Ki-67 nuclear antigen and for apoptosis by TUNEL assay. After 3 days of treatment, all but one of the malignant cell lines showed a significant proportional decrease in the percentage of proliferating cells (46-54% of Ki-67 expressing cells at 0.08 mg/mL AIIB2 and 0.24 mg/mL AIIB2, respectively; $P < 0.02$, Student's *t* test for any AIIB2 dose compared with controls for T4-2, MDA-MB-231, BT-474, and MCF-7; Fig. 1C). The only exception among the five malignant cell lines was SKBR3, which did not show a significant decrease in the percentage of Ki-67-positive cells with AIIB2 treatment. Apoptosis was assayed simultaneously: there was a dramatic increase in TUNEL-positive nuclei for all malignant cell lines (85-88% at 0.08 mg/mL AIIB2 and 0.24 mg/mL AIIB2, respectively; Fig. 1D; $n = 3$). For the MDA-MB-231 cell line, the higher dose of AIIB2 was associated with a statistically significant increase in TUNEL-positive nuclei, whereas the *P* approached significance for the lower dose (hence the absence of the *).

In contrast, the nonmalignant cell line S-1 formed acinar structures when cultured on top of three-dimensional lrECM for 6 days and, unlike colonies made of malignant cells, did not undergo increased apoptosis or cytostasis upon addition of AIIB2 regardless of the dose used (Fig. 1C and D). Similar results were obtained for S-1 cells treated at day 4 (data not shown). In addition, there was no significant change in the distribution of the size or number of total colonies (data not shown). Previous studies have shown that AIIB2 applied to single S-1 cells induce apoptosis (27); however, in the present study, we show that when S-1 cells are in the context of organized structures, they are resistant to apoptosis. This indicated that the signaling context of β_1 integrin is critical to response to AIIB2 treatment: nonmalignant mammary epithelial cells with intact cell-cell and cell-ECM interactions were resistant to the inhibitor. These results confirm and extend studies of conventional apoptotic and chemotherapeutic agents tested previously in the single-cell assay in three-dimensional lrECM (29).

Coexpression of total β_1 integrin, phosphorylated β_1 integrin, and phosphorylated ³⁹⁷FAK among breast cell lines cultured in three-dimensional lrECM. β_1 Integrin expression detected by immunofluorescence was characterized by basolateral localization in nonmalignant S-1 acinar structures and disorganized and aberrant expression in the malignant cell lines. To further characterize β_1 integrin expression, we analyzed cell lysates for total β_1 integrin levels using Western immunoblotting. Total β_1 integrin expression corresponded to that detected using immunofluorescence; three cell lines (S-1, T4-2, and MDA-MB-231) showed relatively higher levels of β_1 integrin compared with SKBR3, BT474, and MCF-7 (Fig. 2A). In addition, fluorescence-activated cell sorting (FACS) analysis confirmed the surface expression of β_1 integrin reflected that detected using immunofluorescence and Western blot (Fig. 2B). We concluded that β_1 integrin expression was variable, and response to β_1 integrin inhibitory antibody did not seem to correlate with total levels of β_1 integrin expression in individual cell lines.

We reasoned that signaling proteins that are critical in β_1 integrin signaling, such as phosphorylation of β_1 integrin cytoplasmic tail (30), or focal adhesion kinase (FAK; refs. 31, 32), may correlate with response to AIIB2 treatment. To test this, protein lysates from the six cell lines propagated in three-dimensional lrECM were used to detect relative coexpression of β_1 integrin, phosphorylated β_1 integrin (p- β_1 integrin), and phosphorylated ³⁹⁷FAK (p-³⁹⁷FAK). We found that p- β_1 integrin levels were relatively lower in S-1, T4-2, and MDA-MB-231 cells compared with SKBR3, BT474, and MCF-7 cell lines, which inversely correlated with total β_1 integrin levels (Fig. 2A). p-³⁹⁷FAK levels did not seem to correlate with total β_1 integrin or p- β_1 integrin levels. Interestingly, p-³⁹⁷FAK levels were lowest in SKBR3 cells, which were refractory to AIIB2-induced cytostasis.

SKBR3 colonies respond to a combination of AIIB2 and Herceptin. The SKBR3 cell line overexpresses erbB2 (HER-2), a

Figure 1. Morphology and response of breast cell lines to β_1 integrin inhibition in three-dimensional lrECM. Five malignant breast cell lines (T4-2, MDA-MB-231, SKBR3, BT474, and MCF-7) and one nonmalignant breast cell line (S-1) were propagated in three-dimensional lrECM and treated with β_1 integrin inhibitory antibody, AIIB2, after colonies were formed. *A*, schema of the three-dimensional lrECM assay used in this study. *B*, *top* and *middle*, phase-contrast micrographs of cultured colonies before and after antibody treatment, respectively. Bar, 20 μ m. *Bottom*, confocal midsections of β_1 integrin immunofluorescence (green) of colonies cultured in three-dimensional lrECM. Phalloidin was used to stain actin filaments (blue), and DAPI was used to stain individual nuclei (red). Bar, 13 μ m for all cell lines shown. *C*, whereas there were no significant changes in Ki-67 or TUNEL expressing cells among nonmalignant S-1 cells after β_1 integrin inhibition, malignant cell lines, except SKBR3, had a significant decrease in Ki-67 expressing cells and a significant increase in TUNEL-positive cells after antibody treatment. Columns, mean ($n = 3$); bars, SE. $P < 0.05$, *t* test.

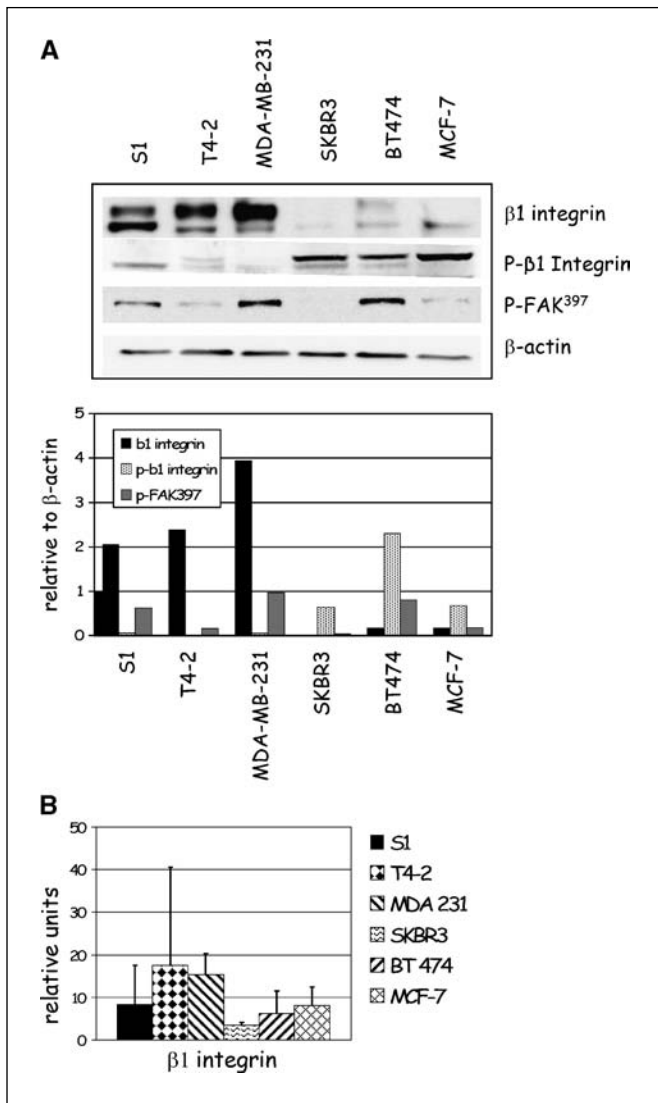


Figure 2. β_1 Integrin, p- β_1 integrin, and p-³⁹⁷FAK are expressed at different levels in breast cell lines in three dimensions. Lysates from five breast cancer cell lines (T4-2, MDA-MB-231, SKBR3, BT474, and MCF-7) and one nonmalignant cell line (S-1) in three-dimensional IrECM were probed by Western immunoblotting for total and p- β_1 integrin and p-³⁹⁷FAK and for surface β_1 integrin expression by FACS analysis. **A**, total β_1 integrin levels are relatively high in S-1, T4-2, and MDA-MB-231 cells compared with SKBR3, BT474, and MCF7 cells. Conversely, p- β_1 integrin levels are relatively low in S-1, T4-2, and MDA-MB-231 cells compared with SKBR3, BT474, and MCF7 cells. Expression of p-³⁹⁷FAK is expressed among all cell lines except SKBR3, where it is undetectable by Western blots. **B**, surface expression of β_1 integrin by FACS analysis corresponds to that seen by immunofluorescence (Fig. 1B) and Western blots (Fig. 1A).

member of the EGF family of growth factor receptors. β_1 integrin has been shown to cooperate with other members of the EGF family, such as erbB1 (19); however, the relationship between HER-2 and β_1 integrin signaling is not well understood. We reasoned that HER-2 signaling was one factor that could contribute to the decreased cytostatic response of SKBR3 cells treated with AIIB2. Herceptin is a monoclonal antibody directed against HER-2 and has a significant role in treatment of patients with HER-2 overexpressing breast cancer (33). Therefore, we tested the effect of Herceptin and AIIB2 in combination in SKBR3 cells. Compared with colonies treated with nonspecific

control IgG, SKBR3 colonies treated with AIIB2 or Herceptin alone showed a proportional decrease in Ki-67-positive cells (44.8% for AIIB2 and 39.1% for Herceptin). However, colonies that were treated with both AIIB2 and Herceptin had an augmented proportional decrease in Ki-67-positive cells (68.8%; $P < 0.05$, χ^2 ; Supplementary Fig. S1).

β_1 integrin inhibition preferentially affects larger tumor masses with a global redistribution in colony size and morphology. To determine the effect of treatment on the colony population as a whole, we counted the total number of cells and then scored for individual colonies by size. Using T4-2 cells as a prototype, we found that β_1 integrin inhibition resulted in a significant decrease in total cell number (Fig. 3A, mean \pm SE; $P < 0.05$, χ^2). To further examine how the treatment influenced the global composition of colonies in the population, we counted the number of cells within each colony after 3 days of treatment. The mean colony size decreased from 12 to 6 cells with treatment reflected by the distribution of the size of colonies (Fig. 3B, mean \pm

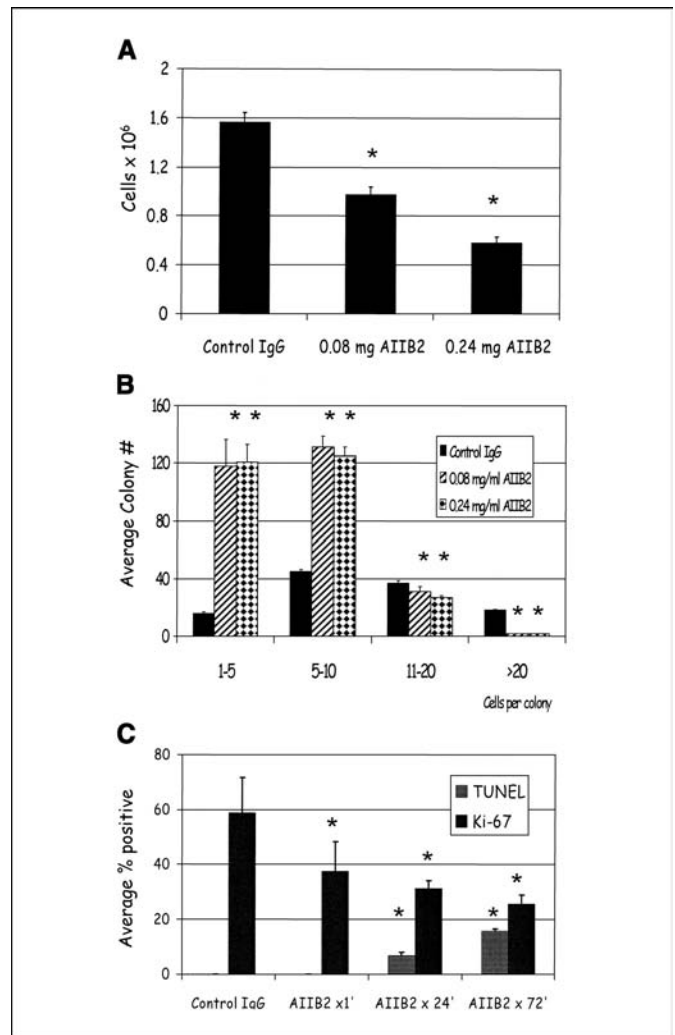
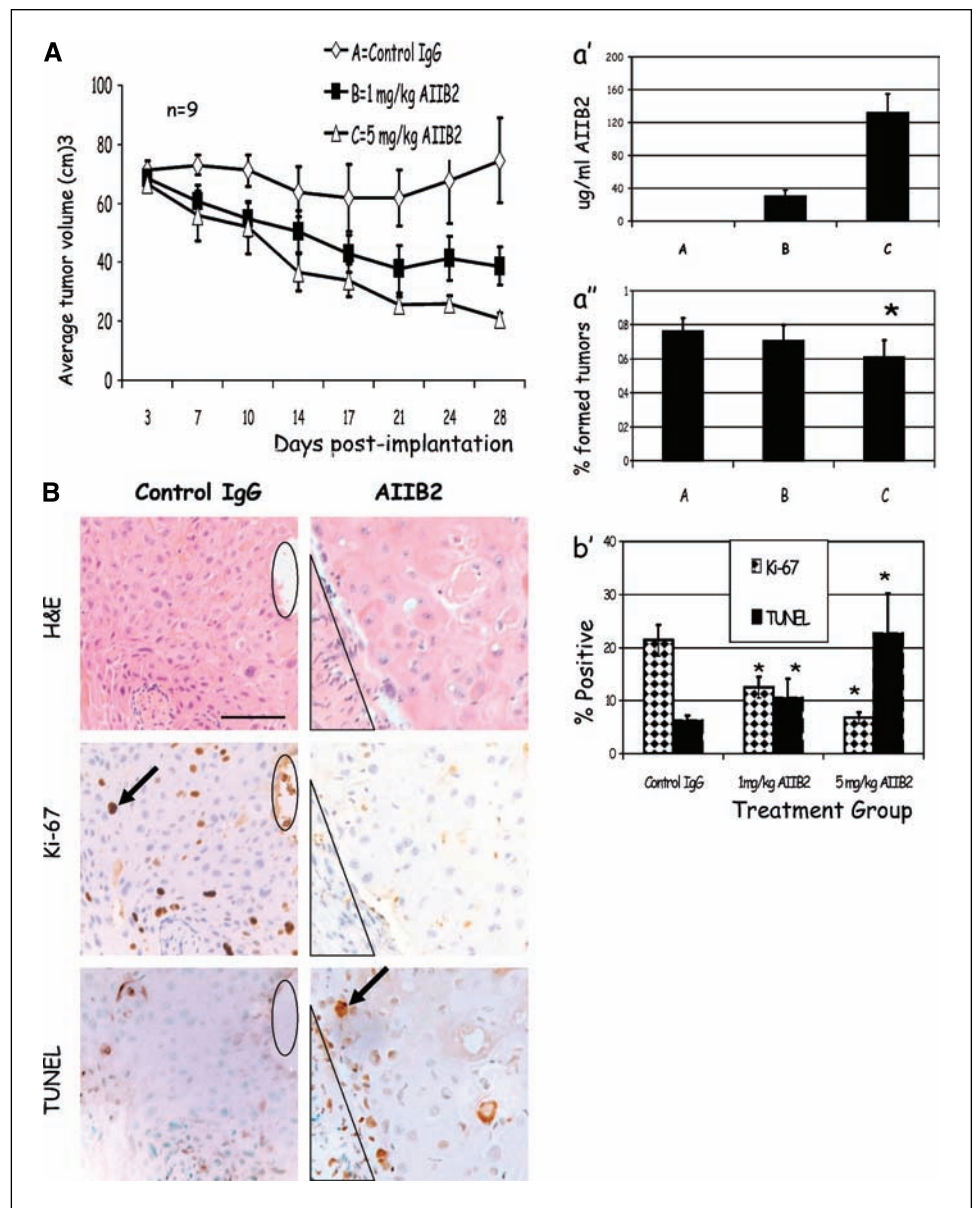


Figure 3. AIIB2 reduces both total cell number and average colony size in malignant cell lines. **A**, average number of T4-2 cells after 3 days of treatment with AIIB2. Columns, mean; bars, SE. $P < 0.05$, χ^2 . **B**, histogram showing the average colony size decreased with AIIB2 compared with controls. Columns, mean; bars, SE. $P < 0.05$, t test. **C**, percentage of Ki-67 and TUNEL expressing nuclei among T4-2 cells 1, 24, and 72 hours after addition of AIIB2 to cultures. Columns, mean; bars, SE. $P < 0.05$, t test.

Figure 4. AIIB2 suppresses tumor growth *in vivo* by enhancing apoptosis and decreasing proliferation. **A**, mean tumor volumes among animals that received 1 mg/kg AIIB2 (■) or 5 mg/kg AIIB2 (△) were significantly smaller than control animals (◆). Points, mean ($n = 9$); bars, SE. **A'**, average serum concentration ($\mu\text{g/mL}$) of AIIB2 at the time of sacrifice was significantly higher in animals receiving AIIB2 compared with control vehicle. Columns, mean; bars, SD. **A''**, average number of animals in each treatment group that had histologic evidence of tumor at the time of sacrifice was significantly lower among treated animals compared to controls. Columns, mean for three separate experiments; bars, SE. *, $P < 0.03$, χ^2 . **B**, micrographs of serial sections of tumors that were scored for apoptosis by the presence of TUNEL-positive nuclei and for proliferation by the presence of Ki-67 nuclear antigen. Black ovals and triangles, coregistered regions in serial sections; arrows, examples of positive staining. **B'**, with AIIB2 treatment, the average number of TUNEL nuclei increased, and the number of Ki-67-positive nuclei decreased. Columns, mean; bars, SE. *, $P < 0.05$, χ^2 . Bar, 247 μm .



SE; $P < 0.05$, t test). Similar results were seen for all other cancer cell lines (data not shown). To investigate the time course and mechanism of these changes, we counted the average number of Ki-67- and TUNEL-positive nuclei in the T4-2 cultures as a function of time after addition of AIIB2 (Fig. 3C, mean \pm SE; $P < 0.05$, t test). The number of proliferating cells decreased dramatically even within 1 hour after addition of AIIB2, indicating an immediate growth arrest. The percentage of TUNEL-positive nuclei increased from 24 to 72 hours.

Treatment with AIIB2 results in decreased tumor formation, increased apoptosis, and cytostasis *in vivo*. We have shown previously that breast cancer cells that have been pretreated with β_1 integrin inhibitors before injection into nude mice have decreased ability to form tumors *in vivo* (17, 26). To determine the efficacy and optimal dose of AIIB2 that effectively inhibits tumor formation *in vivo*, we tested the ability of AIIB2 to inhibit untreated T4-2 cells to form tumors in adult female

$nu^{-/-}$ mice. Animals were implanted with 5 to 10×10^6 T4-2 cells or 10^7 MCF-7 cells either s.c. or into the mammary fat pad on day 0. Three groups of mice ($n = 9$) received biweekly i.p. injections of (a) isotype-matched nonspecific rat IgG1, (b) 1 mg/kg AIIB2, or (c) 5 mg/kg AIIB2 in a blinded fashion beginning on day 4. Tumors were measured biweekly, and volume was estimated by multiplying width \times length \times depth. Compared with tumors propagated in animals that received control IgG, there was a significant dose-dependent decrease in the volume of treated tumors (Fig. 4A) and in the number of animals harboring tumors (Fig. 4A'; $P < 0.03$, χ^2). After 4 weeks, animals were sacrificed, serum was analyzed for AIIB2 levels, and tumors were analyzed for histology. Compared with controls, treated animals had a dose-dependent level of AIIB2 detectable in serum samples (Fig. 4A'', mean \pm SE; $P < 0.05$, χ^2). Representative micrographs of the same coregistered region of a tumor stained with H&E, Ki-67, and TUNEL are shown (Fig. 4B).

Sections from each tumor were evaluated for apoptosis by TUNEL assay and proliferation by Ki-67 (Fig. 4B). Compared with controls, treated tumors had significantly decreased percentage of Ki-67-positive cells and a significantly increased level of TUNEL-positive nuclei (mean \pm SE; $P < 0.05$, χ^2). In addition, tumors treated with 5 mg/kg AIIB2 had significantly higher percentage of caspase-3-positive cells ($11 \pm 2\%$) compared with controls ($3.13 \pm 0.7\%$; $P < 0.05$, χ^2). Similar results were obtained for MCF-7 xenografts treated with AIIB2 *in vivo* (data not shown).

AIIB2 is effective against established tumors *in vivo*. To further evaluate the efficacy of AIIB2 *in vivo*, we allowed MCF-7 cells to continue to grow for ~ 4 weeks and then randomized animals to receive nonspecific rat IgG1, 1 mg/kg AIIB2, or 5 mg/kg AIIB2 for four additional weeks. Compared with controls, treated animals had significantly less tumor growth (Fig. 5A). In addition, histologic analysis showed that treated tumors had significantly fewer Ki-67-positive cells compared with controls (Fig. 5B, mean \pm SE; $P < 0.001$, χ^2) and significantly decreased TUNEL-positive nuclei (Fig. 5B, mean \pm SE; $P < 0.01$, χ^2). Similar results were found for T4-2 xenografts treated *in vivo* (data not shown).

There is no discernible toxicity with β_1 integrin inhibition *in vivo*. Animals were monitored for any signs of toxicity by measuring weekly weight and assessing activity and general appearance. There was no difference in animal weight between the treated or control groups (Fig. 5C), and no discernible toxicity among any groups, up to AIIB2 doses of 20 mg/kg administered biweekly over 4 weeks (data not shown).

Although AIIB2 seems to cross react with murine β_1 integrin,⁶ we sought to further evaluate the potential toxicity of broad β_1 integrin inhibition *in vivo*. Therefore, we used clone Ha2/5, a β_1 integrin function-blocking antibody that recognizes murine β_1 integrin. Adult female *nu^{-/-}* mice were treated with serially increasing doses of antibody from 1 to 20 mg/kg over 4 weeks via biweekly i.p. injection. There were no differences in body weight, activity, overall appearance, or examination at necropsy among animals receiving antibody compared with controls, and no evidence of toxicity among any groups (data not shown).

Discussion

Recent advances in cancer therapy have taken advantage of the aberrant receptors in tumor cells to inhibit growth and enhance the efficacy of conventional cytotoxic treatments (2). β_1 Integrin belongs to a class of cell surface receptors that not only facilitates growth factor receptor signaling but also plays diverse roles in mediating multiple aspects of malignant cell behavior. Indeed, expression of β_1 integrin was shown recently to be necessary for formation of mammary tumors in engineered murine models (4). In addition, β_1 integrin has been shown to enhance survival by mediating resistance to cytotoxic treatment in several cancers (9, 34). The success of any therapy depends on its ability to distinguish between malignant and normal tissues or the therapeutic index. Taking advantage of the modified three-dimensional lrECM culture assay, we show that β_1 integrin inhibitory monoclonal antibody effectively distinguishes between normal and malignant tissue structures. Treatment of malignant

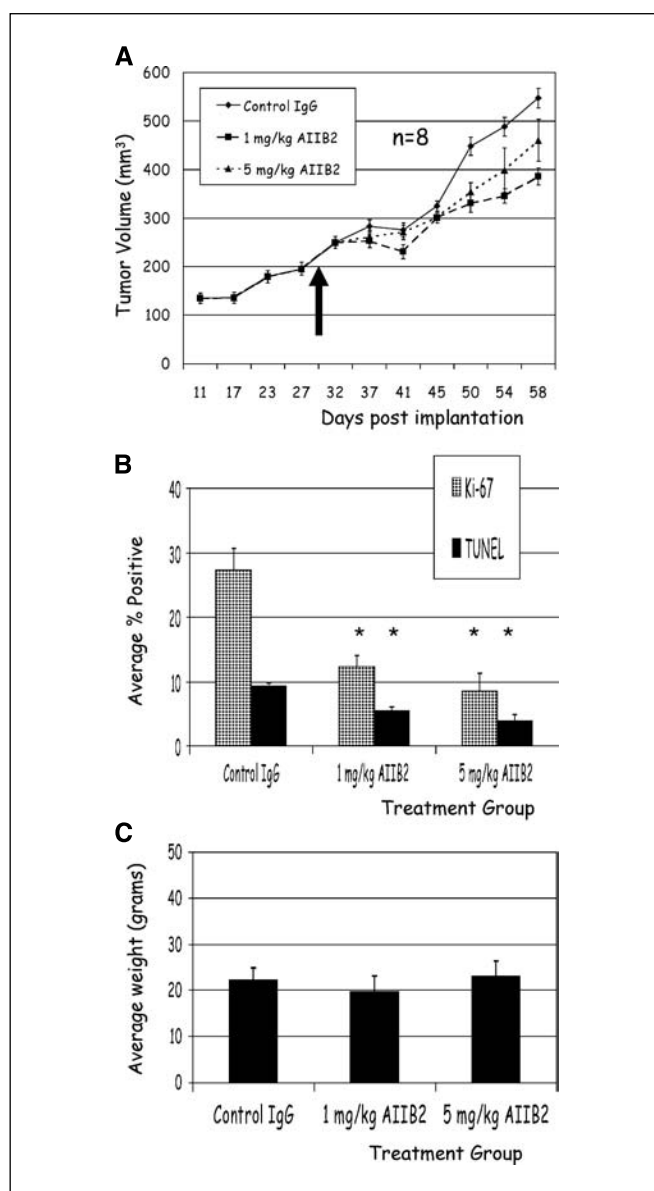


Figure 5. AIIB2 effectively induces cytostasis in established MCF-7 tumors *in vivo* with no toxicity. **A**, animals were randomized to receive treatment or control IgG 4 weeks after MCF-7 cell implantation (arrow, time of randomization at day 30). Mean tumor volumes for animals receiving 1 mg/kg AIIB2 (■) and 5 mg/kg AIIB2 (△) and nonspecific rat IgG1 (◆). Points, mean ($n = 8$); bars, SE. **B**, compared with controls, tumors from animals that received AIIB2 treatment had significantly fewer Ki-67-positive nuclei and fewer TUNEL-positive nuclei. Columns, mean; bars, SE. *, $P < 0.001$, χ^2 . **C**, average weight of control animals, and animals that received AIIB2 treatment were not significantly different at any biweekly time point measured throughout the experiment (data not shown) and at the end of the experiment. Columns, mean; bars, SE.

colonies with AIIB2 resulted in a dramatic loss in total cell number with a concomitant decrease in proliferation and increase in apoptosis. In addition, there was a global redistribution in the malignant colony size and morphology, reflected by a decrease in mean colony size. In contrast, nonmalignant epithelial cells that were capable of forming organized and polar structures with appropriate cell-ECM interactions remained intact and were resistant to β_1 integrin inhibition. *In vivo*, AIIB2 treatment inhibited tumor growth with an associated decrease in proliferation and increase in cell death in early

⁶ Unpublished data.

treated tumors and a decrease in proliferation in treatment of established tumors, with no measurable toxicity to the host. Overall, these results indicate that β_1 integrin inhibition is a potentially viable therapeutic approach in the treatment of breast cancer.

The use of three-dimensional cultures provides a physiologically relevant context in which to emulate cells *in vivo* (35, 36) and has been used previously to investigate novel mechanisms of drug resistance in cancer cells that are demonstrable specifically only in a three-dimensional setting when the appropriate basement membrane molecules are present (37, 38). To model the differences between normal and malignant tissues, we took advantage of the ability of a nonmalignant cell line, HMT-3522-S-1, to undergo normal morphogenesis in three-dimensional lrECM, in contrast to malignant cells that continue to form disorganized invasive colonies. This allowed us to examine the effects of β_1 integrin inhibition on the morphology of cancer cell colonies as a population and to distinguish the potential effects on nonmalignant acini. We had shown previously that nonmalignant cells that were treated with β_1 integrin inhibition as single cells were susceptible to apoptosis (27, 39). However, the response of cells within acinar-like tissue structures where β_1 integrin function is relatively intact has not been investigated. We found that in response to 3 days of AIB2 treatment, all but one malignant cell line in three-dimensional lrECM showed a dramatic loss in total number of cells, coupled with a significant increase in the percentage of apoptotic cells and a significant decrease in the percentage of proliferating cells. In contrast, S-1 cells that formed polar acinar-like structures were entirely resistant to AIB2. These results indicate that most malignant cells that form colonies in three-dimensional lrECM rely on β_1 integrin signaling for proliferation and survival, whereas in the context of an organized structure, cells were either no longer dependent on β_1 integrin signaling for survival, or that β_1 integrin was not accessible to the antibody.

Further analysis of cell cultures during and after AIB2 treatment revealed that the largest cancer cell colonies were being affected, resulting in a global change in the morphology and distribution of proliferating cells, reflected in a decrease in mean colony size. This pattern of multiple residual "tumor foci" was seen also *in vivo* (data not shown). The morphologic characteristics of these clones were distinctly different from the untreated tumors, as were features of cell-cell and cell-ECM interactions. These results have implications for clinical treatment. β_1 Integrin has been implicated in mediating resistance to cytotoxic chemotherapies (9, 10), and inhibition of different tumor types may enhance response by abrogating resistance. In addition, ionizing radiation was shown to up-regulate β_1 integrin in cancer cells (40, 41), and our preliminary studies of β_1 integrin inhibition combined with ionizing radiation are promising and may lead to novel strategies for combinatorial therapies to eradicate or further reduce tumor viability *in vivo*.

Several promising biological therapies aimed at signaling pathways have entered clinical trials; however, despite evidence of response to treatment, useful biomarkers have frequently been difficult to validate (1, 42, 43). For example, the current treatment of cancers with EGFR inhibition illustrates the complexity of some molecular targets and the lack of robust predictive markers that would aid in the selection of individuals for treatment (42). The mechanisms that are involved in cytostasis and apoptosis associated with β_1 integrin inhibition in malignant cells are likely

to involve interactions between multiple signaling pathways. For example, our previous studies have shown that β_1 integrin signaling pathway integrates and cooperates with the EGFR signaling pathway via mitogen-activated protein kinase and phosphatidylinositol 3-kinase (18, 19). In the present study, we found that β_1 integrin expression on the six breast cell lines used was variable. We probed the cell lines for p- β_1 integrin and p-³⁹⁷FAK to investigate potential markers for β_1 integrin signaling activity. Interestingly, p- β_1 integrin expression was inversely correlated with total β_1 integrin, suggesting that either species is required for β_1 integrin signaling to occur. Although p-³⁹⁷FAK is a requisite protein for focal adhesion formation, its role in β_1 integrin signaling in the context of the cell lines we investigated remains unclear. We recognize that β_1 integrin signaling involves several steps, including activation, heterodimerization, ligand binding, and clustering (44, 45); these functional aspects of β_1 integrin signaling activity may not be reflected by the level of receptor expression and/or status of any single signaling protein alone. The major factor that distinguished the nonmalignant S-1 cells and the malignant cell lines is the organization and polarity of β_1 integrin localization, indicating that the context of signaling may be the most important feature that enhances the therapeutic window. Studies are ongoing to investigate which pathways may be the most robust predictors of response in to β_1 integrin inhibition in the clinical setting.

SKBR3 cells were less responsive to β_1 integrin inhibition compared with other cancer cell lines. This cell line is characteristically devoid of E-cadherin and overexpresses growth factor receptor HER-2 features that could contribute to uncoupling of β_1 integrin signaling and survival (46, 47). Interestingly, BT474 cells, which overexpress HER-2 and estrogen receptor (ER), remain sensitive to AIB2. In contrast, SKBR3 cells overexpress HER-2 but are ER negative, a phenotype that has implicated growth factor signaling pathways with resistance to tamoxifen (48). Herceptin, a monoclonal antibody against HER-2, has been shown to down-modulate the HER-2 receptor, resulting in cytostasis (24). We found that the addition of Herceptin to AIB2 in SKBR3 cells in three-dimensional lrECM resulted in a significantly decreased percentage of Ki-67-positive cells compared with cultures treated with AIB2 alone. These data indicate that an additive cytostatic effect is achieved by using the combination of inhibitory antibodies. Further investigations of the features of SKBR3 that may confer resistance to AIB2 are warranted and may help identify subsets of tumors that may respond to a combination of β_1 integrin inhibition and Herceptin or hormonal therapy.

We found that β_1 integrin inhibition was effective in both T4-2 and MCF-7 xenografts in nude mice *in vivo*, confirming our results in three-dimensional lrECM. Similar to the response observed in culture, tumor xenografts treated *in vivo* showed decreased proliferation and increased apoptosis compared with controls in the animals that received treatment beginning 4 days after tumor implantation. In animals where the tumors were treated after 4 weeks of implantation, there was a significant decrease in tumor size and proliferation and a decrease in apoptosis in treated animals compared with controls. The decrease in observed TUNEL-positive cells in the larger tumors could be due to the increased amounts of necrosis, an alternate mechanism of cell death, seen in larger tumors (data not shown).

Toxicity studies using AIB2 and clone Ha2/5 revealed no discernible toxicity in animals, even with 20 mg/kg doses. These

results indicate that β_1 integrin signaling confers growth and survival advantages in cancer cells *in vivo* that can be discriminated from normal β_1 integrin signaling by AIB2. Other mechanisms also should be considered. For example, immune-mediated secondary effects of the antibody have been shown to play a significant role in antibody-mediated therapies (47). We have previously shown that the F(ab')₂ fragments of AIB2 are active in three-dimensional IrECM assays (17), and others have shown that AIB2 binds to a region of β_1 integrin extracellular domain between two putative ligand binding sites that are thought to induce a conformational change (48), resulting in down-modulation of signaling. The activity or presence of Fc-directed immune response *in vivo* has not been isolated from the activity of the F(ab')₂ region per se. These studies, in addition to humanization of the AIB2 clone, are necessary next steps towards clinical drug development.

In summary, β_1 integrin inhibition using monoclonal antibody AIB2 results in cytostasis and apoptosis in malignant breast cancer colonies but not normal tissue structures propagated on top of three-dimensional IrECM gels. The three-dimensional IrECM assay appropriately distinguishes the difference in response between normal structures and malignant

colonies and reveals global changes in morphology associated with treatment. In addition, AIB2 inhibits breast cancer growth *in vivo* by eliciting increased apoptosis and decreased proliferation, with no discernible toxicity to animals. We conclude that β_1 integrin inhibition using monoclonal antibodies is a promising approach to breast cancer treatment, and that the modified three-dimensional IrECM assay and protocol is an appropriate assay for testing differences in malignant and normal cell response to targeted therapeutic agents.

Acknowledgments

Received 8/29/2005; revised 11/12/2005; accepted 11/18/2005.

Grant support: UCSF-REAC; Cooperative Institutional Research Program; NIH P50 Specialized Programs of Research Excellence grant CA CA58207-08 (C. Park); U.S. Department of Energy, Office of Biological and Environmental Research grant DE-AC03-76SF00098 (M.J. Bissell); NIH/National Cancer Institute grants CA64786-09 (M.J. Bissell) and P50 CA112970-01 (J.W. Gray and M.J. Bissell); and U.S. Department of Defense Breast Cancer Research Program's Innovator Award DAMD17-02-1-0438 (M.J. Bissell).

The costs of publication of this article were defrayed in part by the payment of page charges. This article must therefore be hereby marked *advertisement* in accordance with 18 U.S.C. Section 1734 solely to indicate this fact.

We thank Donghui Wang and Evelyn Yao for expert technical assistance.

References

- Mendelsohn J, Baselga J. The EGF receptor family as targets for cancer therapy. *Oncogene* 2000;19:6550-65.
- Slamon DJ, Leyland-Jones B, Shak S, et al. Use of chemotherapy plus a monoclonal antibody against HER2 for metastatic breast cancer that overexpresses HER2. *N Engl J Med* 2001;344:783-92.
- Giancotti FG, Ruoslahti E. Integrin signaling. *Science* 1999;285:1028-32.
- White DE, Kurpios NA, Zuo D, et al. Targeted disruption of β_1 -integrin in a transgenic mouse model of human breast cancer reveals an essential role in mammary tumor induction. *Cancer Cell* 2004;6:159-70.
- Berry MG, Gui GP, Wells CA, Carpenter R. Integrin expression and survival in human breast cancer. *Eur J Surg Oncol* 2004;30:484-9.
- Gui GP, Wells CA, Yeomans P, et al. Integrin expression in breast cancer cytology: a novel predictor of axillary metastasis. *Eur J Surg Oncol* 1996;22:254-8.
- Shaw LM. Integrin function in breast carcinoma progression. *J Mammary Gland Biol Neoplasia* 1999;4:367-76.
- Zutter MM, Krigman HR, Santoro SA. Altered integrin expression in adenocarcinoma of the breast. Analysis by *in situ* hybridization. *Am J Pathol* 1993;142:1439-48.
- Aoudjit F, Vuori K. Integrin signaling inhibits paclitaxel-induced apoptosis in breast cancer cells. *Oncogene* 2001;20:4995-5004.
- Damiano JS. Integrins as novel drug targets for overcoming innate drug resistance. *Curr Cancer Drug Targets* 2002;2:37-43.
- Lewis JM, Truong TN, Schwartz MA. Integrins regulate the apoptotic response to DNA damage through modulation of p53. *Proc Natl Acad Sci U S A* 2002;99:3627-32.
- Sethi T, Rintoul RC, Moore SM, et al. Extracellular matrix proteins protect small cell lung cancer cells against apoptosis: a mechanism for small cell lung cancer growth and drug resistance *in vivo*. *Nat Med* 1999;5:662-8.
- Kawamura T, Endo Y, Yonemura Y, et al. Significance of integrin α_2/β_1 in peritoneal dissemination of a human gastric cancer xenograft model. *Int J Oncol* 2001;18:809-15.
- Fujita S, Watanabe M, Kubota T, et al. Alteration of expression in integrin β_1 -subunit correlates with invasion and metastasis in colorectal cancer. *Cancer Lett* 1995;91:145-9.
- Elliott BE, Ekblom P, Pross H, et al. Anti- β_1 integrin IgG inhibits pulmonary macrometastasis and the size of micrometastases from a murine mammary carcinoma. *Cell Adhes Commun* 1994;1:319-32.
- Bissell MJ, Weaver VM, Lelievre SA, et al. Tissue structure, nuclear organization, and gene expression in normal and malignant breast. *Cancer Res* 1999;59:1757-63; discussion 1763-4s.
- Weaver VM, Petersen OW, Wang F, et al. Reversion of the malignant phenotype of human breast cells in three-dimensional culture and *in vivo* by integrin blocking antibodies. *J Cell Biol* 1997;137:231-45.
- Liu H, Radisky DC, Wang F, Bissell MJ. Polarity and proliferation are controlled by distinct signaling pathways downstream of PI3-kinase in breast epithelial tumor cells. *J Cell Biol* 2004;164:603-12.
- Wang F, Weaver VM, Petersen OW, et al. Reciprocal interactions between β_1 -integrin and epidermal growth factor receptor in three-dimensional basement membrane breast cultures: a different perspective in epithelial biology. *Proc Natl Acad Sci U S A* 1998;95:14821-6.
- Briand P, Petersen OW, Van Deurs B. A new diploid nontumorigenic human breast epithelial cell line isolated and propagated in chemically defined medium. *In Vitro Cell Dev Biol* 1987;23:181-8.
- Hall DE, Reichardt LF, Crowley E, et al. The α_1/β_1 and α_6/β_1 integrin heterodimers mediate cell attachment to distinct sites on laminin. *J Cell Biol* 1990;110:2175-84.
- Tomaselli KJ, Damsky CH, Reichardt LF. Purification and characterization of mammalian integrins expressed by a rat neuronal cell line (PC12): evidence that they function as α/β heterodimeric receptors for laminin and type IV collagen. *J Cell Biol* 1988;107:1241-52.
- Werb Z, Tremble PM, Behrendtsen O, et al. Signal transduction through the fibronectin receptor induces collagenase and stromelysin gene expression. *J Cell Biol* 1989;109:877-89.
- Baselga J, Albanell J, Molina MA, Arribas J. Mechanism of action of trastuzumab and scientific update. *Semin Oncol* 2001;28:4-11.
- Ott RL. Introduction to statistical methods and data analysis. 5th ed. Belmont (CA): Duxbury Press; 2001.
- Wang F, Hansen RK, Radisky D, et al. Phenotypic reversion or death of cancer cells by altering signaling pathways in three-dimensional contexts. *J Natl Cancer Inst* 2002;94:1494-503.
- Howlett AR, Bailey N, Damsky C, et al. Cellular growth and survival are mediated by β_1 integrins in normal human breast epithelium but not in breast carcinoma. *J Cell Sci* 1995;108:1945-57.
- Lelievre SA, Bissell MJ. Three dimensional cell culture: the importance of microenvironment in regulation of function. In: Meyers RA, editor. Encyclopedia of molecular cell biology and molecular medicine. 2nd ed. New York: Wiley; 2005.
- Weaver VM, Lelievre S, Lakin JN, et al. Beta4 integrin-dependent formation of polarized three-dimensional architecture confers resistance to apoptosis in normal and malignant mammary epithelium. *Cancer Cell* 2002;2:205-16.
- Wennerberg K, Fassler R, Warmegard B, Johansson S. Mutational analysis of the potential phosphorylation sites in the cytoplasmic domain of integrin β_{1A} . Requirement for threonines 788-789 in receptor activation. *J Cell Sci* 1998;111:1117-26.
- Yamada KM, Pankov R, Cukierman E. Dimensions and dynamics in integrin function. *Braz J Med Biol Res* 2003;36:959-66.
- Gu J, Tamura M, Pankov R, et al. Shc and FAK differentially regulate cell motility and directionality modulated by PTEN. *J Cell Biol* 1999;146:389-403.
- Romond EH, Perez EA, Bryant J, et al. Trastuzumab plus adjuvant chemotherapy for operable HER2-positive breast cancer. *N Engl J Med* 2005;353:1673-84.
- Truong T, Sun G, Doorly M, et al. Modulation of DNA damage-induced apoptosis by cell adhesion is independently mediated by p53 and c-Abl. *Proc Natl Acad Sci U S A* 2003;100:10281-6.
- Cukierman E, Pankov R, Stevens DR, Yamada KM. Taking cell-matrix adhesions to the third dimension. *Science* 2001;294:1708-12.
- Schmeichel KL, Bissell MJ. Modeling tissue-specific signaling and organ function in three dimensions. *J Cell Sci* 2003;116:2377-88.
- Green SK, Francia G, Isidoro C, Kerbel RS. Anti-adhesive antibodies targeting E-cadherin sensitize multicellular tumor spheroids to chemotherapy *in vitro*. *Mol Cancer Ther* 2004;3:149-59.
- St Croix B, Florens VA, Rak JW, et al. Impact of the cyclin-dependent kinase inhibitor p27Kip1 on resistance of tumor cells to anticancer agents. *Nat Med* 1996;2:1204-10.
- Boudreau N, Werb Z, Bissell MJ. Suppression of apoptosis by basement membrane requires three-dimensional tissue organization and withdrawal from the cell cycle. *Proc Natl Acad Sci U S A* 1996;93:3509-13.

40. Cordes N, Blaese MA, Meineke V, Van Beuningen D. Ionizing radiation induces up-regulation of functional β_1 -integrin in human lung tumour cell lines *in vitro*. *Int J Radiat Biol* 2002;78:347-57.
41. Meineke V, Gilbertz KP, Schilperoort K, et al. Ionizing radiation modulates cell surface integrin expression and adhesion of COLO-320 cells to collagen and fibronectin *in vitro*. *Strahlenther Onkol* 2002;178:709-14.
42. Rosell R, Fossella F, Milas L. Molecular markers and targeted therapy with novel agents: prospects in the treatment of non-small cell lung cancer. *Lung Cancer* 2002;38 Suppl 4:43-9.
43. Sledge GW, Jr. HER-2 stay: the continuing importance of translational research in breast cancer. *J Natl Cancer Inst* 2004;96:725-7.
44. Ruoslahti E. Integrins as signaling molecules and targets for tumor therapy. *Kidney Int* 1997;51:1413-7.
45. Giancotti FG. Complexity and specificity of integrin signalling. *Nat Cell Biol* 2000;2:E13-4.
46. Ojakian GK, Ratcliffe DR, Schwimmer R. Integrin regulation of cell-cell adhesion during epithelial tubule formation. *J Cell Sci* 2001;114:941-52.
47. Celetti A, Garbi C, Consales C, et al. Analysis of cadherin/catenin complexes in transformed thyroid epithelial cells: modulation by β_1 integrin subunit. *Eur J Cell Biol* 2000;79:583-93.
48. Gutierrez MC, Detre S, Johnston S, et al. Molecular changes in tamoxifen-resistant breast cancer: relationship between estrogen receptor, HER-2, and p38 mitogen-activated protein kinase. *J Clin Oncol* 2005;23:2469-76.
49. Clynes RA, Towers TL, Presta LG, Ravetch JV. Inhibitory Fc receptors modulate *in vivo* cytotoxicity against tumor targets. *Nat Med* 2000;6:443-6.
50. Takada Y, Puzon W. Identification of a regulatory region of integrin β_1 subunit using activating and inhibiting antibodies. *J Biol Chem* 1993;268:17597-601.

Three-dimensional culture models of normal and malignant breast epithelial cells

Genee Y Lee, Paraic A Kenny, Eva H Lee & Mina J Bissell

Life Sciences Division, Lawrence Berkeley National Laboratory, MS 977R225A, Berkeley, California 94720, USA. Correspondence should be addressed to M.J.B. (mjbissell@lbl.gov).

Extracellular matrix is a key regulator of normal homeostasis and tissue phenotype¹. Important signals are lost when cells are cultured *ex vivo* on two-dimensional plastic substrata. Many of these crucial microenvironmental cues may be restored using three-dimensional (3D) cultures of laminin-rich extracellular matrix (lrECM)². These 3D culture assays allow phenotypic discrimination between nonmalignant and malignant mammary cells, as the former grown in a 3D context form polarized, growth-arrested acinus-like colonies whereas the latter form disorganized, proliferative and nonpolar colonies³. Signaling pathways that function in parallel in cells cultured on plastic become reciprocally integrated when the cells are exposed to basement membrane-like gels^{4–7}. Appropriate 3D culture thus provides a more physiologically relevant approach to the analysis of gene function and cell phenotype *ex vivo*. We describe here a robust and generalized method for the culturing of various human breast cell lines in three dimensions and describe the preparation of cellular extracts from these cultures for molecular analyses. The procedure below describes the 3D ‘embedded’ assay, in which cells are cultured embedded in an lrECM gel⁸ (Fig. 1). By lrECM, we refer to the solubilized extract derived from the Engelbreth-Holm-Swarm mouse sarcoma cells⁹. For a discussion of user options regarding 3D matrices, see Box 1. Alternatively, the 3D ‘on-top’ assay, in which cells are cultured on top of a thin lrECM gel overlaid with a dilute solution of lrECM, may be used as described in Box 2 (Fig. 1 and Fig. 2).

MATERIALS

REAGENTS

Engelbreth-Holm-Swarm extracellular matrix extract (EHS), growth factor-reduced (Matrigel, BD Biosciences or Cultrex BME, Trevigen)

Diaminophenylindole (DAPI)

Hard-set mounting medium (VECTASHIELD HardSet, Vector Laboratories or ProLong Gold, Invitrogen)

Immunofluorescence (IF) buffer: 0.2% Triton X-100, 0.1%

BSA (radioimmunoassay grade), 0.05% Tween 20 in PBS

(pH 7.4; sterilized, 0.22 µm filter); for long-term storage, add 7.7 mM NaN₃

IF blocking solution: 10% goat serum, 1% goat F(ab')₂ anti-mouse immunoglobulin G (IgG; Caltag) in IF buffer

PBS: 130 mM NaCl, 13 mM Na₂HPO₄, 3.5 mM NaH₂PO₄ (pH 7.4)

PBS-EDTA: 5 mM EDTA, 1 mM NaVO₄, 1.5 mM NaF in PBS

PBS-glycine: 100 mM glycine in PBS



Culturing cells in 3D

PROCEDURE

1| Thaw EHS at 4 °C overnight.

2| Coat prechilled culture surface (for example, dish or well) with a thin layer of EHS. Slowly pipette the appropriate volume of “EHS coat” (Table 1) directly onto surface and spread evenly with a pipette tip or plunger of a 1-ml syringe for smaller areas, or cell lifter for larger areas. Incubate for 15–30 min at 37 °C to allow the EHS to gel (but do not let it overdry).

▲ CRITICAL STEP

3| Trypsinize cells from a monolayer to a single-cell suspension.

Use cells that are healthy and not more than 75% confluent.

4| Aliquot cells to be plated into a 1.5 ml microcentrifuge tube.

To perform drug response assays in 3D cultures^{7,10,11} (Fig. 3 and Supplementary Videos 1 and 2 online), compounds may be added to the culture in one of two manners:

- (i) *Small-molecule inhibitors: add to medium when cells are plated in Step 6 of the main protocol and Step b of the 3D on-top protocol (Box 2). Include the compound in all media changes for the duration of the culture.*
- (ii) *Blocking antibodies: mix with cells before plating in Step 5 of the main protocol and Step b of the 3D on-top protocol (Box 2) to ensure complete exposure of the cells to antibodies. Include the antibody in all media changes for the duration of the culture.*

5| Gently pellet the cells by centrifugation at ~115g and, on ice, resuspend the cells into the appropriate volume of EHS (Table 1).

The number of cells to be plated per milliliter of EHS depends on the growth properties of the cell line and may need some optimization, but we recommend the following ranges: for nonmalignant cells, 0.85×10^6 cells/ml; for malignant cells, $0.50\text{--}0.60 \times 10^6$ cells/ml.

▲ CRITICAL STEP

6| Pipette the mixture of cells and EHS onto the precoated surface. Incubate 30 min at 37 °C to allow EHS to gel. Add the appropriate volume of medium (Table 1).

➡ TROUBLESHOOTING

7| Maintain the culture for 10 d, changing medium every 2 d.

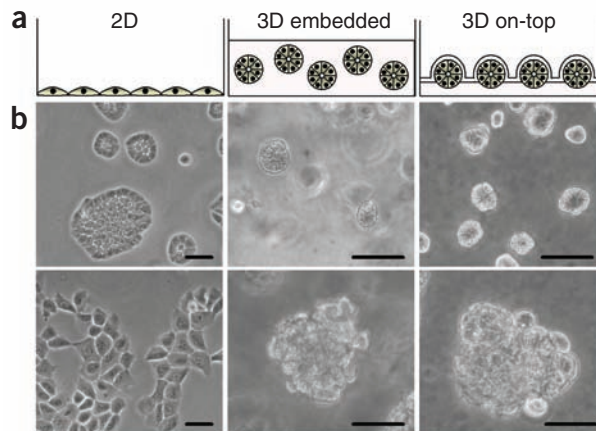


Figure 1 | Breast epithelial cell morphology in different culture conditions. (a) Schematic of nonmalignant breast epithelial cells grown as a monolayer on tissue-culture plastic (left), in the 3D embedded assay (middle) and in the 3D on-top assay (right). (b) Phase-contrast images of nonmalignant HMT-3522 S1 cells grown in the three different culture conditions (top) and malignant HMT-3522 T4-2 cells grown in the same conditions (bottom). Scale bars, 50 μm.

BOX 1 EHS USER'S GUIDE

EHS is available commercially from several sources, including BD Biosciences (Matrigel) and Trevigen (Cultrex Basement Membrane Extract). EHS can also be prepared directly from EHS tumors grown as xenografts²². As EHS is a biological product, its components and properties, including ECM protein and growth factor concentrations, endotoxin levels and stiffness, vary between lots. It is therefore desirable to perform a series of experiments using the same lot number to minimize variation introduced by slight differences in the properties of the EHS. It is also important, when a new lot is obtained, to test whether it is appropriate for culture by performing a side-by-side comparison with cells grown in EHS from a previous lot. We routinely evaluate new lots for the typical and appropriate morphogenesis of nonmalignant and malignant cells along with the expression of several markers of interest. We also exclusively use growth factor-reduced EHS as much of our work is done in the absence of serum and under defined medium conditions. Depending on the nature of the cell type and parameters to be measured, you may develop your own strategy for validation and arrive at your own EHS preferences.

BOX 2 3D ON-TOP ASSAY

As an alternative to the 3D embedded assay, we developed the 3D on-top assay, which requires a shorter amount of time, a decreased amount of EHS, and facilitates imaging as colonies are in a single plane. Therefore, the on-top assay is ideal for time-lapse imaging and also for *in situ* immunostaining of cell lines that form invasive stellate structures in 3D (see Step 8, Option C). Because less EHS is required, it is also a more cost-effective approach.

- (a) Follow Steps 1–4 of the main protocol to prepare the surface and cells for plating.
- (b) Pellet the cells by centrifugation at ~115 g, resuspend in half the “medium volume” (Table 1) and plate onto the coated surface. Allow the cells to settle and attach to the EHS for 10–30 min at 37 °C. *The number of cells to be plated per square centimeter of culture surface area may need some optimization depending on the growth properties of the cell line, but we recommend the following ranges: for nonmalignant cells, 0.25×10^5 cells/cm²; for malignant cells, 0.175 – 0.20×10^5 cells/cm². Cells of some lines tend to aggregate with one another and may not adhere as quickly to the EHS, resulting in cells not resting singly on the layer of EHS or concentrating in the center of the well. Agitation of the plate in the x-y plane at intervals during incubation at 37 °C may assist with preventing cell concentration in the center of the well (do not apply a swirling motion as cells will then accumulate around the edge of the well).*
- (c) Chill the remaining medium on ice and add EHS to 10% volume. Gently add the EHS-medium mixture to the plated culture.
Medium must be thoroughly chilled before addition of EHS to ensure homogenous mixing and even deposition of EHS onto cells in culture. Pipette the EHS-medium mixture down the side of the well to avoid disturbance of the cells or EHS gel.
- (d) Maintain culture for 4 d, replacing EHS-medium mixture every 2 d.
- (e) To perform drug response assays in the 3D on-top assay, see Step 4 of the main protocol.

8 | Colonies may be fully extracted from their 3D culture environment for further analyses, for example, immunostaining, DNA, RNA and protein extraction (Option A, complete extraction). If only an immunostaining endpoint is desired, a complete extraction is often not necessary. An abbreviated procedure may be performed in which the gel is partially broken down, allowing for sufficient dissolution

of polymerized EHS in the sample for immunostaining (Option B, in-well extraction). Alternatively, colonies may be fixed and then immunostained directly in the gel (Option C, whole-culture fixation; proceeding to Box 3, whole-culture immunostaining). This latter method is generally only preferable if a 3D colony you would like to visualize would be disrupted by extraction (as in Fig. 2c) because the immunostaining procedure then requires a much larger amount of antibody per sample and is less flexible as a single culture may only be stained against one set of markers. Frozen sections for subsequent immunostaining may also be obtained after embedding of whole cultures in Optimal Cutting Temperature (OCT) compound. If only RNA extraction is desired, the culture may be directly solubilized by addition of Trizol.

Perform all steps on ice.

- (i) Aspirate the medium and rinse 2× with 1 medium-volume equivalent of ice-cold PBS.
- (ii) Add 2–3 volumes of ice-cold PBS-EDTA. Detach EHS from the bottom of culture surface using a cell lifter (for dishes of diameter ≥35 mm) or by gently scraping the bottom with a pipette tip. Shake gently for 15–30 min.

The 3D-embedded cultures will require a larger volume of PBS-EDTA than 3D on-top cultures and will also take longer to break down.

Extracting cells from 3D cultures

Option A. Complete extraction

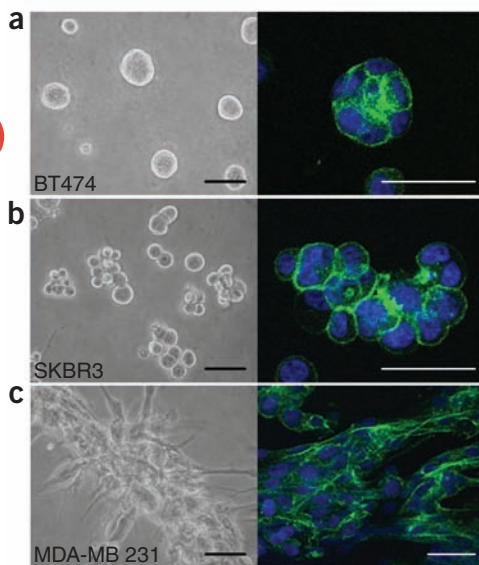


Figure 2 | Breast cancer cell lines in 3D culture. (a–c) Phase-contrast images (left) and confocal cross-sections of Phalloidin staining of F-actin (right) of BT-474 (a), SK-BR-3 (b) and MDA-MB-231 (c) cell lines grown for 4 d in the 3D on-top assay. In a and b, colonies were completely extracted from the gel for immunostaining; in c, colonies were immunostained in the gel. Scale bars, 100 μm (left) and 50 μm (right).



Option B. In-well extraction

Option C. Whole-culture fixation

Immunostaining of 3D cultures

Table 1 | Suggested volumes for 3D culture

	Number of wells	Diameter (mm)	Area (cm ²)	Medium volume (μl)	3D embedded		3D on-top
					EHS coat (μl)	EHS plate (μl)	EHS coat (μl)
Dish	NA	60	28.3	5,000	250	3,600	850
	6	35	9.6	2,000	120	1,200	500
	24	16	2.0	500	50	300	120
Plates	48	10	0.75	200	30	150	80
	96	6	0.26	60	5	75	15
	Chamber slides	4	NA	1.8	500	50	300
	8	NA	0.8	200	30	150	90

Note that the volumes of EHS to be plated are not directly proportional to surface area owing to the meniscus effect. NA, not applicable.

- (iii) Transfer solution to a conical tube. Rinse culture surface once with 0.5 volume of PBS-EDTA and transfer the rinse to the conical tube. Gently shake tube on ice for 15–30 min.
 - (iv) Inspect the tube to check that EHS has dissolved completely (invert tube gently and look for a homogeneous suspension of cell colonies without visible EHS gel fragments). If not, wait longer and/or add more PBS-EDTA.
- To collect colonies for immunostaining, follow (v). Otherwise, proceed to (vi).
- (v) Centrifuge the solution at ~115g for 1–2 min such that cell colonies collect at the bottom of the tube but do not form a tight pellet. Then carefully aspirate the majority of the supernatant. Gently resuspend the colonies in the remaining supernatant. Pipette approximately 15 μl of the colony suspension onto a slide, allow cells to settle and adhere to the glass, and fix the cells using a fixative appropriate for the antigen of interest.

▲ CRITICAL STEP

■ PAUSE POINT Colonies fixed on slides may be stored at –20 °C for several months.

- (vi) Centrifuge the colonies at ~115g for 5 min into a pellet. Aspirate the supernatant, lyse the cells with an appropriate extraction buffer and process using standard procedures¹².
For protein extraction an additional wash with PBS-EDTA will minimize the amount of EHS in the final extract.

■ PAUSE POINT Extracts may be stored at –80 °C for several months.

- (i) Follow Step 8 Option A (i–ii).
- (ii) Check under microscope to verify that majority of EHS has broken apart and colonies have settled to bottom of the well. If not, wait longer and/or add more PBS-EDTA.
- (iii) Carefully aspirate the majority of the supernatant. Pipette approximately 15 μl of the colonies in solution onto a slide, allow cells to settle and adhere to the glass, and fix them.

▲ CRITICAL STEP

■ PAUSE POINT Cultures fixed on slides may be stored at –20 °C for several months.

- (i) Aspirate the medium and rinse 2× with 1 medium-volume equivalent of ice-cold PBS.
- (ii) Fix culture with 4% paraformaldehyde at room temperature (18–23 °C) for 10 min.
- (iii) Stop fixation by aspirating 4% paraformaldehyde and adding at least 2× medium-volume PBS-glycine for 10 min; wash once with PBS and store in PBS.

■ PAUSE POINT Fixed cultures may be stored at 4 °C for up to 4 d.

9| To immunostain the 3D cultures, first wash slides 3× with PBS-glycine for 10 min at room temperature.

This immunostaining procedure applies to cultures fixed on slides generated in Step 8 Option A or B (Figs. 2a,b and 3) and, with modifications indicated in Box 3, also to fixed whole cultures generated in Step 8 Option C (Fig. 2c).

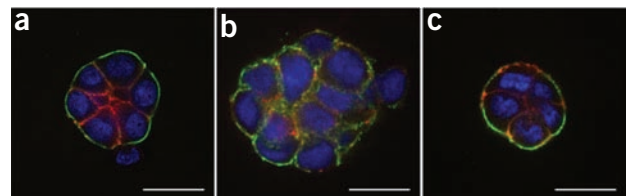


Figure 3 | 3D drug response assay. (a–c) HMT-3522 S1 (a), HMT-3522 T4-2 (b) and HMT-3522 T4-2 treated with an EGFR inhibitor, AG1478 (c) were cultured in the 3D on-top assay for 4 d. Colonies were then extracted and immunostained against α6 integrin (green) and β-catenin (red). Nuclei were counterstained with DAPI (blue). Confocal sections through the centers of the colonies are shown. Scale bar, 20 μm.

BOX 3 WHOLE-CULTURE IMMUNOSTAINING

When performing whole-culture immunostaining in a well, the general procedure for immunostaining may be applied (see Steps 9–18), with some slight modifications:

- Washes are performed in the well and require careful pipetting and aspiration; if cultures are not treated gently, colonies may detach from the EHS and be lost. It is advisable to check cultures frequently under a microscope to ensure they are still attached. We suggest using 2× medium-volume equivalents for washes; for antibody incubations, 0.5× volume is sufficient.
- Samples immunostained in a chamber slide may be mounted directly after removal of the chamber and aspiration of excess fluid.
- Samples immunostained in a tissue-culture well should be removed and mounted on a slide for long-term storage and higher-quality imaging.

10| To block slides, spread 100 µl of IF blocking solution over the fixed cells with a strip of Parafilm, and incubate the slides for 1.5 h, at room temperature in a humid chamber.
The anti-mouse F(ab')₂ fragments in the IF blocking solution block against immunoreactive mouse IgG species in EHS.

11| Stain cultures with the primary antibody of interest diluted in 100 µl of IF buffer for 2 h at room temperature in a humid chamber.

12| Wash slides 3× for 20 min in IF buffer in a Coplin jar at room temperature.

13| Incubate slides with a secondary antibody diluted in 100 µl of IF buffer for 45 min at room temperature in a humid chamber.

14| Wash slides 1× with IF buffer for 20 min, and then 2× with PBS for 10 min at room temperature.

15| Counterstain the nuclei with DAPI (0.5 µg/ml in PBS) for 5 min at room temperature.

16| Wash slides in PBS for 10 min at room temperature.

17| To mount slides, spread one drop of hard-set mounting medium with a number 1½ coverslip and allow to set overnight at 4 °C.

Take care to avoid forming bubbles when mounting.

■ **PAUSE POINT** Mounted slides may be stored at –20 °C for several months.

18| Owing to the thickness of the samples, confocal microscopy is ideal for imaging 3D cultures.

➔ **TROUBLESHOOTING**

TROUBLESHOOTING TABLE

PROBLEM	SOLUTION
Step 6 Cells are not suspended and have settled to the bottom of the EHS gel.	If the cell-EHS mixture in Step 5 is diluted with medium before setting, the cells may settle to the bottom of the gel. Be sure to aspirate the majority of the supernatant to avoid this problem.
Step 18 Excess EHS causes immunostaining background.	Colonies fully extracted from the EHS gel as in Step 8 Option A should have little or no background. Partial extraction of colonies by Step 8 Option B may result in background if EHS is not sufficiently broken down, and a haze or cloud of EHS adheres to cells. To avoid this, increase both the volume of PBS-EDTA used and increase the incubation time in Step 8, Option A (ii).

CRITICAL STEPS

Step 2 Culture surfaces must be prechilled and coated on ice to ensure even spreading of EHS. Pipette EHS slowly and directly onto culture surface to avoid formation of bubbles, which may allow cells to come in direct contact with the culture surface and begin to spread as a monolayer beneath the gel. Note that the viscosity of EHS causes it to form a meniscus in the well, the effect of which increases with decreasing well size. Thus, for 3D on-top cultures, the smaller the well size, the less flat the plane of plating will be.





Step 5 After aspiration of the supernatant, gently flick the tube to loosen the cell pellet so that when EHS is added, the cells are in a single cell suspension. Pipette carefully when mixing to avoid bubbles.

Step 8, Option A (v) Centrifugation time will depend on the size of your colonies and may require some optimization. Larger colonies will settle on their own and may only require a pulse to collect at the bottom of the tube whereas smaller colonies may have only just collected in the conical area of the tube after 2 minutes of centrifugation.

The amount of aspiration required to achieve the balance between getting a high number of colonies on the slide in a relatively low volume of liquid may require some practice. If the volume of liquid used to pipette a sufficient number of colonies is too high it may decrease the efficiency of fixation. The slides may sit for some time to allow excess liquid to evaporate, but do not allow the cells to dry out completely at any point as this will alter the cell structure.

Step 8, Option B (iii) See second comment in Critical Steps, Step 8, Option A (v).

COMMENTS

Here we describe a generalized protocol for monotypic 3D breast epithelial cell culture in the presence of IrECM, an approach that has proved to be extremely informative in our laboratory and those of others. For instance, we recently used the 3D on-top assay to analyze the correlations between colony morphology and gene expression in a large panel of breast cancer cell lines¹³. Other workers have succeeded in culturing cell types from a wide variety of tissues using these techniques (summarized in ref. 14) and informative protocols have been published for several of these systems^{15–20}. Although much of this work has been performed using EHS, other 3D substrata, such as collagen I gels, are excellent for assays of mammary gland branching morphogenesis²¹, and we are watching with interest the development of additional synthetic and natural 3D substrata. Using these approaches, we hope to develop functional organotypic cultures comprised of multiple cell types—including epithelial, myoepithelial, stromal and endothelial—to more appropriately model signaling and cell-cell interactions in an environment similar to complex breast tissue.

Note: Supplementary information is available on the Nature Methods website.

ACKNOWLEDGMENTS

The protocol described here has been the work of many members of the Bissell laboratory over many years. We apologize to those whose work could not be cited owing to space limitations and have cited reviews where possible. This work was supported by grants from the Office of Biological and Environmental Research of the US Department of Energy (DE-AC03-76SF00098 and a Distinguished Fellow Award to M.J.B.), the US National Cancer Institute (CA64786 to M.J.B.; CA57621 to Zena Werb and M.J.B.) and the Breast Cancer Research Program of the US Department of Defense (Innovator Award DAMD17-02-1-438 to M.J.B.).

COMPETING INTERESTS STATEMENT

The authors declare no competing financial interests.

Published online at <http://www.nature.com/naturemethods/>

Reprints and permissions information is available online at <http://npg.nature.com/reprintsandpermissions>

<ol style="list-style-type: none"> 1. Bissell, M.J., Radisky, D.C., Rizki, A., Weaver, V.M. & Petersen, O.W. The organizing principle: microenvironmental influences in the normal and malignant breast. <i>Differentiation</i> 70, 537–546 (2002). 2. Bissell, M.J., Kenny, P.A. & Radisky, D.C. Microenvironmental regulators of tissue structure and function also regulate tumor induction and progression: the role of extracellular matrix and its degrading enzymes. <i>Cold Spring Harb. Symp. Quant. Biol.</i> 70, 343–356 (2005). 3. Petersen, O.W., Ronnov-Jessen, L., Howlett, A.R. & Bissell, M.J. Interaction with basement membrane serves to rapidly distinguish growth and differentiation pattern of normal and malignant human breast epithelial cells. <i>Proc. Natl. Acad. Sci. USA</i> 89, 9064–9068 (1992). 4. Anders, M. <i>et al.</i> Disruption of 3D tissue integrity facilitates adenovirus infection by deregulating the coxsackievirus and adenovirus receptor. <i>Proc. Natl. Acad. Sci. USA</i> 100, 1943–1948 (2003). 5. Bissell, M.J., Rizki, A. & Mian, I.S. Tissue architecture: the ultimate regulator of breast epithelial function. <i>Curr. Opin. Cell Biol.</i> 15, 753–762 (2003). 6. Wang, F. <i>et al.</i> Phenotypic reversion or death of cancer 	<ol style="list-style-type: none"> cells by altering signaling pathways in three-dimensional contexts. <i>J. Natl. Cancer Inst.</i> 94, 1494–1503 (2002). 7. Wang, F. <i>et al.</i> Reciprocal interactions between beta1-integrin and epidermal growth factor receptor in three-dimensional basement membrane breast cultures: a different perspective in epithelial biology. <i>Proc. Natl. Acad. Sci. USA</i> 95, 14821–14826 (1998). 8. Liu, H., Radisky, D.C., Wang, F. & Bissell, M.J. Polarity and proliferation are controlled by distinct signaling pathways downstream of PI3-kinase in breast epithelial tumor cells. <i>J. Cell Biol.</i> 164, 603–612 (2004). 9. Kleinman, H.K. <i>et al.</i> Isolation and characterization of type IV procollagen, laminin, and heparan sulfate proteoglycan from the EHS sarcoma. <i>Biochemistry</i> 21, 6188–6193 (1982). 10. Weaver, V.M. <i>et al.</i> Reversion of the malignant phenotype of human breast cells in three-dimensional culture and in vivo by integrin blocking antibodies. <i>J. Cell Biol.</i> 137, 231–245 (1997). 11. Weaver, V.M. <i>et al.</i> beta4 integrin-dependent formation of polarized three-dimensional architecture confers resistance to apoptosis in normal and malignant mammary epithelium. <i>Cancer Cell</i> 2, 205–216 (2002).
---	---

12. Sambrook, J., Fritsch, E.F. & Maniatis, T. *Molecular Cloning: A Laboratory Manual* (Cold Spring Harbor Laboratory Press, Cold Spring Harbor, New York, 1989).
13. Kenny, P.A. *et al.* The morphologies of breast cancer cell lines in three-dimensional assays correlate with their profiles of gene expression. *Mol. Oncol.* (in the press).
14. Kleinman, H.K. & Martin, G.R. Matrigel: basement membrane matrix with biological activity. *Semin. Cancer Biol.* **15**, 378–386 (2005).
15. Auerbach, R., Lewis, R., Shinnars, B., Kubai, L. & Akhtar, N. Angiogenesis assays: a critical overview. *Clin. Chem.* **49**, 32–40 (2003).
16. Debnath, J., Muthuswamy, S.K. & Brugge, J.S. Morphogenesis and oncogenesis of MCF-10A mammary epithelial acini grown in three-dimensional basement membrane cultures. *Methods* **30**, 256–268 (2003).
17. Toda, S. *et al.* A new organotypic culture of thyroid tissue maintains three-dimensional follicles with C cells for a long term. *Biochem. Biophys. Res. Commun.* **294**, 906–911 (2002).
18. Tonge, D., Edstrom, A. & Ekstrom, P. Use of explant cultures of peripheral nerves of adult vertebrates to study axonal regeneration *in vitro*. *Prog. Neurobiol.* **54**, 459–480 (1998).
19. Vaughan, M.B., Ramirez, R.D., Wright, W.E., Minna, J.D. & Shay, J.W. A three-dimensional model of differentiation of immortalized human bronchial epithelial cells. *Differentiation* **74**, 141–148 (2006).
20. Wang, R. *et al.* Three-dimensional co-culture models to study prostate cancer growth, progression, and metastasis to bone. *Semin. Cancer Biol.* **15**, 353–364 (2005).
21. Fata, J.E., Werb, Z. & Bissell, M.J. Regulation of mammary gland branching morphogenesis by the extracellular matrix and its remodeling enzymes. *Breast Cancer Res.* **6**, 1–11 (2004).
22. Kibbey, M.C. Maintenance of the EHS sarcoma and matrigel preparation. *Methods Cell Sci.* **16**, 227–230 (1994).

available at www.sciencedirect.comwww.elsevier.com/locate/molonc

The morphologies of breast cancer cell lines in three-dimensional assays correlate with their profiles of gene expression

Paraic A. Kenny^{a,1}, Genee Y. Lee^{a,1}, Connie A. Myers^{a,2}, Richard M. Neve^a,
Jeremy R. Semeiks^a, Paul T. Spellman^a, Katrin Lorenz^{a,3}, Eva H. Lee^a,
Mary Helen Barcellos-Hoff^a, Ole W. Petersen^b, Joe W. Gray^a,
Mina J. Bissell^{a,*}

^aLife Sciences Division, Lawrence Berkeley National Laboratory, University of California, One Cyclotron Road, MS 977-225A, Berkeley, CA 94720, USA

^bStructural Cell Biology Unit, Institute of Medical Anatomy, The Panum Institute, University of Copenhagen, DK-2200 Copenhagen N, Denmark

ARTICLE INFO

Article history:

Received 31 January 2007

Accepted 1 February 2007

Available online 14 March 2007

Keywords:

Breast cancer

3D culture

Extracellular matrix

Gene expression profiling

Signal transduction

ABSTRACT

3D cell cultures are rapidly becoming the method of choice for the physiologically relevant modeling of many aspects of non-malignant and malignant cell behavior *ex vivo*. Nevertheless, only a limited number of distinct cell types have been evaluated in this assay to date. Here we report the first large scale comparison of the transcriptional profiles and 3D cell culture phenotypes of a substantial panel of human breast cancer cell lines. Each cell line adopts a colony morphology of one of four main classes in 3D culture. These morphologies reflect, at least in part, the underlying gene expression profile and protein expression patterns of the cell lines, and distinct morphologies were also associated with tumor cell invasiveness and with cell lines originating from metastases. We further demonstrate that consistent differences in genes encoding signal transduction proteins emerge when even tumor cells are cultured in 3D microenvironments.

© 2007 Federation of European Biochemical Societies.
Published by Elsevier B.V. All rights reserved.

1. Introduction

Mechanistic studies of human cancer are largely reliant on *ex vivo* culture of established cell lines. The overwhelming majority of these studies are performed using immortalized cell lines cultured on two-dimensional plastic substrata. Non-malignant mammary epithelial cells, as well as other differentiated cell types, rapidly lose many aspects of the differentiated state upon dissociation and culture on plastic substrata (Bissell et al., 1973; Bissell and Tilles, 1971; Bissell, 1981; Emerman and Pitelka, 1977). Over many decades, we and others have

proposed (Bissell et al., 1982) and demonstrated (Barcellos-Hoff et al., 1989; Roskelley et al., 1995; Schmidhauser et al., 1992; Streuli et al., 1991, 1995; Streuli and Bissell, 1990) that signals from the extracellular matrix play crucial roles in the establishment and maintenance of tissue specificity of non-malignant mammary cells. We have shown that functional and morphological differentiation can be largely restored by growing cells in a reconstituted basement membrane which provides in culture the crucial cues from extracellular matrix proteins to which these cells respond *in vivo* (Barcellos-Hoff et al., 1989; Li et al., 1987; Petersen et al., 1992) and these culture

* Corresponding author. Tel.: +1 510 486 4365; Fax: +1 510 486 5586.

E-mail address: mjbissell@lbl.gov (M.J. Bissell).

¹ These authors contributed equally to this report.

² Present address: Division of Neuropathology, Washington University School of Medicine, St. Louis, MO 63110, USA.

³ Present address: Department of Molecular Medicine, Max Planck Institute of Biochemistry, 82152 Martinsried, Germany.

techniques are now being used to study differentiated function in several tissues (reviewed in Kleinman and Martin, 2005; Schmeichel and Bissell, 2003).

We extended these studies to malignant human breast cells and reported in 1992 that non-malignant and malignant cells can be distinguished rapidly and reliably when grown in three-dimensional (3D) laminin-rich extracellular matrix (lrECM) cultures (Petersen et al., 1992). Non-malignant cells (e.g. HMT-3522 S1) undergo a small number of rounds of cell division, after which they organize into polarized, growth-arrested colonies with many of the morphological features of mammary acini (Petersen et al., 1992). This ability to correctly sense the cues from the basement membrane and organize into acini is shared by the other non-malignant breast epithelial cells which we have studied: MCF-10A (Muthuswamy et al., 2001; Petersen et al., 1992) and 184 (Fournier et al., 2006). In contrast, malignant cells – both established cell lines and cells from primary tumors – adopt a variety of colony morphologies but share some common aspects – loss of tissue polarity, a disorganized architecture and a failure to arrest growth (Park et al., 2006; Petersen et al., 1992).

Crucially, our studies have shown that signal transduction pathways in non-malignant cells are integrated in 3D lrECM cultures in ways not observed when cells are cultured as monolayers. Initially, we reported that the expression and activity of β 1-integrin and EGFR are reciprocally downregulated in breast cancer cells treated with various signaling inhibitors, but only when cultured on 3D substrata (Wang et al., 1998). In another example, T4-2 cells treated with PI3-Kinase inhibitors undergo a reversion of the malignant phenotype in 3D culture, with downregulation of EGFR, β 1-integrin and upregulation of PTEN – changes which are only seen in cells grown on lrECM – while proximal markers of drug efficacy (e.g. pAkt and pGSK3 β) responded similarly in cells grown on both substrata (Liu et al., 2004). We have also shown crucial differences in apoptotic sensitivity in response to chemotherapeutic agents for non-malignant and malignant breast cell lines in 2D and 3D culture (Weaver et al., 2002), further underscoring the relative value of 3D models over more conventional approaches. More recently we have defined a gene expression signature from acini formed from non-malignant breast epithelial cells in 3D lrECM and showed that human breast tumors sharing this pattern had a significantly better prognosis (Fournier et al., 2006). These 3D culture models also have played a key role in our validation of two new molecular targets in breast cancer, β 1-integrin (Park et al., 2006; Weaver et al., 1997) and TACE/ADAM17 (Kenny and Bissell, 2007). These data have raised the question of the extent to which monolayer cultures may be failing to recapitulate signaling *in vivo* (Bissell et al., 2003, 1999).

Whereas there are dramatic morphological (and hence biochemical) differences between normal and malignant cells in 2D and 3D (Bissell et al., 2005; Petersen et al., 1992), the cancer cells are much less sensitive to environmental perturbations. Nevertheless, it is becoming clear that even tumor cells respond to chemotherapy and other factors differently in different microenvironments. Much is known about the gene expression patterns of different breast cancer cell lines on tissue culture plastic (Neve et al., 2006; Perou et al., 1999), yet a comprehensive analysis of the phenotype of a large panel of breast cancer cell lines in 3D culture has been lacking to date. We

asked whether we could detect differences in morphology of the breast cancer cell lines in 3D and whether these differences could be correlated with aspects of gene expression. We focused on a large panel of breast cancer cell lines which largely recapitulate the diversity of gene expression patterns and mutational and genomic aberrations found in breast tumors *in vivo* (Chin et al., 2006; Neve et al., 2006). Here, we report the morphological phenotype of 25 of these breast cell lines grown in 2D and 3D cultures, and their gene expression profiles under these same conditions. These data reveal that breast cancer cell lines generally form colonies with one of four distinctive morphologies and that culture in a 3D microenvironment results in significant and reproducible gene expression changes, even in malignant cells.

2. Results

Twenty-five established epithelial cell lines originally derived from reduction mammoplasty or breast tumors were cultured in a 3D culture assay in which cells are seeded singly on top of a thin gel comprised of laminin-rich extracellular matrix (Lee et al., 2007; Park et al., 2006), overlaid with medium containing a small amount of additional lrECM and analyzed after 4 days. In this study we compare 25 cell lines using the following endpoints: 3D morphology, proliferation index at this time point, and expression level and activity of several key signaling proteins. Additionally, we performed Affymetrix gene expression analysis of cells cultured on both substrata.

2.1. Cell lines exhibit distinct morphologies when cultured in the 3D lrECM on the ‘on-top’ assay

Whereas the panel of cell lines adopted largely non-distinct morphologies when cultured as monolayers, dramatic differences emerged when grown on a 3D lrECM substratum. The 3D morphologies of these cell lines were characterized by phase contrast microscopy and localization of F-actin in colonies at the culture endpoint. We classified the cell lines into four distinct morphological groups referred to as: Round, Mass, Grape-like and Stellate. Representative examples of each class are shown in Figure 1, and the morphology of each of the cell lines in the panel is shown in Figure 2. The Round cell class include HCC1500, MCF-12A, MDA-MB-415, MPE-600, and S1; these form round colonies on top of gels as viewed by phase contrast microscopy and have nuclei that are organized in a regular manner around the center of the colony as assessed by confocal microscopy. The Mass class, BT-474, BT-483, HCC70, HCC1569, MCF-7, T4-2 and T-47D, form colonies which may also have round colony outlines by phase contrast microscopy, but are distinguished from the Round morphological grouping by their disorganized nuclei and filled colony centers (colonies of the Round morphology occasionally form lumens, although the frequency varies greatly between the cell lines). The Grape-like class, AU565, CAMA-1, MDA-MB-361, MDA-MB-453, MDA-MB-468, SK-BR-3, UACC-812, ZR-75-1 and ZR-75-B, form colonies with poor cell-cell contacts and are distinguished by their grape-like appearance. This phenotype is readily apparent by phase contrast microscopy in most of the cell lines grouped in this

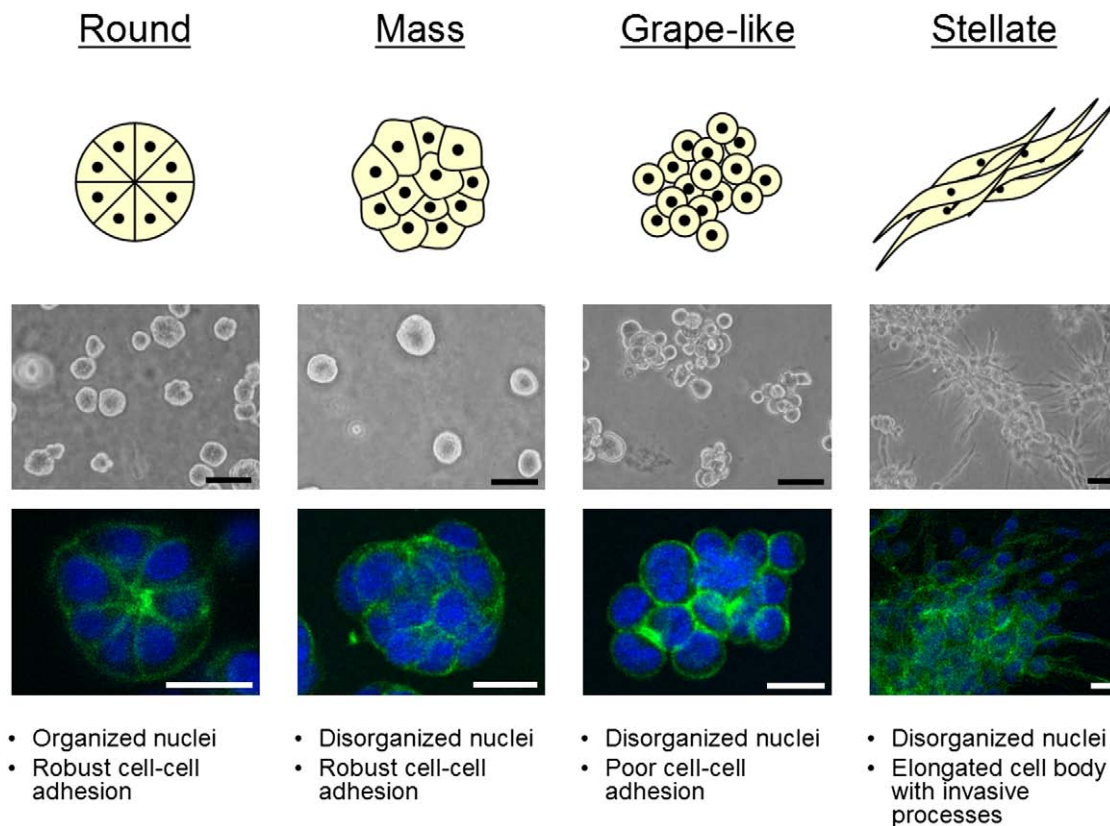


Figure 1 – Breast cell line colony morphologies in 3D culture fall into four distinct groups. A panel of 25 breast cell lines were cultured in three-dimensions and grouped into four distinct morphologies. A schematic and key descriptors of each morphology is shown in addition to phase contrast and F-actin and nuclear fluorescence images of representative cell lines of each morphology: for Round, S1 is shown; Mass, BT-474; Grape-like, SK-BR-3; and Stellate, MDA-MB-231. Scale bars: phase contrast, 50 μm ; fluorescence, 20 μm .

morphology but is particularly obvious when F-actin localization is visualized using phalloidin staining. Although by phase contrast microscopy, UACC-812 and ZR-75-B appear mass-like, F-actin staining of these colonies clearly shows a lack of robust cell–cell adhesion and they were therefore classed in the Grape-like morphology. Lastly, the Stellate class, BT-549, Hs578T, MDA-MB-231 and MDA-MB-436, are distinguished by their invasive phenotype in 3D culture, with stellate projections that often bridge multiple cell colonies.

2.2. Proliferation analysis

We determined the proliferation index of these 25 cell lines at the endpoint of the 3D IrECM assay by indirect immunofluorescence against Ki67 antigen (Table 1). The proportion of nuclei staining positive for Ki67 at this time point (Table 1) did not show any significant correlation to colony morphology (ANOVA, $P = 0.92$), Sorlie/Perou tumor class (ANOVA, $P = 0.30$), ER status (t-test, $P = 0.23$) or whether the cell line was derived from a primary tumor or a metastasis (t-test, $P = 0.35$).

2.3. Expression of signaling proteins

Protein lysates were isolated from cell colonies for western blotting against proteins involved in key signaling processes and in cell–cell interactions (Figure 3). Many of the known

major aspects of protein expression in the panel of cell lines are reflected in this analysis. MDA-MB-468 had the highest levels of EGFR, consistent with their reported amplification of this gene (Filmus et al., 1985). This cell line also had the highest levels of EGFR activity, the second highest being found in T4-2 cells, in which this gene is also amplified (Briand et al., 1996).

Two immunoreactive bands were seen for $\beta 1$ -integrin; the lower and upper bands have been reported to correspond to the partially and fully glycosylated forms, respectively (Bellis, 2004). Interestingly, the protein recognized in the upper band was more highly expressed in six cell lines, while the variant of lower apparent molecular weight was the predominant isoform in 14 of the cell lines. The upper band was most common in the Stellate cells.

Several cell lines had significant levels of phosphorylated Akt, including HCC1569, CAMA-1, BT-549, ZR-75-1 and MDA-MB-468, all of which have no functional PTEN. Other lines, which have activating mutations in the gene encoding PI3-Kinase have somewhat lower, but still substantial levels of pAkt (BT-474, MCF-7 and T-47D) suggesting that PTEN loss may have a more potent effect on activation of Akt than PIK3CA activation. MDA-MB-415 also expressed high levels of pAkt, although to our knowledge defects in this pathway in this cell line have not yet been reported.

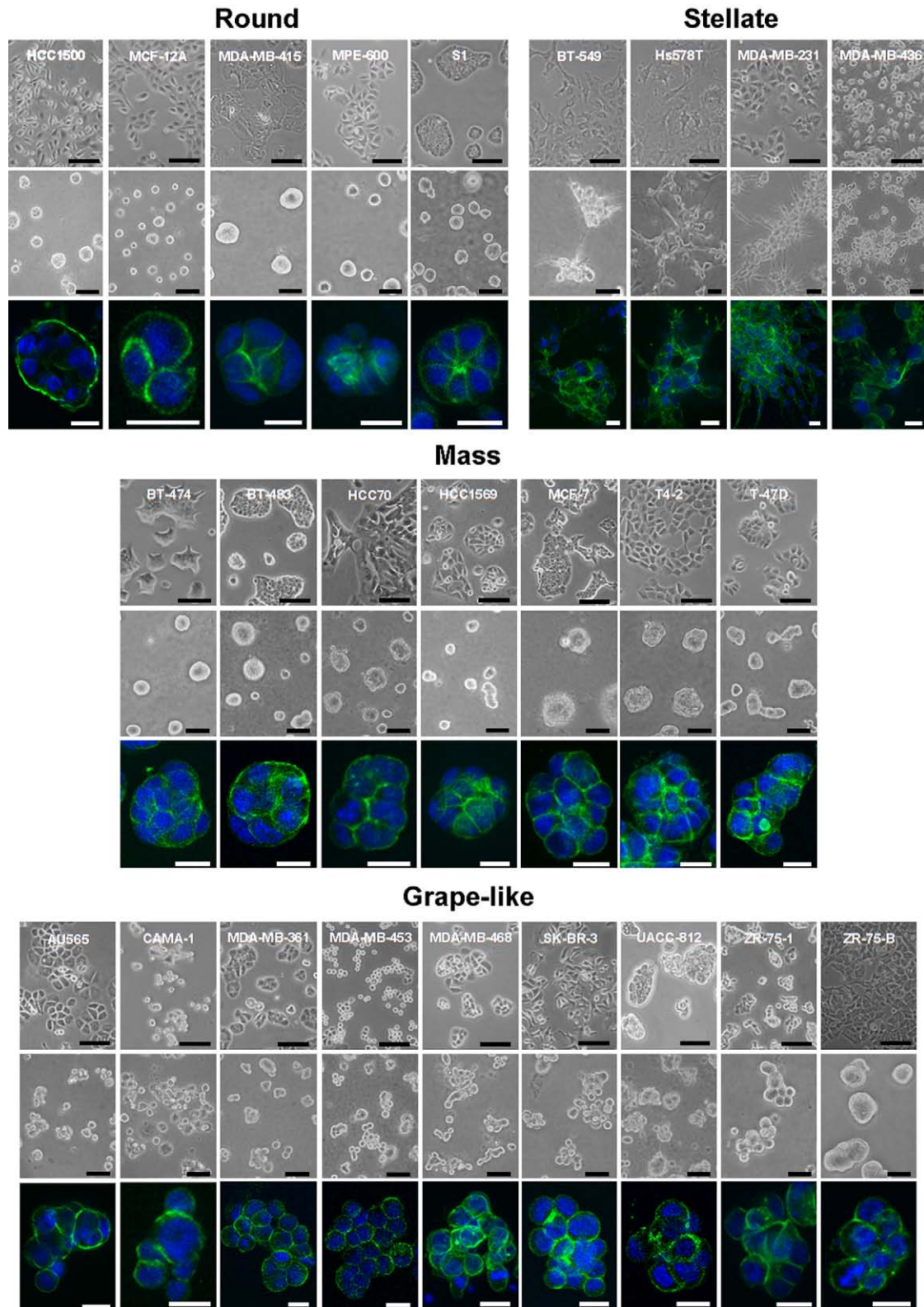


Figure 2 – Morphologies of breast cell lines cultured in two- and three-dimensions. Phase contrast images of the complete panel of 25 breast cell lines cultured on tissue culture plastic (top panel) and in the 3D IrECM assay (middle panel) are shown grouped by 3D morphological classification: Round, Mass, Grape-like and Stellate. 3D cultures were stained for F-actin and nuclei were counterstained with DAPI. Optical sections of representative colonies are shown for all cell lines (bottom panel) with the exception of MDA-MB-468 for which a Z projection with maximum intensity projection (Image J) is shown (because of the high degree of dimensionality of the colonies generated by this cell line, optical sections appear to show single cells not evidently part of the same colony). Scale bars: top panel, 100 μm ; middle panel, 50 μm ; bottom panel, 20 μm .

Table 1 – Breast cell line characteristics

3D morphology	Cell line	ER	PgR	ERBB2 amp.	Mutational status	Tumor type	Tissue source	Tumorigenicity	Tumor classification	Proliferation index (3D) (%)
Round	HCC1500	+	+		N/A	DC	P	Unknown	Basal B	85.9
	MCF-12A	–	–		N/A	F	P	No	Basal B	9.42
	MDA-MB-415	+	–		TP53	AC	M (PE)	No	Luminal	6.02
	MPE-600 ^a	+	–		N/A	IDC	Unknown ^a	Unknown	Luminal	35.3
	S1 ^b	–	–		N/A	F	P	No	Basal B	31
Mass	BT-474	+	+	+	PIK3CA	IDC	P	Yes	Luminal	19.2
	BT-483	+	+		N/A	PIDC	P	Yes	Luminal	25
	HCC70	–	–		N/A	DC	P	Unknown	Basal A	6.82
	HCC1569	–	–		PTEN, TP53	MC	P	Unknown	Basal A	43.1
	MCF-7	+	+		CDKN2A, PIK3CA	IDC	M (PE)	Yes	Luminal	56.7
	T4-2 ^b	–	–		TP53 ^e	F	P	Yes	Basal B	61.6
	T-47D	+	+		PIK3CA, TP53	IDC	M (PE)	Yes	Luminal	53.4
Grape-like	AU565 ^c	–	–	+	None	AC	M (PE)	Unknown	Luminal	53.36
	CAMA-1	+	+		PTEN, VHL	AC	M (PE)	Yes	Luminal	53.4
	MDA-MB-361	+	+	+	None	AC	M (Br)	Yes	Luminal	4.43
	MDA-MB-453	–	–	+	CDH1, PIK3CA	AC	M (PE)	No	Luminal	72.5
	MDA-MB-468	–	–		MADH4, PTEN, RB1, TP53	AC	M (PE)	Yes	Basal A	82.4
	SK-BR-3 ^c	–	–	+	N/A	AC	M (PE)	Yes	Luminal	35.2
	UACC-812	+	–	+	None	IDC	P	Unknown	Luminal	3.95
	ZR-75-1 ^d	+	+		N/A	IDC	M (As)	Yes	Luminal	5.88
	ZR-75-B ^d	+	+		N/A	IDC	M (As)	Unknown	Luminal	22.1
Stellate	BT-549	–	–		RB1, TP53	PIDC	P	Yes	Basal B	23
	Hs578T	–	–		CDKN2A, HRAS, TP53	CS	P	Yes	Basal B	44.2
	MDA-MB-231	–	–		BRAF, CDKN2A, KRAS, TP53	AC	M (PE)	Yes	Basal B	49.5
	MDA-MB-436	–	–		N/A	AC	M (PE)	Yes	Basal B	66.5

Relevant characteristics of non-malignant and malignant breast cell lines used are organized by 3D morphology and summarized here. Estrogen receptor (ER), progesterone receptor (PgR), ERBB2 amplification status (ERBB2 amp.), primary tumor type, tissue source, experimental tumorigenicity, defined as the ability of a cell line to form tumors in an immunocompromised mouse model, and tumor classification, based on previously published data (Lacroix and Leclercq, 2004; Neve et al., 2006), are indicated. Data on mutations were extracted from the Cancer Genome Project at the Sanger Institute (<http://www.sanger.ac.uk/genetics/CGP/CellLines/>) for all available cell lines unless otherwise indicated. Cell lines for which mutational status was not available are indicated as N/A. Genes tested in all cell lines: APC, BRAF, CDH1, CDKN2A, CTNNB1, EGFR, HRAS, KRAS, MADH4, NRAS, PIK3CA, PTEN, RB1, STK11, TP53, VHL; additional genes tested in BT-549, Hs578T, MCF-7, MDA-MB-231 and T-47D: BRCA1, BRCA2, ERBB2, FLT3, PDGFRA. The proliferation index of cell lines cultured for 4 days in 3D defined as the percentage of nuclei staining positive for Ki67 antigen is also shown.

Abbreviations: AC, adenocarcinoma; As, ascites; Br, brain; CS, carcinosarcoma; DC, ductal carcinoma; F, fibrocystic disease; IDC, invasive ductal carcinoma; M, metastasis; MC, metaplastic carcinoma; P, primary; PE, pleural effusion; PIDC, papillary invasive ductal carcinoma.

a MPE-600 was developed by Vysis International, Inc.

b T4-2 is a tumorigenic cell line derived from S1 *in vitro*.

c AU565 and SK-BR-3 were derived from the same patient.

d ZR-75-B was cloned from ZR-75-1.

e T4-2 is not included in the Sanger Institute Cancer Genome Project, but a TP53 mutation in the cell line was reported in (Moyret et al., 1994).

Most cell lines had similar levels of β -catenin, with the exception of some of the E-Cadherin negative cells such as SK-BR-3 and AU565. This is consistent with the role of E-cadherin in stabilizing a pool of β -catenin in adherens junctions, with the loss of E-Cadherin leading to the rapid turnover of cytosolic β -catenin in these cell lines which express the CTNNB1 gene but have a high activity of the β -catenin turnover pathway (Orford et al., 1997).

Each of the Stellate cell lines lacked E-cadherin, and the Grape-like cell lines generally had lower levels than the other two groups, most probably reflecting the more limited cell–cell interactions observed in colonies with this morphology. In many cases, E-cadherin negativity was consistent with the reported deletions in this panel of cell lines (Hiraguri et al.,

1998). Two cell lines, CAMA-1 and MPE-600, were positive for E-cadherin, but the immunoreactive bands were of a slightly different size to the 120 KDa band found in the other cell lines. MPE-600 has been reported to have a deletion of exon 9, while CAMA-1 has a mutation in the splice acceptor site of exon 12 (van de Wetering et al., 2001).

The highest levels of ErbB2 were found in cell lines of the Grape-like and Mass categories. Cells of the Round category expressed moderate levels of ErbB2, while this protein was not detected in Stellate cells. AU565, BT-474, HCC1569, SK-BR-3, MDA-MB-361, MDA-MB-453, and UACC-812 have been reported to have amplified this gene (Lacroix and Leclercq, 2004 and references therein; Neve et al., 2006). Of the remaining cell lines with high levels of ErbB2, BT-483

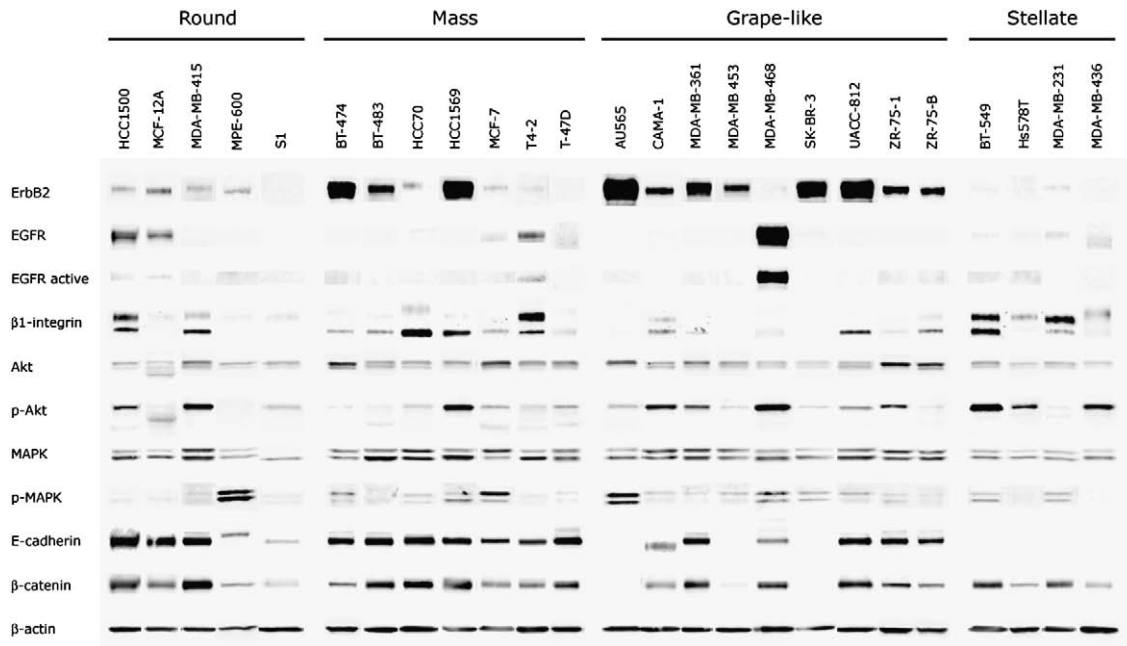


Figure 3 – Western blot analysis of breast cell lines cultured in 3D. Western blot analysis of the indicated proteins is shown. Equal amounts of protein were loaded per lane, and lysates of S1 and T4-2 were run on all separate blots as to control for equal loading and exposure time. Signal from control cell lines were semi-quantitatively normalized across blots using S1 or T4-2 signal for each protein in Adobe Photoshop. Normalized protein profiles for each cell line were then aligned and grouped by morphology in this composite figure (see Section 4 for additional detail).

and ZR-75-1 are not amplified at the ErbB2 locus (Kallioniemi et al., 1992; Kraus et al., 1987), however, both are known to overexpress ErbB2 (Gazdar et al., 1998; Kraus et al., 1987).

2.4. Gene expression profiling of breast epithelial cells grown in two- and three-dimensions

We determined the gene expression profile of 24 of the 25 cell lines in 2D and 3D cultures. During the period in which these studies were performed, the array platform being utilized was upgraded from the Affymetrix high-density oligonucleotide array cartridge system to the newer, Affymetrix high throughput array (HTA) GeneChip system. To ensure the validity of our inter-platform comparison (for a detailed description, please see Section 4), we analyzed a number of samples on both platforms. These samples clustered together following the cross-platform normalization, indicating that the approach is valid and robust. In total, 89 samples from 24 different cell lines were analyzed, 47 in 2D and 42 in 3D. Replicates were not averaged and are presented as individual samples to provide additional confidence in the robustness of our inter-platform comparison and clustering approach. These data have been deposited in the Array Express database (<http://www.ebi.ac.uk/arrayexpress/>; accession number E-TABM-244). Figure 4 represents unsupervised hierarchical clustering of the 89 samples.

In agreement with the earlier report from one of our laboratories (Neve et al., 2006), the cell lines grouped into two broad clusters which have similarities to the Luminal and Basal subclasses described by Perou et al. (2000) in human breast cancer cases. As described by Neve et al. (2006) the Basal cell lines could be further subdivided into two groups,

Basal A and Basal B. The cell lines of the HMT-3522 series (non-malignant S1 and malignant T4-2) cluster with the non-malignant MCF-12A cell line in the Basal B subclass. Given that the malignant T4-2 cells were derived from S1 cells by selection in culture (rather than over many years of mutation and evolution under the complex selective pressures in a cancer patient), it is perhaps unsurprising, but also intriguing that it clusters with those of a more normal phenotype. The HCC1500 cell line is an outlier of this group, distinct from the other cells with a basal phenotype. In 3D culture, this cell line (although tumor-derived) still retains some aspects of the normal mammary gland morphology and has been occasionally observed to form colonies with nuclear organization around a central lumen with apical F-actin localization (data not shown).

While the Basal/Luminal delineation seems to be the strongest driver of the clustering pattern, cell lines of similar morphologies within these sub-types frequently clustered together suggesting that the gene expression pattern of the cells is a strong determinant of colony morphology (Figure 4). All four of the Stellate cell lines are more similar to each other than to cell lines of any other morphology, while all of the Round cell lines of the Basal subtype clustered together. Among the Luminal subtype, five of the seven Grape-Like cell lines cluster together and there is a sub-cluster of two Round cell lines in a larger cluster of mostly Mass cell lines.

2.5. 2D versus 3D expression comparison

From the hierarchical clustering, it is clear that the 2D and 3D expression profiles of the individual cell lines cluster together, independently of the substratum on which they were cultured.

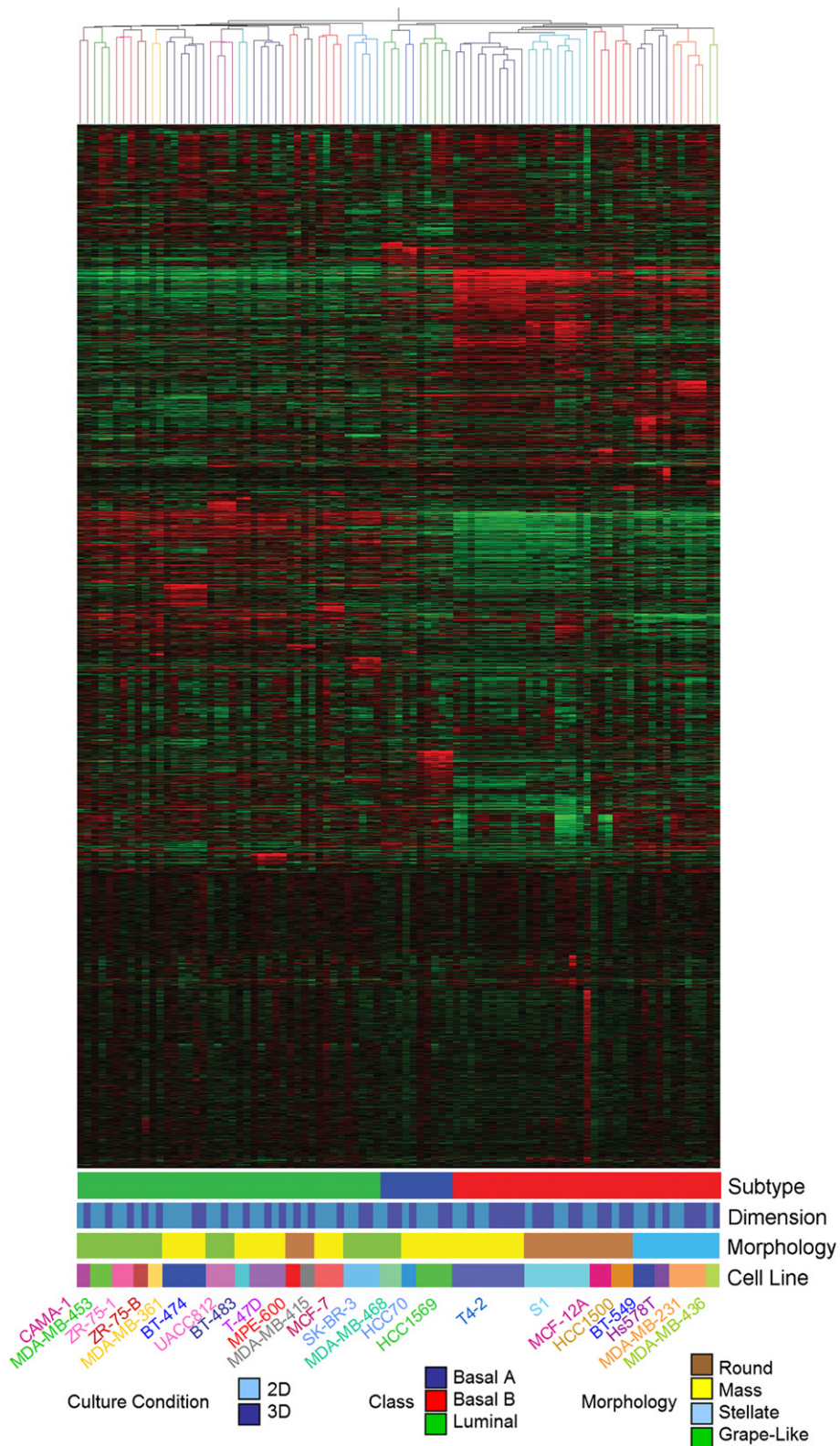


Figure 4 – Gene expression profiling of breast cell lines grown in two- and three-dimensions. Unsupervised hierarchical clustering of 89 samples representing 24 non-malignant and malignant breast cell lines cultured on either tissue culture plastic (2D) or IrECM (3D). Tree branches are colored to indicate cell line identity (see key on bottom of figure). Also colored in the key are the morphological group and the tumor classification to which each cell line belongs.

These data indicate that 3D culture did not effect a consistent and widespread change in gene expression causing each cell line to adopt a substantially different and common program of gene expression. Nevertheless, it is also clear that the 3D microenvironment did effect significant changes in the gene expression profiles of these cancer cell lines.

To identify those genes which respond consistently to the 3D culture microenvironment in all of the cell lines, we averaged all of the replicates for each cell line under each culture condition and tested whether there was a set of genes which distinguished cell lines grown in 2D versus those grown in 3D (ANOVA, cutoff $P < 0.00025$). We identified 96 Affymetrix probes which were strongly up/downregulated consistently across the majority of the cell lines (Figure 5). These data indicate that, although cell line identity and the Luminal/Basal phenotype make a strong contribution to the gene expression profiles, the culture microenvironment and substratum also exert significant effects.

Of these 96 Affymetrix probes, 41 corresponded to genes with annotated functions. We used Gene Ontology annotations (Ashburner et al., 2000) to determine whether particular molecular functions were statistically overrepresented in this set. These genes and their Gene Ontology classifications are shown in Figure 6. Of the eight classifications found, one – “signal transducer activity” – was statistically significantly overrepresented in the set of genes which differ between 2D and 3D culture ($P = 0.0201$). The “enzyme regulator activity” class almost reached statistical significance ($P = 0.0509$). Given that many signal transduction molecules are regulated at the level of phosphorylation and other protein modifications rather than at transcriptional levels, we expect that the actual changes at the level of cellular signaling would be even more striking than the gene expression arrays indicate. These data provide additional support for our contention that regulation of signal transduction is substantially different in cells cultured on basement membrane gels (Liu et al., 2004; Wang et al., 1998; Weaver et al., 2002, 1997).

3. Discussion

The utility of the 3D culture models to explore aspects of the normal and malignant phenotypes in culture has now been widely recognized and many workers have adopted these approaches to study cancers of the breast and of other tissues (reviewed in Schmeichel and Bissell, 2003). One recent fruitful avenue has been to take non-malignant cells, e.g. S1 or MCF-10A which form acini in 3D cultures, and specifically overexpress or ablate expression of potentially cancer-relevant genes and analyze the effects of the manipulation on the ability of these cells to execute acinar morphogenesis (Debnath et al., 2002, 2003; Gunawardane et al., 2005; Irie et al., 2005; Isakoff et al., 2005; Muthuswamy et al., 2001; Overholtzer et al., 2006; Reginato et al., 2003; Wrobel et al., 2004; Zhan et al., 2006). Many of these reports have shown that the effects of activation of oncogenes or inactivation of tumor-suppressor genes are profoundly different in cells cultured in different microenvironments. Setting the “oncogenic lesion” a priori has allowed the dissection of the potential contribution of individual components to various aspects

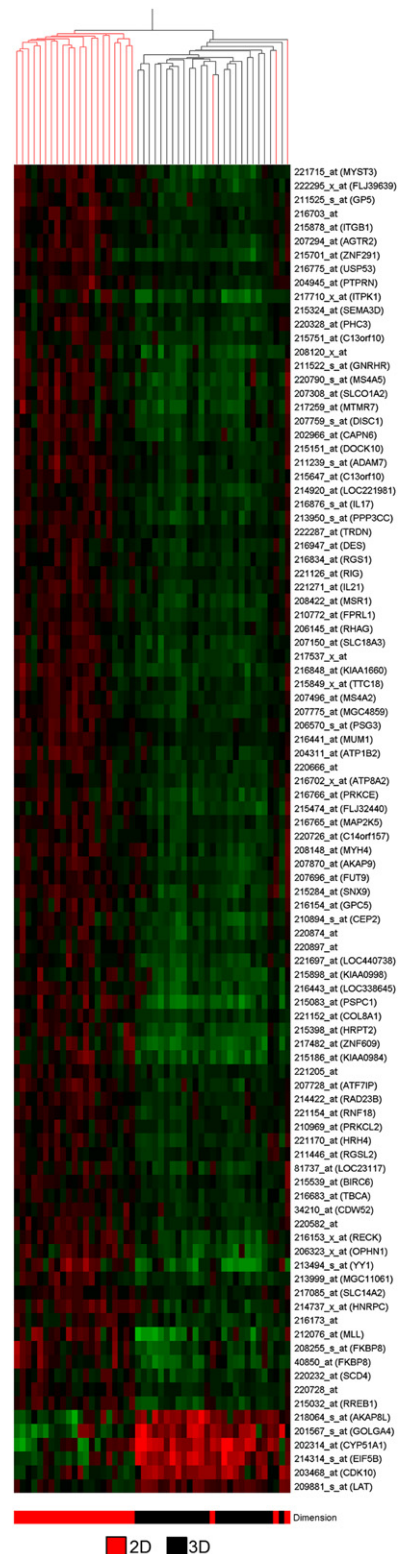


Figure 5 – Genes which distinguish 2D and 3D culture conditions. All replicates were averaged so that each condition represents one cell line in either 2D or 3D culture. The 22215 Affymetrix probes were tested for association with the parameter, Dimension, using a cutoff of $P < 0.00025$, corrected for multiple comparisons using the Benjamini and Hochberg test. Ninety-six probes significantly distinguished the expression profiles of cells grown on plastic from those grown on IrECM at this level of significance.

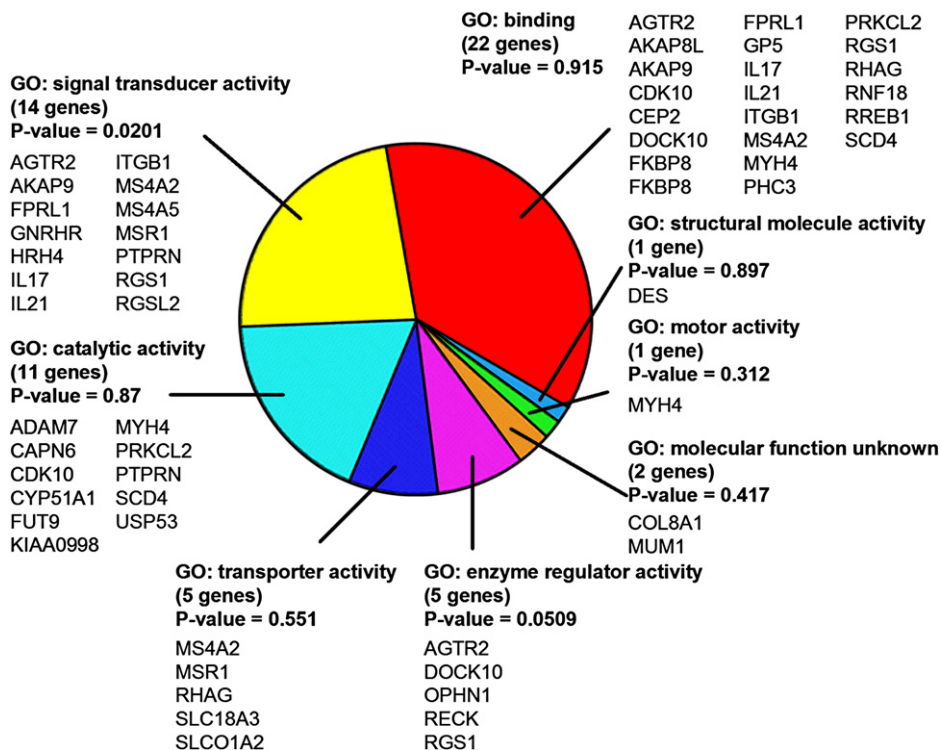


Figure 6 – Gene Ontology analysis of genes distinguishing cells grown in 2D and 3D culture conditions. Gene Ontology analysis of the 41 of the 96 genes shown in Figure 5 for which Gene Ontology annotations were available. Genes encoding proteins involved in signal transduction are significantly overrepresented in this set ($P = 0.0201$), while genes encoding proteins involved in the regulation of enzyme activity almost achieved statistical significance ($P = 0.0509$).

of the malignant phenotype and has provided a wealth of useful information. In these systems it is possible to examine one, two or perhaps three factors acting in concert, but the technical difficulties with these experiments, and the intrinsic gene selection bias in experimental design resulting from our incomplete knowledge of cancer cell biology and of the endogenous aberrations in the host cells, impose a significant constraint on the utility of this widely used approach.

Unlike such models developed in tissue culture, the cell lines in our panel were selected for the ability to proliferate to form clinically relevant and often invasive and metastatic tumors in women. The exposure to these strong evolutionary pressures *in vivo*, promoting such phenotypes as angiogenic potential, resistance to growth inhibitory cues and ability to survive in circulation and at sites distant from the primary tumor – may be more likely to represent relevant cancer models than those constructed in the laboratory. This panel recapitulates, in large part, the full spectrum of interacting mutations and aberrations found in human breast cancer cases (Neve et al., 2006). These include those alterations of which we already have a good understanding and many alterations – “unknown unknowns” – of which we are still ignorant. In this way, our experimental approaches are not biased strongly by prior assumptions, and the sample set is sufficiently diverse to allow us and other workers to choose individual cell lines based on the data provided here to test specific hypotheses. More importantly, perhaps, we should consider these assays and paradigms as we explore ways of testing and selecting current and future chemotherapeutics.

We had previously reported, in a much smaller sample set, that breast cancer cell lines adopt a variety of morphologies in 3D culture and share a number of common properties which distinguish them from non-malignant breast epithelial cells – specifically, a failure to arrest growth and form organized, polarized colonies in response to cues from the extracellular matrix. Here we not only expand on the previous work, but show the plasticity and the diversity of the malignant cells themselves when grown on top of 3D gels. We describe four distinct morphological classes which show correlations with the underlying gene and protein expression patterns. Interestingly, eight of the nine Grape-Like cells were isolated from tumor metastases. In general, these cells formed less closely associated colonies with reduced cell–cell adhesion compared to cell lines of the other morphologies. This may reflect, in part, the acquisition of the ability to break away from their neighbors in the primary tumor over the course of their evolution as they acquired the ability to metastasize.

We previously reported that breast cancer cell lines belonging to the Basal B category were much more invasive by Boyden chamber assays than those belonging to the Basal A and Luminal categories (Neve et al., 2006). The two outliers in this correlation were MCF-10A and MCF-12A, both Basal B but highly un-invasive. Interestingly, both of these cell lines fall under the Round class by 3D morphology (Muthuswamy et al., 2001 and Figure 2). Of the other eight Basal B cell lines which are highly invasive, six cell lines are of the Stellate 3D morphology: three are described in full here (BT-549, Hs578T, MDA-MB-231) and we have also characterized the

other three (HBL-100, MDA-MB-157, SUM 159PT) as Stellate; data not shown). MDA-MB-436 has been shown to be invasive by similar *in vitro* assays (Albini et al., 1987). Thus far, all of the cell lines we have characterized as Stellate have been shown to be invasive in commonly used *in vitro* assays, suggesting the utility of the 3D colony morphology as a functional assay for invasive potential.

In the model we have studied most intensively, malignant T4-2 of the HMT-3522 series, we have used the 3D culture assay to identify a number of signaling nodes which regulate proliferation and architecture of the cells in response to a number of signaling inhibitors (for review see Bissell et al., 2003). In this assay, the disorganized, apolar phenotype of the T4-2 cells can be 'reverted' to a phenotype much more closely approximating that of non-malignant breast acini (and the reverted structures show a profound reduction in tumorigenicity *in vivo*). We determined that the level of signaling downstream of both EGFR and β 1-integrin are critical for the maintenance or reversion of the malignant phenotype in this cell line (Wang et al., 1998; Weaver et al., 1997) and have made substantial inroads into understanding how the key signals may be elicited (Kenny and Bissell, 2007) and transduced (Liu et al., 2004). We expanded this analysis to a small number of other breast cancer cell lines in 3D cultures (MDA-MB-231, MCF-7 and Hs578T) and demonstrated the feasibility of using combinatorial approaches to identify the key deregulated pathways in these cell lines (Wang et al., 2002). Large scale studies of tumor cells in this culture context offer the possibility of rapidly identifying the key molecular vulnerabilities in ways not requiring intensive gene expression or proteomic analyses. The demonstration by Nevins and co-workers that gene expression profiles can be used to predict sensitivity and resistance to different chemotherapeutic agents (Bild et al., 2006; Potti et al., 2006) is exciting and could be used to shortlist compounds for testing in this assay. Since we have shown that resistance to a number of chemotherapeutic agents are dramatically increased by tissue (acinar) polarity in 3D cultures, it would be interesting to explore if signatures from 3D models are better at predicting drug sensitivity *in vivo* than profiles derived from cells cultured on 2D plastic substrata.

In addition to providing important physical and biochemical cues to adhesion receptors, the gelatinous extracellular matrices provide significantly more pliable microenvironments than tissue culture plastic and are thus, in these very important respects, considerably closer to the microenvironments within which cells exist *in vivo*. We and others have repeatedly demonstrated that this environment allows cells to self-organize transcriptionally (Schmidhauser et al., 1992; Xu et al., *in press*), architecturally (Petersen et al., 1992; Roskelley et al., 1994) and at the level of nuclear organization (Lelievre et al., 1998; Maniotis et al., 2005) to express differentiated functions lost in cells grown on tissue culture plastic. We have provided much data suggesting that signal transduction is integrated in cells grown on laminin-containing gels in ways which are fundamentally different from cells grown on plastic. That the differentiated state of so many non-malignant cell types is restored *ex vivo* under the 3D conditions we have defined argues that the signaling events observed are significantly closer to the cognate events *in vivo*. These

concepts are now supported further by the systematic differences observed in 2D versus 3D in the expression of genes encoding signaling proteins in malignant cells. The data support our contention that even malignant cells are plastic and dependent on their microenvironmental signals for survival, growth and metastasis (Bissell and Radisky, 2001). This study, reporting the initial characterization of the growth kinetics, morphology and gene expression patterns of this panel of cell lines in physiologically relevant culture substrata, represents an important initial step to realizing the full potential of thinking in three-dimensions.

4. Experimental procedures

4.1. Cell culture

HMT-3522 S1 (S1) and HMT-3522 T4-2 (T4-2) mammary epithelial cells were maintained on tissue culture plastic as previously described (Briand et al., 1996; Briand et al., 1987; Petersen et al., 1992; Weaver et al., 1997). The following human breast cell lines were maintained on tissue culture plastic in the following manners: CAMA-1, Hs578T, MCF-7, MDA-MB-231, MDA-MB-361, MDA-MB-415, MDA-MB-436, MDA-MB-453, MDA-MB-468, MPE-600, SK-BR-3, UACC-812 were propagated in DMEM/H-21 (Invitrogen) with 10% fetal bovine serum (Gemini); AU565, BT-474, BT-483, BT-549, HCC70, HCC1500, HCC1569, T-47D, ZR-75-1, ZR-75-B were propagated in RPMI 1640 (Invitrogen) with 10% fetal bovine serum; and MCF-12A was propagated in DMEM/F-12 (Invitrogen) with 10 ng/ml insulin, 100 ng/ml cholera toxin, 500 ng/ml hydrocortisone, 20 ng/ml EGF (Sigma), and 5% fetal bovine serum. Three-dimensional laminin-rich extracellular matrix (3D lrECM) on-top cultures (Lee et al., 2007) were prepared by trypsinization of cells from tissue culture plastic, seeding of single cells on top of a thin gel of Engelbreth-Holm-Swarm (EHS) tumor extract (Matrigel: BD Biosciences; Cultrex BME: Trevigen), and addition of medium containing 5% EHS. Cell lines with Round 3D morphology were seeded at a density of 3.1×10^4 cells per cm^2 ; cell lines with Stellate 3D morphology were seeded at 1.6×10^4 cells per cm^2 ; all other cell lines were seeded at 2.1×10^4 cells per cm^2 . All 3D lrECM cell cultures were maintained in H14 medium with 1% fetal bovine serum, with the exception of S1 and T4-2 which were maintained in their propagation medium, for 4 days with media change every 2 days.

4.2. Expression analysis

Colonies were isolated from 3D cultures by dissolution in PBS/EDTA as previously described (Lee et al., 2007). Purified total cellular RNA was extracted using RNeasy Mini Kit with on-column DNase digestion (Qiagen). RNA was quantified by measuring optical density at A260 and quality was verified by agarose gel electrophoresis. Affymetrix microarray analysis was performed using either the Affymetrix high-density oligonucleotide array human HG-U133A chip cartridge system or the Affymetrix High Throughput Array (HTA) GeneChip system, in which HG-U133A chips are mounted on pegs arranged in a 96 well format.

4.2.1. Data processing

A multi-step process was used in order to be able to perform a robust comparison of expression data generated at different times on two separate array platforms. Robust multi-array analysis (RMA) (Irizarry et al., 2003) was performed separately on data generated on both platforms. The data sets from each platform were then row-centered separately by subtracting a constant from all probesets across samples, such that the mean of each probeset equaled zero. The row-centered data sets were then combined and row-centered together. These data have been deposited in the Array Express database (<http://www.ebi.ac.uk/arrayexpress/>; accession number E-TABM-244).

4.3. Immunofluorescence and image acquisition

Immunofluorescence assays were performed as previously described (Lee et al., 2007). In brief, cells were either isolated from 3D cultures and fixed onto glass slides with 4% paraformaldehyde or 1:1 methanol:acetone or fixed directly in culture with 4% paraformaldehyde. Cells were blocked and stained with either fluorescein-labeled phalloidin (Molecular Probes) diluted 1:500 or anti-Ki67 antigen (Vector Laboratories) diluted 1:500 followed by Texas Red-labeled secondary antibody. Nuclei were counterstained with diaminophenylindole (DAPI; Sigma). Slides were mounted with VECTASHIELD Hardset Mounting Medium (Vector Laboratories).

Proliferation index was assessed by quantification of proportion of cells positive for Ki67 antigen. The number of nuclei positive for Ki67 antigen was scored by eye and divided by the total number of nuclei. The mean number of total nuclei counted per cell line was 441, with a minimum of 119.

Confocal analysis was performed using either a Zeiss LSM 410 laser scanning confocal system or a Solamere Technology Group spinning disk confocal system comprised of a Zeiss Axiovert 200M inverted microscope, Yokagawa CSU10 confocal scan head and Stanford Photonics XR/Mega-10 ICCD camera, run by QED InVivo software (Media Cybernetics). Images were analysed using ImageJ (National Institutes of Health) and Adobe Photoshop.

4.4. Western blotting

Cells were isolated from 3D cultures as described above, lysed in 2% SDS in PBS containing 1 mM sodium orthovanadate, 1.5 mM sodium fluoride (Sigma), and 1× protease inhibitor cocktail set I (Calbiochem), and homogenized by sonication. Equal amounts of protein were fractionated by SDS-PAGE, transferred to nitrocellulose membranes and probed with antibodies against the following proteins: Akt, E-cadherin, β -catenin, EGFR, activated EGFR, β 1-integrin (BD Biosciences), phosphorylated S473 Akt, ErbB2, MAPK, phosphorylated T202 and T204 MAPK (Cell Signaling Technology). β -actin (Sigma) was used as a loading control. Blots were developed with SuperSignal West Femto Maximum Sensitivity Substrate (Pierce) and visualized with a FluorChem 8900 imager (Alpha Innotech). Lysates from S1 and T4-2 cells were run on all separate blots in order for signals from cell lines run at different times to be semi-quantitatively compared. Normalization across separate blots was performed in Adobe Photoshop.

First, the sizes of all protein bands were normalized across blots by measuring the width of all T4-2 protein bands with the Ruler tool and resizing blots to equalize the widths while maintaining a fixed aspect ratio. Next, normalization of signal of each protein blotted was performed by using the Eyedropper tool to measure and equalize maximum band intensities of either S1 or T4-2 across all blots. Signal from T4-2 (being generally stronger than S1) was used for normalization except for phosphorylated MAPK and phosphorylated Akt. For normalization of saturated β 1-integrin and β -actin signal, the size of the saturated bands was used for normalization. After normalization was complete, protein bands were aligned and all layers were flattened.

Acknowledgements

These investigations were initially made possible by an Innovator award from the Department of Defense Breast Cancer Research Program (DAMD17-02-1-0438) to M.J.B. and additionally by a Distinguished Scientist Award and a grant from the US Department of Energy, Office of Biological and Environmental Research (DE-AC03 SF0098), and in part by the National Cancer Institute (R01 CA064786 to M.J.B. and O.W.P. and U54 CA112970 to J.W.G.). P.A. Kenny was supported by postdoctoral training fellowships from the Susan G. Komen Breast Cancer Foundation (#2000-223) and the Department of Defense Breast Cancer Research Program (DAMD17-00-1-0224).

REFERENCES

- Albini, A., Iwamoto, Y., Kleinman, H.K., Martin, G.R., Aaronson, S.A., Kozlowski, J.M., McEwan, R.N., 1987. A rapid in vitro assay for quantitating the invasive potential of tumor cells. *Cancer Research* 47, 3239–3245.
- Ashburner, M., Ball, C.A., Blake, J.A., Botstein, D., Butler, H., Cherry, J.M., Davis, A.P., Dolinski, K., Dwight, S.S., Eppig, J.T., et al., 2000. Gene ontology: tool for the unification of biology. The Gene Ontology Consortium. *Nature Genetics* 25, 25–29.
- Barcellos-Hoff, M.H., Aggeler, J., Ram, T.G., Bissell, M.J., 1989. Functional differentiation and alveolar morphogenesis of primary mammary cultures on reconstituted basement membrane. *Development* 105, 223–235.
- Bellis, S.L., 2004. Variant glycosylation: an underappreciated regulatory mechanism for beta1 integrins. *Biochimica et Biophysica Acta* 1663, 52–60.
- Bild, A.H., Yao, G., Chang, J.T., Wang, Q., Potti, A., Chasse, D., Joshi, M.B., Harpole, D., Lancaster, J.M., Berchuck, A., et al., 2006. Oncogenic pathway signatures in human cancers as a guide to targeted therapies. *Nature* 439, 353–357.
- Bissell, D.M., Hammaker, L.E., Meyer, U.A., 1973. Parenchymal cells from adult rat liver in nonproliferating monolayer culture. I. Functional studies. *Journal of Cell Biology* 59, 722–734.
- Bissell, D.M., Tilles, J.G., 1971. Morphology and function of cells of human embryonic liver in monolayer culture. *Journal of Cell Biology* 50, 222–231.
- Bissell, M.J., 1981. The differentiated state of normal and malignant cells or how to define a “normal” cell in culture. *International Review of Cytology* 70, 27–100.

- Bissell, M.J., Hall, H.G., Parry, G., 1982. How does the extracellular matrix direct gene expression? *Journal of Theoretical Biology* 99, 31–68.
- Bissell, M.J., Kenny, P.A., Radisky, D.C., 2005. Microenvironmental regulators of tissue structure and function also regulate tumor induction and progression: the role of extracellular matrix and its degrading enzymes. *Cold Spring Harbor Symposia on Quantitative Biology* 70, 343–356.
- Bissell, M.J., Radisky, D., 2001. Putting tumours in context. *Nature Reviews Cancer* 1, 46–54.
- Bissell, M.J., Rizki, A., Mian, I.S., 2003. Tissue architecture: the ultimate regulator of breast epithelial function. *Current Opinion in Cell Biology* 15, 753–762.
- Bissell, M.J., Weaver, V.M., Lelievre, S.A., Wang, F., Petersen, O.W., Schmeichel, K.L., 1999. Tissue structure, nuclear organization, and gene expression in normal and malignant breast. *Cancer Research* 59, 1757–1763s (Discussion 1763s–1764s).
- Briand, P., Nielsen, K.V., Madsen, M.W., Petersen, O.W., 1996. Trisomy 7p and malignant transformation of human breast epithelial cells following epidermal growth factor withdrawal. *Cancer Research* 56, 2039–2044.
- Briand, P., Petersen, O.W., Van Deurs, B., 1987. A new diploid nontumorigenic human breast epithelial cell line isolated and propagated in chemically defined medium. *In Vitro Cellular and Developmental Biology* 23, 181–188.
- Chin, K., Devries, S., Fridlyand, J., Spellman, P.T., Roydasgupta, R., Kuo, W.L., Lapuk, A., Neve, R.M., Qian, Z., Ryder, T., et al., 2006. Genomic and transcriptional aberrations linked to breast cancer pathophysiologies. *Cancer Cell* 10, 529–541.
- Debnath, J., Mills, K.R., Collins, N.L., Reginato, M.J., Muthuswamy, S.K., Brugge, J.S., 2002. The role of apoptosis in creating and maintaining luminal space within normal and oncogene-expressing mammary acini. *Cell* 111, 29–40.
- Debnath, J., Walker, S.J., Brugge, J.S., 2003. Akt activation disrupts mammary acinar architecture and enhances proliferation in an mTOR-dependent manner. *Journal of Cell Biology* 163, 315–326.
- Emerman, J.T., Pitelka, D.R., 1977. Maintenance and induction of morphological differentiation in dissociated mammary epithelium on floating collagen membranes. *In Vitro* 13, 316–328.
- Filmus, J., Pollak, M.N., Cailleau, R., Buick, R.N., 1985. MDA-468, a human breast cancer cell line with a high number of epidermal growth factor (EGF) receptors, has an amplified EGF receptor gene and is growth inhibited by EGF. *Biochemical and Biophysical Research Communications* 128, 898–905.
- Fournier, M.V., Martin, K.J., Kenny, P.A., Xhaja, K., Bosch, I., Yaswen, P., Bissell, M.J., 2006. Gene expression signature in organized and growth-arrested mammary acini predicts good outcome in breast cancer. *Cancer Research* 66, 7095–7102.
- Gazdar, A.F., Kurvari, V., Virmani, A., Gollahon, L., Sakaguchi, M., Westerfield, M., Kodagoda, D., Stasny, V., Cunningham, H.T., Wistuba, I.I., et al., 1998. Characterization of paired tumor and non-tumor cell lines established from patients with breast cancer. *International Journal of Cancer* 78, 766–774.
- Gunawardane, R.N., Sgroi, D.C., Wrobel, C.N., Koh, E., Daley, G.Q., Brugge, J.S., 2005. Novel role for PDEF in epithelial cell migration and invasion. *Cancer Research* 65, 11572–11580.
- Hiraguri, S., Godfrey, T., Nakamura, H., Graff, J., Collins, C., Shayesteh, L., Doggett, N., Johnson, K., Wheelock, M., Herman, J., et al., 1998. Mechanisms of inactivation of E-cadherin in breast cancer cell lines. *Cancer Research* 58, 1972–1977.
- Irie, H.Y., Pearline, R.V., Grueneberg, D., Hsia, M., Ravichandran, P., Kothari, N., Natesan, S., Brugge, J.S., 2005. Distinct roles of Akt1 and Akt2 in regulating cell migration and epithelial-mesenchymal transition. *Journal of Cell Biology* 171, 1023–1034.
- Irizarry, R.A., Bolstad, B.M., Collin, F., Cope, L.M., Hobbs, B., Speed, T.P., 2003. Summaries of Affymetrix GeneChip probe level data. *Nucleic Acids Research* 31, e15.
- Isakoff, S.J., Engelman, J.A., Irie, H.Y., Luo, J., Brachmann, S.M., Pearline, R.V., Cantley, L.C., Brugge, J.S., 2005. Breast cancer-associated PIK3CA mutations are oncogenic in mammary epithelial cells. *Cancer Research* 65, 10992–11000.
- Kallioniemi, O.P., Kallioniemi, A., Kurisu, W., Thor, A., Chen, L.C., Smith, H.S., Waldman, F.M., Pinkel, D., Gray, J.W., 1992. ERBB2 amplification in breast cancer analyzed by fluorescence in situ hybridization. *Proceedings of the National Academy of Sciences of the United States of America* 89, 5321–5325.
- Kenny, P.A., Bissell, M.J., 2007. Targeting TACE-dependent EGFR ligand shedding in breast cancer. *Journal of Clinical Investigation* 117, 337–345.
- Kleinman, H.K., Martin, G.R., 2005. Matrigel: basement membrane matrix with biological activity. *Seminars in Cancer Biology* 15, 378–386.
- Kraus, M.H., Popescu, N.C., Amsbaugh, S.C., King, C.R., 1987. Overexpression of the EGF receptor-related proto-oncogene erbB-2 in human mammary tumor cell lines by different molecular mechanisms. *EMBO Journal* 6, 605–610.
- Lacroix, M., Leclercq, G., 2004. Relevance of breast cancer cell lines as models for breast tumours: an update. *Breast Cancer Research and Treatment* 83, 249–289.
- Lee, G.Y., Kenny, P.A., Lee, E.H., Bissell, M.J., 2007. 3D culture models of normal and malignant breast epithelial cells. *Nature Methods* 4, 359–365.
- Lelievre, S.A., Weaver, V.M., Nickerson, J.A., Larabell, C.A., Bhaumik, A., Petersen, O.W., Bissell, M.J., 1998. Tissue phenotype depends on reciprocal interactions between the extracellular matrix and the structural organization of the nucleus. *Proceedings of the National Academy of Sciences of the United States of America* 95, 14711–14716.
- Li, M.L., Aggeler, J., Farson, D.A., Hatier, C., Hassell, J., Bissell, M.J., 1987. Influence of a reconstituted basement membrane and its components on casein gene expression and secretion in mouse mammary epithelial cells. *Proceedings of the National Academy of Sciences of the United States of America* 84, 136–140.
- Liu, H., Radisky, D.C., Wang, F., Bissell, M.J., 2004. Polarity and proliferation are controlled by distinct signaling pathways downstream of PI3-kinase in breast epithelial tumor cells. *Journal of Cell Biology* 164, 603–612.
- Maniotis, A.J., Valyi-Nagy, K., Karavitis, J., Moses, J., Boddipali, V., Wang, Y., Nunez, R., Setty, S., Arbieva, Z., Bissell, M.J., et al., 2005. Chromatin organization measured by AluI restriction enzyme changes with malignancy and is regulated by the extracellular matrix and the cytoskeleton. *American Journal of Pathology* 166, 1187–1203.
- Moyret, C., Madsen, M.W., Cooke, J., Briand, P., Theillet, C., 1994. Gradual selection of a cellular clone presenting a mutation at codon 179 of the p53 gene during establishment of the immortalized human breast epithelial cell line HMT-3522. *Experimental Cell Research* 215, 380–385.
- Muthuswamy, S.K., Li, D., Lelievre, S., Bissell, M.J., Brugge, J.S., 2001. ErbB2, but not ErbB1, reinitiates proliferation and induces luminal repopulation in epithelial acini. *Nature Cell Biology* 3, 785–792.
- Neve, R.M., Chin, K., Fridlyand, J., Yeh, J., Baehner, F.L., Fevr, T., Clark, L., Bayani, N., Coppe, J.P., Tong, F., et al., 2006. A collection of breast cancer cell lines for the study of functionally distinct cancer subtypes. *Cancer Cell* 10, 515–527.
- Orford, K., Crockett, C., Jensen, J.P., Weissman, A.M., Byers, S.W., 1997. Serine phosphorylation-regulated ubiquitination and degradation of beta-catenin. *Journal of Biological Chemistry* 272, 24735–24738.
- Overholzer, M., Zhang, J., Smolen, G.A., Muir, B., Li, W., Sgroi, D.C., Deng, C.X., Brugge, J.S., Haber, D.A., 2006. Transforming properties of YAP, a candidate oncogene on the chromosome 11q22 amplicon. *Proceedings of the National*

- Academy of Sciences of the United States of America 103, 12405–12410.
- Park, C.C., Zhang, H., Pallavicini, M., Gray, J.W., Baehner, F., Park, C.J., Bissell, M.J., 2006. Beta1 integrin inhibitory antibody induces apoptosis of breast cancer cells, inhibits growth, and distinguishes malignant from normal phenotype in three dimensional cultures and in vivo. *Cancer Research* 66, 1526–1535.
- Perou, C.M., Jeffrey, S.S., van de Rijn, M., Rees, C.A., Eisen, M.B., Ross, D.T., Pergamenschikov, A., Williams, C.F., Zhu, S.X., Lee, J.C., et al., 1999. Distinctive gene expression patterns in human mammary epithelial cells and breast cancers. *Proceedings of the National Academy of Sciences of the United States of America* 96, 9212–9217.
- Perou, C.M., Sorlie, T., Eisen, M.B., van de Rijn, M., Jeffrey, S.S., Rees, C.A., Pollack, J.R., Ross, D.T., Johnsen, H., Akslen, L.A., Fluge, O., Pergamenschikov, A., Williams, C., Zhu, S.X., Lonning, P.E., Borresen-Dale, A.L., Brown, P.O., Botstein, D., 2000. Molecular portraits of human breast tumors. *Nature* 406, 747–752.
- Petersen, O.W., Ronnov-Jessen, L., Howlett, A.R., Bissell, M.J., 1992. Interaction with basement membrane serves to rapidly distinguish growth and differentiation pattern of normal and malignant human breast epithelial cells. *Proceedings of the National Academy of Sciences of the United States of America* 89, 9064–9068.
- Potti, A., Dressman, H.K., Bild, A., Riedel, R.F., Chan, G., Sayer, R., Cragun, J., Cottrill, H., Kelley, M.J., Petersen, R., et al., 2006. Genomic signatures to guide the use of chemotherapeutics. *Nature Medicine* 12, 1294–1300.
- Reginato, M.J., Mills, K.R., Paulus, J.K., Lynch, D.K., Sgroi, D.C., Debnath, J., Muthuswamy, S.K., Brugge, J.S., 2003. Integrins and EGFR coordinately regulate the pro-apoptotic protein Bim to prevent anoikis. *Nature Cell Biology* 5, 733–740.
- Roskelley, C.D., Desprez, P.Y., Bissell, M.J., 1994. Extracellular matrix-dependent tissue-specific gene expression in mammary epithelial cells requires both physical and biochemical signal transduction. *Proceedings of the National Academy of Sciences of the United States of America* 91, 12378–12382.
- Roskelley, C.D., Srebrow, A., Bissell, M.J., 1995. A hierarchy of ECM-mediated signalling regulates tissue-specific gene expression. *Current Opinion in Cell Biology* 7, 736–747.
- Schmeichel, K.L., Bissell, M.J., 2003. Modeling tissue-specific signaling and organ function in three dimensions. *Journal of Cell Science* 116, 2377–2388.
- Schmidhauser, C., Casperon, G.F., Myers, C.A., Sanzo, K.T., Bolten, S., Bissell, M.J., 1992. A novel transcriptional enhancer is involved in the prolactin- and extracellular matrix-dependent regulation of beta-casein gene expression. *Molecular Biology of the Cell* 3, 699–709.
- Streuli, C.H., Bailey, N., Bissell, M.J., 1991. Control of mammary epithelial differentiation: basement membrane induces tissue-specific gene expression in the absence of cell–cell interaction and morphological polarity. *Journal of Cell Biology* 115, 1383–1395.
- Streuli, C.H., Bissell, M.J., 1990. Expression of extracellular matrix components is regulated by substratum. *Journal of Cell Biology* 110, 1405–1415.
- Streuli, C.H., Schmidhauser, C., Bailey, N., Yurchenco, P., Skubitz, A.P., Roskelley, C., Bissell, M.J., 1995. Laminin mediates tissue-specific gene expression in mammary epithelia. *Journal of Cell Biology* 129, 591–603.
- van de Wetering, M., Barker, N., Harkes, I.C., van der Heyden, M., Dijk, N.J., Hollestelle, A., Klijn, J.G., Clevers, H., Schutte, M., 2001. Mutant E-cadherin breast cancer cells do not display constitutive Wnt signaling. *Cancer Research* 61, 278–284.
- Wang, F., Hansen, R.K., Radisky, D., Yoneda, T., Barcellos-Hoff, M.H., Petersen, O.W., Turley, E.A., Bissell, M.J., 2002. Phenotypic reversion or death of cancer cells by altering signaling pathways in three-dimensional contexts. *Journal of the National Cancer Institute* 94, 1494–1503.
- Wang, F., Weaver, V.M., Petersen, O.W., Larabell, C.A., Dedhar, S., Briand, P., Lupu, R., Bissell, M.J., 1998. Reciprocal interactions between beta1-integrin and epidermal growth factor receptor in three-dimensional basement membrane breast cultures: a different perspective in epithelial biology. *Proceedings of the National Academy of Sciences of the United States of America* 95, 14821–14826.
- Weaver, V.M., Lelievre, S., Lakins, J.N., Chrenek, M.A., Jones, J.C., Giancotti, F., Werb, Z., Bissell, M.J., 2002. Beta4 integrin-dependent formation of polarized three-dimensional architecture confers resistance to apoptosis in normal and malignant mammary epithelium. *Cancer Cell* 2, 205–216.
- Weaver, V.M., Petersen, O.W., Wang, F., Larabell, C.A., Briand, P., Damsky, C., Bissell, M.J., 1997. Reversion of the malignant phenotype of human breast cells in three-dimensional culture and in vivo by integrin blocking antibodies. *Journal of Cell Biology* 137, 231–245.
- Wrobel, C.N., Debnath, J., Lin, E., Beausoleil, S., Roussel, M.F., Brugge, J.S., 2004. Autocrine CSF-1R activation promotes Src-dependent disruption of mammary epithelial architecture. *Journal of Cell Biology* 165, 263–273.
- Xu, R., Spencer, V.A., Bissell, M.J., 2007. Extracellular matrix-regulated gene expression requires cooperation of SWI/SNF and transcription factors. *Journal of Biological Chemistry*, in press.
- Zhan, L., Xiang, B., Muthuswamy, S.K., 2006. Controlled activation of ErbB1/ErbB2 heterodimers promote invasion of three-dimensional organized epithelia in an ErbB1-dependent manner: implications for progression of ErbB2-overexpressing tumors. *Cancer Research* 66, 5201–5208.